

# Neutrino-induced coherent $\pi^+$ production in C, CH, Fe and Pb at $\langle E_\nu \rangle \sim 6$ GeV

M.A. Ramírez,<sup>1,2</sup> S. Akhter,<sup>3</sup> Z. Ahmad Dar,<sup>4,3</sup> F. Akbar,<sup>3</sup> V. Ansari,<sup>3</sup> M. V. Ascencio,<sup>5,\*</sup> M. Sajjad Athar,<sup>3</sup> A. Bashyal,<sup>6,†</sup> L. Bellantoni,<sup>7</sup> A. Bercellie,<sup>8</sup> M. Betancourt,<sup>7</sup> A. Bodek,<sup>8</sup> J. L. Bonilla,<sup>2</sup> A. Bravar,<sup>9</sup> H. Budd,<sup>8</sup> G. Caceres,<sup>10,‡</sup> T. Cai,<sup>8</sup> G.A. Díaz,<sup>8</sup> H. da Motta,<sup>10</sup> S.A. Dytman,<sup>11</sup> J. Felix,<sup>2</sup> L. Fields,<sup>12</sup> A. Filkins,<sup>4</sup> R. Fine,<sup>8,§</sup> H. Gallagher,<sup>13</sup> A. Ghosh,<sup>14,10</sup> S.M. Gilligan,<sup>6</sup> R. Gran,<sup>15</sup> E. Granados,<sup>2</sup> D.A. Harris,<sup>16,7</sup> S. Henry,<sup>8</sup> D. Jena,<sup>7</sup> S. Jena,<sup>17</sup> J. Kleykamp,<sup>8,¶</sup> A. Klustová,<sup>18</sup> M. Kordosky,<sup>4</sup> D. Last,<sup>1</sup> A. Lozano,<sup>10</sup> X.-G. Lu,<sup>19,20</sup> E. Maher,<sup>21</sup> S. Manly,<sup>8</sup> W.A. Mann,<sup>13</sup> C. Mauger,<sup>1</sup> K.S. McFarland,<sup>8</sup> B. Messerly,<sup>11,\*\*</sup> J. Miller,<sup>14</sup> O. Moreno,<sup>4,2</sup> J.G. Morfín,<sup>7</sup> D. Naples,<sup>11</sup> J.K. Nelson,<sup>4</sup> C. Nguyen,<sup>22</sup> A. Olivier,<sup>8</sup> V. Paolone,<sup>11</sup> G.N. Perdue,<sup>7,8</sup> K.-J. Plows,<sup>20</sup> R.D. Ransome,<sup>23</sup> D. Ruterborries,<sup>8</sup> H. Schellman,<sup>6</sup> H. Su,<sup>11</sup> M. Sultana,<sup>8</sup> V.S. Syrotenko,<sup>13</sup> E. Valencia,<sup>4,2</sup> N.H. Vaughan,<sup>6</sup> A.V. Waldron,<sup>18</sup> B. Yaeggy,<sup>14,††</sup> and L. Zazueta<sup>4</sup>

(The MINER $\nu$ A Collaboration)

<sup>1</sup>Department of Physics and Astronomy, University of Pennsylvania, Philadelphia, PA 19104

<sup>2</sup>Campus León y Campus Guanajuato, Universidad de Guanajuato, Lascurain de Retana No. 5, Colonia Centro, Guanajuato 36000, Guanajuato México.

<sup>3</sup>Department of Physics, Aligarh Muslim University, Aligarh, Uttar Pradesh 202002, India

<sup>4</sup>Department of Physics, William & Mary, Williamsburg, Virginia 23187, USA

<sup>5</sup>Sección Física, Departamento de Ciencias, Pontificia Universidad Católica del Perú, Apartado 1761, Lima, Perú

<sup>6</sup>Department of Physics, Oregon State University, Corvallis, Oregon 97331, USA

<sup>7</sup>Fermi National Accelerator Laboratory, Batavia, Illinois 60510, USA

<sup>8</sup>Department of Physics and Astronomy, University of Rochester, Rochester, New York 14627 USA

<sup>9</sup>University of Geneva, 1211 Geneva 4, Switzerland

<sup>10</sup>Centro Brasileiro de Pesquisas Físicas, Rua Dr. Xavier Sigaud 150, Urca, Rio de Janeiro, Rio de Janeiro, 22290-180, Brazil

<sup>11</sup>Department of Physics and Astronomy, University of Pittsburgh, Pittsburgh, Pennsylvania 15260, USA

<sup>12</sup>Department of Physics, University of Notre Dame, Notre Dame, Indiana 46556, USA

<sup>13</sup>Physics Department, Tufts University, Medford, Massachusetts 02155, USA

<sup>14</sup>Departamento de Física, Universidad Técnica Federico Santa María, Avenida España 1680 Casilla 110-V, Valparaíso, Chile

<sup>15</sup>Department of Physics, University of Minnesota – Duluth, Duluth, Minnesota 55812, USA

<sup>16</sup>York University, Department of Physics and Astronomy, Toronto, Ontario, M3J 1P3 Canada

<sup>17</sup>Department of Physical Sciences, IISER Mohali, Knowledge City, SAS Nagar, Mohali - 140306, Punjab, India

<sup>18</sup>The Blackett Laboratory, Imperial College London, London SW7 2BW, United Kingdom

<sup>19</sup>Department of Physics, University of Warwick, Coventry, CV4 7AL, UK

<sup>20</sup>Oxford University, Department of Physics, Oxford, OX1 3PJ United Kingdom

<sup>21</sup>Massachusetts College of Liberal Arts, 375 Church Street, North Adams, MA 01247

<sup>22</sup>University of Florida, Department of Physics, Gainesville, FL 32611

<sup>23</sup>Rutgers, The State University of New Jersey, Piscataway, New Jersey 08854, USA

(Dated: June 28, 2023)

MINER $\nu$ A has measured the  $\nu_\mu$ -induced coherent  $\pi^+$  cross section simultaneously in hydrocarbon (CH), graphite (C), iron (Fe) and lead (Pb) targets using neutrinos from 2 to 20 GeV. The measurements exceed the predictions of the Rein-Sehgal and Berger-Sehgal PCAC based models at multi-GeV  $\nu_\mu$  energies and at produced  $\pi^+$  energies and angles,  $E_\pi > 1$  GeV and  $\theta_\pi < 10^\circ$ . Measurements of the cross-section ratios of Fe and Pb relative to CH reveal the effective  $A$ -scaling to increase from an approximate  $A^{1/3}$  scaling at few GeV to an  $A^{2/3}$  scaling for  $E_\nu > 10$  GeV.

In neutrino-induced coherent pion production the nucleons in the nucleus recoil in phase under the impact of an incident neutrino. The nucleus remains in its initial quantum state and recoils with an energy below the detection threshold of most neutrino detectors. A  $\pi$  meson and a lepton are created, both with relatively small angles with respect to the incoming neutrino. Both charged (CC) and neutral current (NC) interactions can occur, induced by a neutrino or anti-neutrino of any flavor, according to  $\nu_l + A \rightarrow l + \pi + A$ , where  $\nu_l$  is a neutrino of flavor  $l$ ,  $A$  is the nucleus, and  $l$  and  $\pi$ , a lepton and a pion of the proper charge, respectively. The four-momentum transfer to the nucleus,

$$|t| = \left| (p_\nu - p_l - p_\pi)^2 \right| \approx \left( \sum_{i=l,\pi} \mathbf{p}_i^T \right)^2 + \left( \sum_{i=l,\pi} E_i - p_i^L \right)^2, \quad (1)$$

must be between  $|t_{min}| \simeq [(Q^2 + m_\pi^2)/2E_\pi]^2$  [1], and  $|t_{max}| = 1/R_N^2$  [2] for the interaction to happen, where  $p_\nu$ ,  $p_l$  and  $p_\pi$  are the neutrino, lepton and pion four-momenta, respectively;  $\mathbf{p}^T$  and  $p^L$  are the lepton's or pion's transverse and longitudinal momenta, respectively;  $E$  is the lepton's or pion's total energy,  $Q^2$  is the square of the four-momentum transferred by the neu-

trino,  $m_\pi$  is the pion mass, and  $R_N$  is the nuclear radius.

Historically, most experiments [2–17] used the Rein-Sehgal model (R-S) [18] to simulate coherent  $\pi$  production. It is based on Adler’s Partially Conserved Axial Current (PCAC) theorem [19], which relates the neutrino-nucleus inelastic cross section to the pion-nucleus elastic cross section, assuming the incoming neutrino and the outgoing lepton are parallel (when  $Q^2 = 0$ ), and neglecting the lepton mass. The CC channel differential cross section is

$$\frac{d^3\sigma_{coh}^{CC}}{dQ^2 dy d|t|} \Big|_{Q^2=0} = \frac{G_F^2 f_\pi^2}{2\pi^2} \frac{1-y}{y} \frac{d\sigma^{\pi^\pm A}}{d|t|}, \quad (2)$$

where  $y = \nu/E_\nu = (E_\nu - E_\mu)/E_\nu \approx E_\pi/E_\nu$ ,  $f_\pi^2$  is the pion decay constant,  $E_\nu$  is the neutrino energy, and  $d\sigma^{\pi^\pm A}/d|t|$  is the pion-nucleus elastic cross section. The model extrapolates Eq. (2) to  $Q^2 > 0$  with a form factor  $[m_A^2 / (m_A^2 + Q^2)]^2$ , where  $m_A \approx 1$  GeV is the axial-vector mass.

CC coherent pion production is an important background for CC quasi-elastic interactions in  $\nu_\mu$ -disappearance measurements [20], when the  $\pi^+$  is misreconstructed as a proton. It is also a significant fraction of MINERvA’s own CC1 $\pi^+$  sample [21]. Both are very valuable for upcoming neutrino oscillation analyses in the few-GeV region [22, 23].

By using  $|t|$  to isolate signal-like events, MINERvA was the first experiment to observe the CC coherent  $\pi^\pm$  in that energy region, using  $\nu_\mu$  and  $\bar{\nu}_\mu$  beams on a hydrocarbon (CH) target [24, 25]. These and two later publications [26, 27] used an improved version of the R-S model that includes the lepton mass [28, 29].

Prior to this work, all published results on coherent pion production used a single target with mass number  $A \leq 40$  ( $A \leq 80$  for NC) [2–17, 24–27]. Compared to the previous MINERvA measurement, the present work uses data from a more energetic and more intense beam [30], and from a longer exposure, representing an increase of the protons on target (POT), from  $\sim 3 \times 10^{20}$  to  $\sim 10.5 \times 10^{20}$ . This paper presents measurements carried out simultaneously on four different samples: hydrocarbon (CH), graphite (C), steel (Fe) and lead (Pb). Absolute cross sections and ratios to scintillator (CH) are reported for nuclei with a wide range of  $A$  values: 12, 56 and 207.

These measurements are obtained using the NuMI beam line at the Fermi National Accelerator Laboratory [31] where 120-GeV protons colliding on a graphite target, create hadrons which are focused using a pair of magnetic horns, and sent to a decay pipe where they create a beam of muon-neutrinos, with  $\langle E_\nu \rangle \sim 6.0$  GeV [30], made of  $\sim 95\%$   $\nu_\mu$ , and  $\sim 5\%$  of  $\bar{\nu}_\mu$ ,  $\nu_e$  and  $\bar{\nu}_e$  [32]. The neutrino beam is simulated with a Geant4 model [33, 34].

The MINERvA detector consists of an inner detector

made of an upstream “nuclear target” and a downstream “tracker” region, and an outer detector composed of electromagnetic (ECAL) and hadronic (HCAL) calorimeters [35]. The nuclear target region is  $\sim 1.4$  m long with five different passive materials: solid C, Fe, and Pb; and liquid He and H<sub>2</sub>O, all installed in seven targets. Following the beam direction, solid targets are labeled from 1 to 5. Targets 1, 2 and 5 had segments of Fe and Pb, and thickness of  $\sim 2.6$  cm in targets 1 and 2, and  $\sim 1.3$  cm in target 5. Target 3 had C, Fe, and Pb segments, with thickness of  $\sim 7.6$  cm,  $\sim 2.9$  cm and  $\sim 2.6$  cm, respectively. Target 4 was made of Pb with a thickness of  $\sim 0.8$  cm. Eight planes of tracking plastic scintillator (CH) were placed between the targets (only four between targets 4 and 5). Different target positions and thicknesses tried to equalize mass, acceptance and particle containment; maximize event rates, vertex and track resolution; and minimize the energy threshold of particles exiting the passive materials. The tracker region is  $\sim 2.7$  m long and made of 120 scintillator planes. Planes consist of 127 triangular prism scintillator strips with 33-mm base, 17-mm height, and varying length to form an hexagonal plane. Planes are rotated by 60° with respect to adjacent ones, enabling three-dimensional reconstruction. The detector’s single hit position resolution is  $\sim 3$  mm and the time resolution is 3 ns [35]. The ECAL surrounds the inner detector, and the HCAL surrounds the ECAL. The former (latter) consists of planes of lead (iron) and scintillator to contain and track electromagnetically (strongly) interacting particles. Located 2 m downstream of MINERvA, the MINOS near detector [36, 37] served as a magnetized spectrometer to determine muon charge and momentum.

The signal process is CC coherent interactions on C, Fe and Pb, induced by a  $\nu_\mu$  from 2 to 20 GeV. Events with pion angle larger than 70 degrees cannot be tracked and have zero efficiency. Events in the nuclear target (tracker) region with muon angle larger than 13 degrees have an efficiency of  $\sim 1\%$  ( $\sim 4\%$ ) due to MINOS acceptance. The percentage of simulated signal events in these categories is  $\sim 5\%$  for CH and C, and  $\sim 2\%$  for Fe and Pb.

Neutrino interactions are simulated using a modified version of the GENIE event generator v2.12.6 [38, 39]. The signal’s cross section is given by the R-S model with the lepton mass correction. Background processes (Fig. 1) in increasing hadronic invariant mass  $W$ , are: CC quasielastic (QE), correlated pairs of nucleons (2p2h), resonant  $\pi^+$  production (Non-QE,  $W < 1.4$  or RES), inelastic scattering ( $1.4 < W < 2.0$  or INE) and deep inelastic scattering ( $W > 2.0$  or DIS). Quasielastic scattering is simulated using the Llewellyn-Smith model [40] with an axial-vector form factor from a z-expansion fit to deuterium data [41] and a correction from the Valencia Random Phase Approximation (RPA) [42]. The 2p2h process is simulated with the Valencia model [43–45] and modified according to a “low recoil” fit by MINERvA [46]. Resonant pion production uses the Rein-Sehgal model

[47] with its normalization increased 15% based on fits from a deuterium data analysis [48], plus an additional *ad hoc* suppression for  $Q^2 < 0.7$  [ $\text{GeV}/c^2$ ] due to collective nuclear effects [49]. Inelastic interactions use a tuned model of discrete baryon resonances [47], and the Bodek-Yang model for the transition region to DIS, as well as non-resonant pion production across the full  $W$  range [50], that was reduced by 43% based on a tune to the same deuterium data [48]. These tunes to GENIE are labeled as the MINERvA tune v4.4.1 [51].

Final state particles coming from the GENIE simulation are propagated through the detector using a Geant4 simulation of the detector's geometry and material composition, light yield and energy deposition of the particles in the scintillator, and their hadronic and electromagnetic interactions [52, 53]. The detector's energy scale was established by making sure that simulated through-going muons agreed with data in both light yield and reconstructed energy deposition. The detector's simulated response to different particles is validated in a test beam measurement [54], and the effects of accidental activity, electronics charge and time resolution were also included [35].

Scintillator strips with deposited energy greater than 1 MeV are grouped per plane according to their position and time, into “clusters”. These are grouped with clusters in adjacent planes to form tracks. Backwards-projected tracks find interaction vertices. Angles are measured between the simulated beam direction and the direction of the track in its first planes downstream of the vertex.

This analysis isolates events with two tracks from a common vertex. The reconstructed momentum of the muon candidate is the addition of the momentum determined by range inside MINERvA plus its momentum determined by range or curvature inside MINOS. The pion candidate has to be fully contained inside MINERvA, so  $|t|$  can be measured. The pion total energy is reconstructed calorimetrically from all the energy not associated with the muon, given the assumption  $E_\nu \approx E_\pi + E_\mu$  from Eq. (1), where  $E_\mu$  is the muon's total energy.

The reconstructed interaction vertex is defined as the upstream end of the muon track, and it is required to be inside the fiducial volume under study. The CH fiducial volume is 108 planes long ( $\sim 2.4$  m) centered in the tracker region with the area of a 0.85-m apothem hexagon [55]. The fiducial volume in the passive targets, is the area times the thickness of the segment of interest. For the passive materials, the vertex is projected into the  $z$  center of the target, where the  $(x, y)$  coordinate determines the segment (material). Events from different targets but same material, are combined into a single sample.

The reconstructed neutrino energy must be between 2 and 20 GeV to remove events with mis-reconstructed muon energy [34]. To reject protons from quasielastic

and resonance production backgrounds,  $dE/dx$ -based  $\chi^2$  compared to pion and proton hypotheses of the pion candidate track are built. A log likelihood ratio [56] between the hypotheses removes (keeps)  $\sim 70\%$  ( $\sim 87\%$ ) of protons (pions) according to the simulation.

The energy of the vertex region ( $E_{vtx}$ ), defined as a 200-mm radius, 7-plane height cylinder centered at the interaction vertex, must be consistent with the energy deposited by one minimum-ionizing charged pion and one muon. The  $E_{vtx}$  distribution of simulated signal events is fit to a Gaussian function, and events within  $\pm 1\sigma$  of the mean are selected. Due to different target thickness,  $\langle E_{vtx} \rangle$  is target-dependent, varying from  $\sim 60$  to  $\sim 95$  MeV. This cut removes (keeps)  $\sim 86\%$  ( $\sim 60\%$ ) of the background (signal).

Due to their proximity to tracking scintillator planes, the C, Fe and Pb samples have contamination from events occurring in scintillator upstream and downstream of the passive material. These events are considered background, and are tuned using the plastic regions between passive targets as sidebands. There is an “upstream” and a “downstream” plastic sideband for each passive material. The tuned plastic backgrounds represent  $\sim 13\%$ ,  $\sim 14\%$  and  $\sim 21\%$  of the C, Fe and Pb selected samples, respectively.

After removing events with high  $E_{vtx}$ , and subtracting the plastic background, all samples in Fig. 1 show a signal dominance at low  $|t|$ . For heavier nuclei, the signal shrinks to a lower  $|t|$  region as  $R_N$  increases. The C distribution has a significant excess of RES and INE events from  $\sim 0.025$  to  $\sim 0.5$  [ $\text{GeV}/c^2$ ] compared to CH, despite both being interactions on Carbon. This is due to the  $\sim 7.6$ -cm thickness of the C segment, where one or more pions from those backgrounds are absorbed inside the passive material, which allows the event to pass the  $E_{vtx}$  cut.

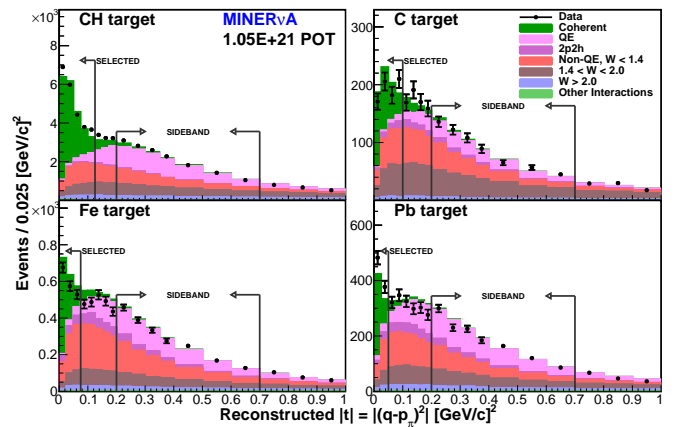


FIG. 1. Reconstructed  $|t|$  distributions after  $E_{vtx}$  cut and background tuning: CH, C, Fe and Pb, in reading order. Regions in between arrows are the sidebands for background tuning. Events to the left of the lower- $|t|$  arrow, are selected.

A high  $|t|$  sideband ( $0.2 < |t| < 0.7$  [ $\text{GeV}/c^2$ ]) is used to tune the QE, RES (Non-QE,  $W < 1.4$ ), INE ( $1.4 < W < 2.0$ ) and DIS ( $W > 2.0$ ) backgrounds. Due to their small content, “Coherent” and “Other Interactions” (NC-,  $\bar{\nu}_\mu$ - or  $\bar{\nu}_e$ -induced) are not tuned, and 2p2h is considered QE during the tuning. Because the C target has limited statistics, two modifications were made to the fit for that target only: RES and INE were combined, and the QE and DIS scale factors were replaced by their CH counterparts. The scale factors for each of the backgrounds are in the supplemental material.

Events with  $|t| < (0.1, 0.125, 0.075, \text{and } 0.05)$  [ $\text{GeV}/c^2$ ] were selected for C, CH, Fe and Pb, respectively. More than 99% of GENIE true signal events are below those cuts. After the  $|t|$  cut and background subtraction, there are  $14855 \pm 433$  CH,  $303 \pm 41$  C,  $726 \pm 89$  Fe and  $492 \pm 41$  Pb candidate events.

An iterative unfolding approach [57] was used to correct the background-subtracted distributions for resolution effects. The unfolded distributions were then efficiency-corrected. The cross sections were extracted according to the expression  $\sigma = N^{DATA\ eff}/(\Phi T)$ , where  $N^{DATA\ eff}$  is the background-subtracted, unfolded and efficiency-corrected data,  $\Phi$  is the incident neutrino flux, and  $T$  the number of C, Fe or Pb nuclei. The largest sources of inefficiency come predominantly from well-understood random processes, which supports the assumption that the non-detected events have the same relative background composition.

The extracted cross sections are compared to the R-S model (GENIE v2.12.6) and to the Berger-Sehgal (B-S) model (GENIE v3.0.6) [58–60]. The latter is also PCAC-based, and also includes the muon mass correction, but uses pion-carbon data [1] to model the elastic pion-nucleus cross section, instead of pion-deuterium data as the R-S model.

Figure 2 shows the total cross section as a function of  $E_\nu$ , with the flux integrated per bin, where both models under-predict the reaction rate at high neutrino energies in the four materials. Inner (outer) error bars are the statistical (statistical+systematic) uncertainties. The differential cross sections with respect to  $E_\pi$  and  $\theta_\pi$ , are flux-averaged from  $2 < E_\nu < 20$  GeV. In  $d\sigma/dE_\pi$  (Fig. 3) there is a clear disagreement between the models and the data of the two heavier nuclei, for low (high)  $E_\pi$  in iron (lead). Figure 4 shows that the models also under-predict the  $d\sigma/d\theta_\pi$  cross section at very forward angles in all materials. Notably, forward pion production in the heavier nuclei is enhanced relative to scattering on carbon, where for lead, the cross section becomes negligible for  $\theta_\pi > 30^\circ$ .

The simultaneous neutrino exposure of the various targets enables precise measurement of cross section ratios thanks to the same beam configuration in all targets at any given time. Figure 5 shows the cross section ratios

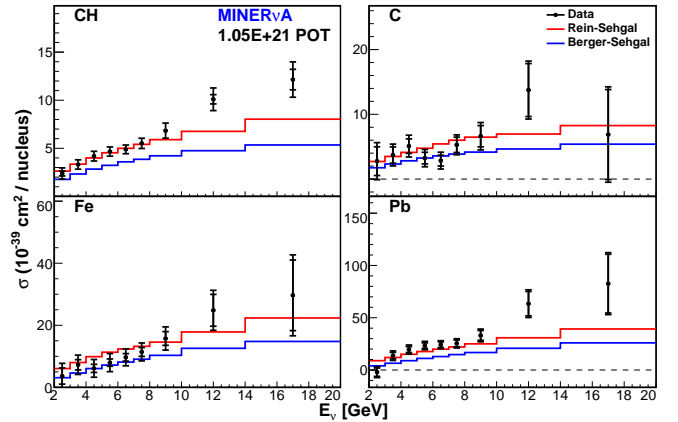


FIG. 2. Total cross sections as function of  $E_\nu$ : CH, C, Fe, and Pb, in reading order. Data is compared to the R-S (red) and B-S (blue) models.

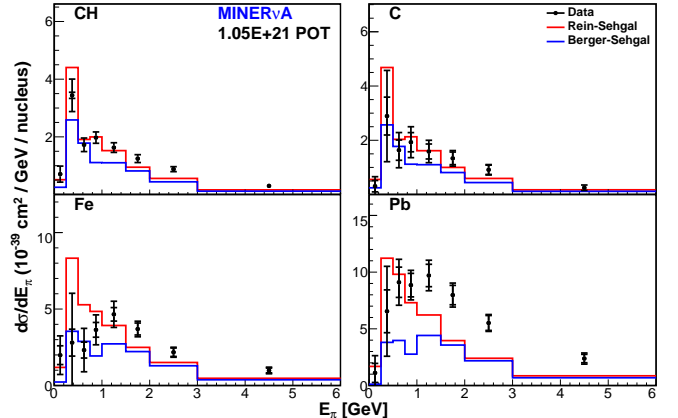


FIG. 3. Differential cross sections as function of  $E_\pi$ : CH, C, Fe, and Pb, in reading order. Data is compared to the R-S (red) and B-S (blue) models.

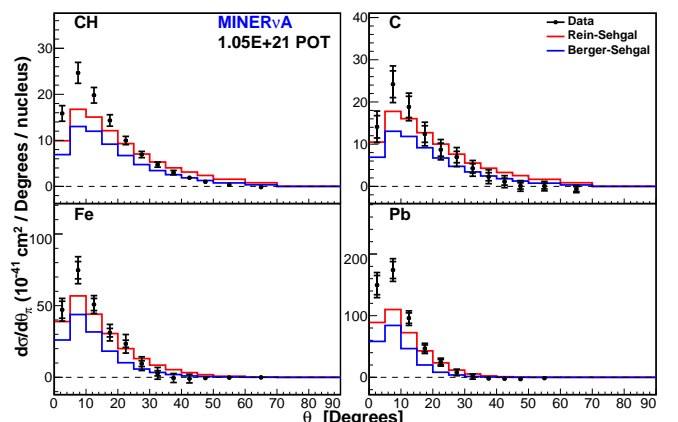


FIG. 4. Differential cross sections as function of  $\theta_\pi$ : CH, C, Fe, and Pb, in reading order. Data is compared to the R-S (red) and B-S (blue) models.

as a function of  $E_\nu$ :  $\sigma_C/\sigma_{CH}$ ,  $\sigma_{Fe}/\sigma_{CH}$  and  $\sigma_{Pb}/\sigma_{CH}$ .

As expected, the former is consistent with unity [61]. The CH cross sections used to calculate the ratios, were reweighted to use a flux that matched the flux used to calculate the C, Fe or Pb cross sections [21].

The R-S and B-S models predict a scaling of the cross-section with respect to the mass number  $A$  and practically energy independent (horizontal dashed lines in Fig. 5),  $\sim A^{1/3}$  [18, 62] and  $\sim A^{2/3}$  [3, 63], respectively. The PCAC-based Belkov-Kopeliovich (B-K) model predicts a scaling close to  $A^{1/3}$  at low pion energy but close to  $A^{2/3}$  at high pion energy [64, 65]. In terms of neutrino energy, the B-K model predicts a scaling of  $\sim A^{1/3}$  ( $\sim A^{2/3}$ ) at neutrino energies below (above)  $\sim 10$  GeV [66].

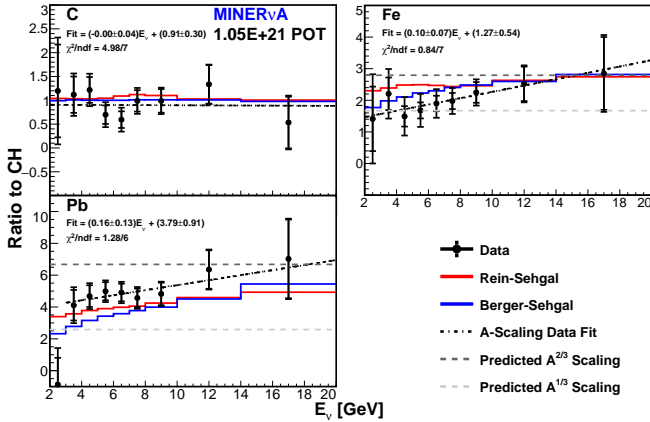


FIG. 5. Cross section ratios as function of  $E_\nu$ :  $\sigma_C/\sigma_{CH}$ ,  $\sigma_{Fe}/\sigma_{CH}$ , and  $\sigma_{Pb}/\sigma_{CH}$ , in reading order. The upper (lower) dashed line is the ratio predicted by an  $A^{2/3}$  ( $A^{1/3}$ ) scaling. The slope is the best  $A$ -scaling fit. The 2–3 GeV bin is not included in the  $\sigma_{Pb}/\sigma_{CH}$  fit due to the null cross section in lead in that bin (Fig. 2).

The measured  $\sigma_{Fe}/\sigma_{CH}$  resembles the trend predicted by B-K, where below  $\sim 8$  GeV there is a clear agreement with the  $A^{1/3}$  scaling, and a better agreement with the  $A^{2/3}$  scaling above  $\sim 10$  GeV, with a constant increase in between. A similar trend occurs for the measured  $\sigma_{Pb}/\sigma_{CH}$  but with an  $A$ -scaling larger than predicted below 10 GeV.

The statistical uncertainty of the total cross section dominates in the three passive materials (Fig. 6). The largest systematic uncertainties are related to the detector's geometry and particles interacting in it (Detector Model), like the muon energy deposition in MINERvA and MINOS [67]. Uncertainties associated with the “Interaction Model”, come from GENIE and the uncertainties from the MINERvA tune v.4.4.1. The “Physics Sideband” is the uncertainty on the backgrounds scale factors, plus a “per-bin” uncertainty covering for the remaining disagreement between data and the simulation in the high  $|t|$  sideband.

The “Flux” uncertainty comes from the uncertainty on the beam line parameters, and hadron interactions [34].

It was further constrained from 7.6% to 3.9% using a neutrino-electron scattering measurement [68].

Other sources of uncertainty are the discrepancy in the detector mass; modifications to the QE-like background (Low Recoil and RPA); low  $Q^2$  suppression of resonant pion production; and the uncertainty on the plastic background scale factors (Plastic Sideband). They contribute less than  $\sim 5\%$  ( $\sim 15\%$ ) to the total cross section uncertainty in CH (C, Fe and Pb). The CH sample provides the most precise measurement of the interaction so far, reducing the total uncertainty from  $\sim 25\%$  to  $\sim 15\%$  compared to the previous MINERvA measurement [25]. Cross section ratios have a further reduction of some systematic uncertainties, in particular the flux, reduced by  $\sim 75\%$  of itself (Fig. 6).

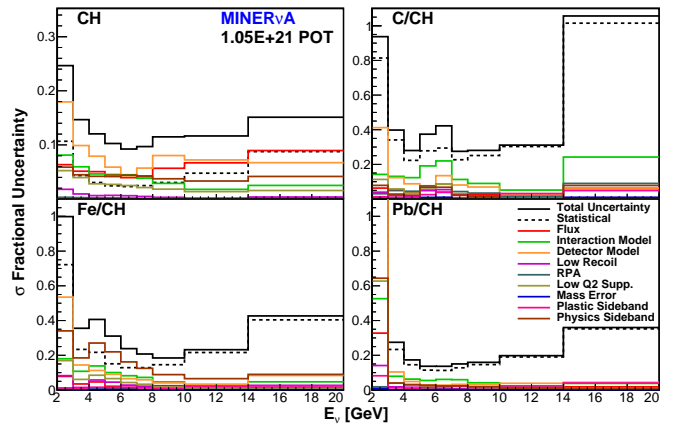


FIG. 6. Uncertainties in the total cross section as a function of  $E_\nu$ : CH, C/CH, Fe/CH, and Pb/CH, in reading order. The systematic uncertainties are described in the text.

The measurements in this letter represent the first simultaneous measurement of the interaction in multiple materials and the first measurement in nuclei with  $A > 40$  ( $^{56}\text{Fe}$  and  $^{207}\text{Pb}$ ), from which cross section ratios with respect to CH are measured. The data indicates that the R-S and B-S PCAC models do not accurately describe the angular dependence on  $\theta_\pi$ , the energy-dependence on  $E_\pi$ , or the  $A$ -dependence. While the  $\sigma_{Fe}/\sigma_{CH}$  qualitatively agrees with the B-K model's energy-dependent  $A$ -scaling,  $\sigma_{Pb}/\sigma_{CH}$  does not, at least at low  $E_\nu$ .

The estimate of the cross sections A-scaling provided in this letter could be used to extrapolate to materials where measurements do not exist or the statistics are limited, like  $\text{H}_2\text{O}$  for Hyper-K or Ar for DUNE. For the latter, pion production will make up around three quarters of the detected neutrino-induced events.

This document was prepared by members of the MINERvA Collaboration using the resources of the Fermi National Accelerator Laboratory (Fermilab), a U.S. Department of Energy, Office of Science, HEP User Facility. Fermilab is managed by Fermi Research Alliance,

LLC (FRA), acting under Contract No. DE-AC02-07CH11359. These resources included support for the MINERvA construction project, and support for construction also was granted by the United States National Science Foundation under Award No. PHY-0619727 and by the University of Rochester. Support for participating scientists was provided by NSF and DOE (USA); by CAPES and CNPq (Brazil); by CoNaCyT (México); by Proyecto Basal FB 0821, CONICYT PIA ACT1413, and Fondecyt 3170845 and 11130133 (Chile); by CONCYTEC (Consejo Nacional de Ciencia, Tecnología e Innovación Tecnológica), DGI-PUCP (Dirección de Gestión de la Investigación - Pontificia Universidad Católica del Perú), and VRI-UNI (Vice-Rectorate for Research of National University of Engineering) (Perú); NCN Opus Grant No. 2016/21/B/ST2/01092 (Poland); by Science and Technology Facilities Council (UK); by EU Horizon 2020 Marie Skłodowska-Curie Action; by a Cottrell Postdoctoral Fellowship from the Research Corporation for Scientific Advancement; by an Imperial College London President's PhD Scholarship. We thank the MINOS Collaboration for use of its near detector data. Finally, we thank the staff of Fermilab for support of the beam line, the detector, and computing infrastructure. M.A. Ramírez specially acknowledges support from a Postdoctoral Fellowship from the University of Pennsylvania.

- 
- \* Now at Iowa State University, Ames, IA 50011, USA  
 † Now at High Energy Physics/Center for Computational Excellence Department, Argonne National Lab, 9700 S Cass Ave, Lemont, IL 60439  
 ‡ now at Department of Physics and Astronomy, University of California at Davis, Davis, CA 95616, USA  
 § Now at Los Alamos National Laboratory, Los Alamos, New Mexico 87545, USA  
 ¶ now at Department of Physics and Astronomy, University of Mississippi, Oxford, MS 38677  
 \*\* Now at University of Minnesota, Minneapolis, Minnesota 55455, USA  
 †† Now at Department of Physics, University of Cincinnati, Cincinnati, Ohio 45221, USA
- [1] E. A. Paschos, A. Kartavtsev and G. J. Gounaris, Coherent pion production by neutrino scattering off nuclei, Phys. Rev. D **74**, 054007 (2006)
  - [2] P. Vilain *et al.* (CHARM II), Coherent single charged pion production by neutrinos, Phys. Lett. B **313**, 267-275 (1993)
  - [3] (Achen-Padova) H. Faissner, E. Frenzel, M. Grimm, T. Hansl-Kozanecka, D. Hoffmann, E. Radermacher, D. Rein, H. Reithler, U. Samm and L. M. Sehgal, *et al.*, Observation of neutrino and anti-neutrino induced coherent neutral pion production off  $^{27}\text{Al}$ , Phys. Lett. B **125**, 230-236 (1983)
  - [4] E. Isiksal, D. Rein and J. G. Morfin, Evidence for neutrino and anti-neutrino induced coherent  $\pi^0$  production, Phys. Rev. Lett. **52**, 1096-1099 (1984)
  - [5] P. Marage *et al.* (WA59), Observation of coherent diffractive charged current interactions of anti-neutrinos on neon nuclei, Phys. Lett. B **140**, 137-141 (1984)
  - [6] F. Bergsma *et al.* (CHARM), Measurement of the cross-section of coherent  $\pi^0$  production by muon neutrino and anti-neutrino neutral current interactions on nuclei, Phys. Lett. B **157**, 469-474 (1985)
  - [7] H. J. Grabosch *et al.* (SKAT), Coherent pion production in neutrino and anti-neutrino interactions on nuclei of heavy freon molecules, Z. Phys. C **31**, 203 (1986)
  - [8] C. Baltay, M. Bregman, D. Caroumbalis, L. D. Chen, M. Hibbs, J. T. Liu, J. Okamitsu, G. Ormazabal, A. C. Schaffer and K. Shastri, *et al.*, Evidence for coherent neutral pion production by high-energy neutrinos, Phys. Rev. Lett. **57**, 2629-2632 (1986)
  - [9] P. Marage *et al.* (BEBC WA59), Coherent single pion production by anti-neutrino charged current interactions and test of PCAC, Z. Phys. C **31**, 191-197 (1986)
  - [10] M. Aderholz *et al.* (E632), Coherent production of  $\pi^+\pi^-$  mesons by charged current interactions of neutrinos and anti-neutrinos on neon nuclei at the Tevatron, Phys. Rev. Lett. **63**, 2349 (1989)
  - [11] P. Marage *et al.* (BEBC WA59), Coherent production of  $\pi^+$  mesons in  $\nu$ -neon interactions, Z. Phys. C **43**, 523-526 (1989)
  - [12] S. Willocq *et al.* (E632), Coherent production of single pions and rho mesons in charged current interactions of neutrinos and anti-neutrinos on neon nuclei at the Fermilab Tevatron, Phys. Rev. D **47**, 2661-2674 (1993)
  - [13] M. Hasegawa *et al.* (K2K), Search for coherent charged pion production in neutrino-carbon interactions, Phys. Rev. Lett. **95**, 252301 (2005)
  - [14] A. A. Aguilar-Arevalo *et al.* (MiniBooNE), First observation of coherent  $\pi^0$  production in neutrino nucleus interactions with  $E_\nu < 2$  GeV, Phys. Lett. B **664**, 41-46 (2008)
  - [15] K. Hiraide *et al.* (SciBooNE), Search for charged current coherent pion production on carbon in a few-GeV neutrino beam, Phys. Rev. D **78**, 112004 (2008)
  - [16] C. T. Kullenberg *et al.* (NOMAD), A measurement of coherent neutral pion production in neutrino neutral current interactions in NOMAD, Phys. Lett. B **682**, 177-184 (2009)
  - [17] Y. Kurimoto *et al.* (SciBooNE), Improved measurement of neutral current coherent  $\pi^0$  production on carbon in a few-GeV neutrino beam, Phys. Rev. D **81**, 111102 (2010)
  - [18] D. Rein and L. M. Sehgal, Coherent  $\pi^0$  production in neutrino reactions, Nucl. Phys. B **223**, 29-44 (1983)
  - [19] S. L. Adler, Tests of the conserved vector current and partially conserved axial-vector current hypotheses in high-energy neutrino reactions, Phys. Rev. **135**, B963-B966 (1964)
  - [20] D. G. Michael *et al.* [MINOS], Phys. Rev. Lett. **97**, 191801 (2006) doi:10.1103/PhysRevLett.97.191801 [[arXiv:hep-ex/0607088](#) [hep-ex]].
  - [21] A. Bercellie *et al.* [MINERvA], [[arXiv:2209.07852](#) [hep-ex]].
  - [22] R. Acciarri *et al.* [DUNE], [[arXiv:1512.06148](#) [physics.ins-det]].
  - [23] K. Abe *et al.* [Hyper-Kamiokande Proto-], PTEP **2015**, 053C02 (2015) doi:10.1093/ptep/ptv061 [[arXiv:1502.05199](#) [hep-ex]].
  - [24] A. Higuera *et al.* (MINERvA), Measurement of coherent production of  $\pi^\pm$  in neutrino and anti-neutrino beams on carbon from  $E_\nu$  of 1.5 to 20 GeV, Phys. Rev. Lett. **113**,

- no.26, 261802 (2014)
- [25] A. Mislove *et al.* (MINERvA), Measurement of total and differential cross sections of neutrino and antineutrino coherent  $\pi^\pm$  production on carbon, Phys. Rev. D **97**, no.3, 032014 (2018)
- [26] R. Acciarri *et al.* (ArgoNeuT), First measurement of neutrino and anti-neutrino coherent charged pion production on argon, Phys. Rev. Lett. **113**, no.26, 261801 (2014) [erratum: Phys. Rev. Lett. **114**, no.3, 039901 (2015)]
- [27] K. Abe *et al.* (T2K), Measurement of coherent  $\pi^+$  production in low energy neutrino-carbon scattering, Phys. Rev. Lett. **117**, no.19, 192501 (2016)
- [28] S. L. Adler, Adventures in theoretical physics: selected papers of Stephen L. Adler: drafts of commentaries,
- [29] D. Rein and L. M. Sehgal, PCAC and the deficit of forward muons in  $\pi^+$  production by neutrinos, Phys. Lett. B **657**, 207-209 (2007)
- [30] R. Ainsworth, P. Adamson, B. C. Brown, D. Capista, K. Hazelwood, I. Kourbanis, D. K. Morris, M. Xiao and M. J. Yang, High intensity operation using proton stacking in the Fermilab Recycler to deliver 700 kW of 120 GeV proton beam, Phys. Rev. Accel. Beams **23**, no.12, 121002 (2020)
- [31] P. Adamson, K. Anderson, M. Andrews, R. Andrews, I. Anghel, D. Augustine, A. Aurisano, S. Avvakumov, D. S. Ayres and B. Baller, *et al.*, The NuMI neutrino beam, Nucl. Instrum. Meth. A **806**, 279-306 (2016)
- [32] M. Betancourt *et al.* (MINERvA), Direct measurement of nuclear dependence of charged current quasielasticlike neutrino interactions using MINERvA, Phys. Rev. Lett. **119**, no.8, 082001 (2017)
- [33] S. Agostinelli *et al.* (GEANT4), GEANT4 - a simulation toolkit, Nucl. Instrum. Meth. A **506**, 250-303 (2003)
- [34] L. Aliaga *et al.* (MINERvA), Neutrino flux predictions for the NuMI beam, Phys. Rev. D **94**, no.9, 092005 (2016)
- [35] L. Aliaga *et al.* (MINERvA), Design, calibration, and performance of the MINERvA detector, Nucl. Instrum. Meth. A **743**, 130-159 (2014)
- [36] I. Ambats *et al.* (MINOS), The MINOS detectors technical design report,
- [37] D. G. Michael *et al.* (MINOS), The Magnetized steel and scintillator calorimeters of the MINOS experiment, Nucl. Instrum. Meth. A **596**, 190-228 (2008)
- [38] C. Andreopoulos, A. Bell, D. Bhattacharya, F. Cavanna, J. Dobson, S. Dytman, H. Gallagher, P. Guzowski, R. Hatcher and P. Kehayias, *et al.*, The GENIE neutrino Monte Carlo generator, Nucl. Instrum. Meth. A **614**, 87-104 (2010)
- [39] C. Andreopoulos, C. Barry, S. Dytman, H. Gallagher, T. Golan, R. Hatcher, G. Perdue and J. Yarba, The GENIE neutrino Monte Carlo generator: physics and user manual,
- [40] C. H. Llewellyn Smith, Neutrino reactions at accelerator energies, Phys. Rept. **3**, 261-379 (1972)
- [41] A. S. Meyer, M. Betancourt, R. Gran and R. J. Hill, Deuterium target data for precision neutrino-nucleus cross sections, Phys. Rev. D **93**, no.11, 113015 (2016)
- [42] J. Nieves, J. E. Amaro and M. Valverde, Inclusive quasi-elastic neutrino reactions, Phys. Rev. C **70**, 055503 (2004) [erratum: Phys. Rev. C **72**, 019902 (2005)]
- [43] J. Nieves, I. Ruiz Simo and M. J. Vicente Vacas, Inclusive charged-current neutrino-nucleus reactions, Phys. Rev. C **83**, 045501 (2011)
- [44] R. Gran, J. Nieves, F. Sanchez and M. J. Vicente Vacas, Neutrino-nucleus quasi-elastic and 2p2h interactions up to 10 GeV, Phys. Rev. D **88**, no.11, 113007 (2013)
- [45] J. Schwehr, D. Cherdack and R. Gran, GENIE implementation of IFIC Valencia model for QE-like 2p2h neutrino-nucleus cross section, [\[arXiv:1601.02038 \[hep-ph\]\]](https://arxiv.org/abs/1601.02038).
- [46] P. A. Rodrigues *et al.* (MINERvA), Identification of nuclear effects in neutrino-carbon interactions at low three-momentum transfer, Phys. Rev. Lett. **116**, 071802 (2016)
- [47] D. Rein and L. M. Sehgal, Neutrino excitation of baryon resonances and single pion production, Annals Phys. **133**, 79-153 (1981)
- [48] P. Rodrigues, C. Wilkinson and K. McFarland, Constraining the GENIE model of neutrino-induced single pion production using reanalyzed bubble chamber data, Eur. Phys. J. C **76**, no.8, 474 (2016)
- [49] P. Stowell *et al.* (MINERvA), Tuning the GENIE pion production model with MINERvA data, Phys. Rev. D **100**, no.7, 072005 (2019)
- [50] A. Bodek, I. Park and U. k. Yang, Improved low  $Q^2$  model for neutrino and electron nucleon cross sections in few GeV region, Nucl. Phys. B Proc. Suppl. **139**, 113-118 (2005)
- [51] D. Ruterbories *et al.* [MINERvA], Phys. Rev. Lett. **129** (2022) no.2, 021803 doi:10.1103/PhysRevLett.129.021803 [\[arXiv:2203.08022 \[hep-ex\]\]](https://arxiv.org/abs/2203.08022).
- [52] A. B. Kaidalov, The quark-gluon structure of the pomeron and the rise of inclusive spectra at high-energies, Phys. Lett. B **116**, 459-463 (1982)
- [53] M. P. Guthrie, R. G. Alsmiller and H. W. Bertini, Calculation of the capture of negative pions in light elements and comparison with experiments pertaining to cancer radiotherapy, Nucl. Instrum. Meth. **66**, 29-36 (1968)
- [54] L. Aliaga *et al.* (MINERvA), MINERvA neutrino detector response measured with test beam data, Nucl. Instrum. Meth. A **789**, 28-42 (2015)
- [55] MINERvA uses a right-handed coordinate system with the y axis pointing upwards and the z axis pointing into the detector parallel to the floor, and almost parallel to the beam plane.
- [56] J. Neyman and E. S. Pearson, On the problem of the most efficient tests of statistical hypotheses, Phil. Trans. Roy. Soc. Lond. A **231**, no.694-706, 289-337 (1933)
- [57] G. D'Agostini, A Multidimensional unfolding method based on Bayes' theorem, Nucl. Instrum. Meth. A **362**, 487-498 (1995)
- [58] J. Tena-Vidal *et al.* (GENIE), Phys. Rev. D **104**, no.7, 072009 (2021)
- [59] P. Stowell, C. Wret, C. Wilkinson, L. Pickering, *et al.*, 2017, Journal of Instrumentation **12**, P01016
- [60] C. Berger and L. M. Sehgal, Phys. Rev. D **79**, 053003 (2009)
- [61] Diffractive scattering in H was not measured, and no correction is applied for its contribution to the coherent cross section in CH because those events are removed by the vertex energy cut.
- [62] K. S. Lackner, Coherent meson production as a test for neutral weak currents of exotic space-time structure, Nucl. Phys. B **153**, 526-545 (1979)
- [63] J. Hufner, Pions interact with nuclei, Phys. Rept. **21**, 1-79 (1975)
- [64] B. Z. Kopeliovich, I. Schmidt and M. Sidzikov, Phys. Rev. D **84**, 033012 (2011) doi:10.1103/PhysRevD.84.033012 [\[arXiv:1107.2845\]](https://arxiv.org/abs/1107.2845)

- [hep-ph]].
- [65] B. Z. Kopeliovich, I. Schmidt and M. Sidzikov, Phys. Rev. D **85**, 073003 (2012) doi:10.1103/PhysRevD.85.073003 [[arXiv:1201.4053](https://arxiv.org/abs/1201.4053) [hep-ph]].
- [66] A. A. Belkov and B. Z. Kopeliovich, Adler relation and neutrino production of single hadrons, Sov. J. Nucl. Phys. **46**, 499 (1987) JINR-E2-86-595.
- [67] M. F. Carneiro *et al.* (MINERvA), High-statistics measurement of neutrino quasielasticlike scattering at 6 GeV on a hydrocarbon target, Phys. Rev. Lett. **124**, no.12, 121801 (2020)
- [68] E. Valencia *et al.* (MINER $\nu$ A), Constraint of the MINER $\nu$ A medium energy neutrino flux using neutrino-electron elastic scattering, Phys. Rev. D **100**, no.9, 092001 (2019)

## Supplemental Material

## Background scale factors

Material	Incoherent backgrounds					Plastic scintillator backgrounds			
	$\alpha_{QE}$	$\alpha_{RES}$	$\alpha_{INE}$	$\alpha_{DIS}$	$\chi^2/ndf$	$\alpha_{US}$	$\chi^2/ndf$	$\alpha_{DS}$	$\chi^2/ndf$
CH	$1.22 \pm 0.02$	$1.29 \pm 0.04$	$0.60 \pm 0.02$	$0.65 \pm 0.03$	281/30	—	—	—	—
C	$1.22 \pm 0.02$	$1.17 \pm 0.05$	$1.17 \pm 0.05$	$0.65 \pm 0.03$	105/30	$1.14 \pm 0.01$	10/4	$1.10 \pm 0.008$	57/5
Fe	$1.40 \pm 0.07$	$1.15 \pm 0.09$	$0.58 \pm 0.06$	$1.08 \pm 0.14$	89/30	$1.16 \pm 0.008$	36/8	$1.18 \pm 0.004$	153/19
Pb	$1.09 \pm 0.05$	$0.66 \pm 0.07$	$0.50 \pm 0.05$	$0.98 \pm 0.14$	119/30	$1.16 \pm 0.005$	90/13	$1.16 \pm 0.006$	75/19

TABLE I. Background scale factors: Quasi-Elastic ( $\alpha_{QE}$ ), Resonance ( $\alpha_{RES}$ ), Inelastic ( $\alpha_{INE}$ ), DIS ( $\alpha_{DIS}$ ), Upstream ( $\alpha_{US}$ ) and Downstream ( $\alpha_{DS}$ ) plastic.

$d\sigma/dQ^2$ ,  $d\sigma/d\theta_\mu$  and  $d\sigma/dE_\mu$  cross sections in CH, C, Fe and Pb

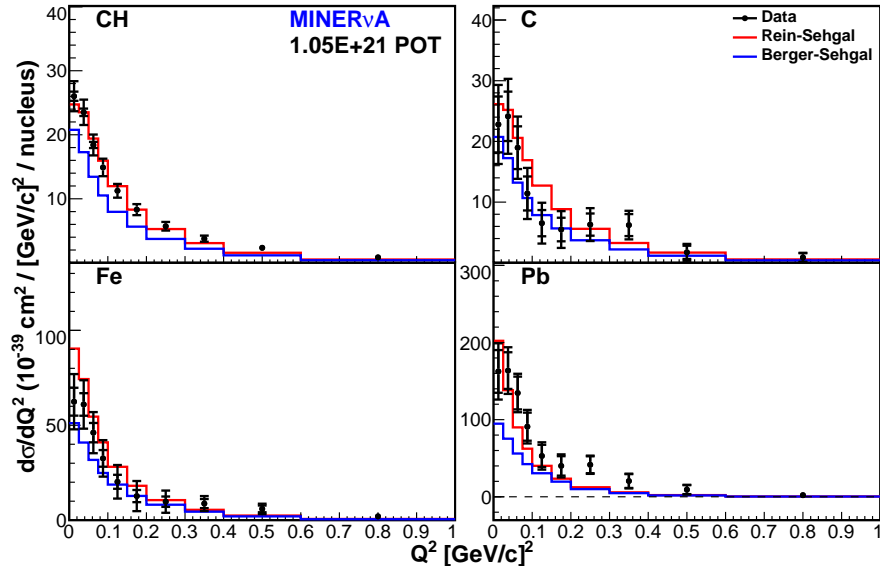


FIG. 7. Differential cross sections as function of  $Q^2$ : CH, C, Fe, and Pb, in reading order. Data is compared to the R-S (red) and B-S (blue) models.

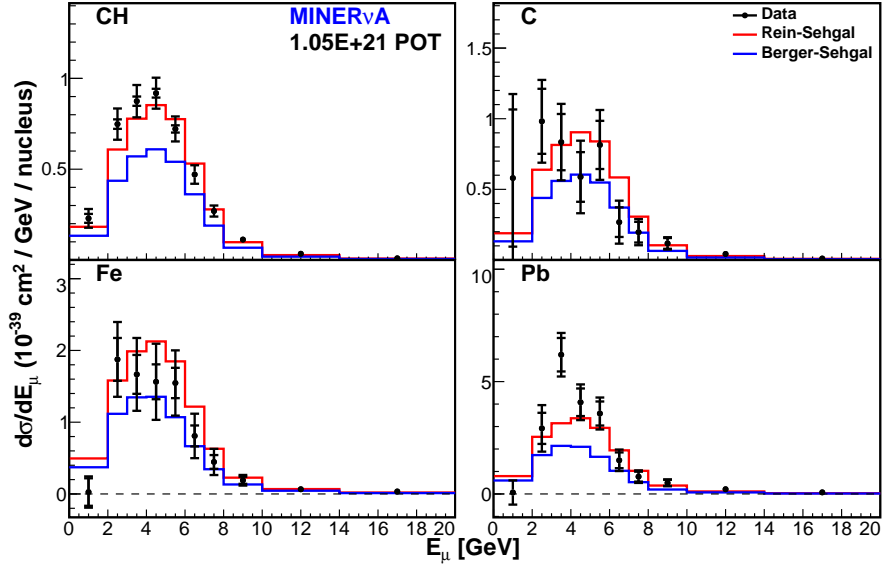


FIG. 8. Differential cross sections as function of  $E_\mu$ : CH, C, Fe, and Pb, in reading order. Data is compared to the R-S (red) and B-S (blue) models.

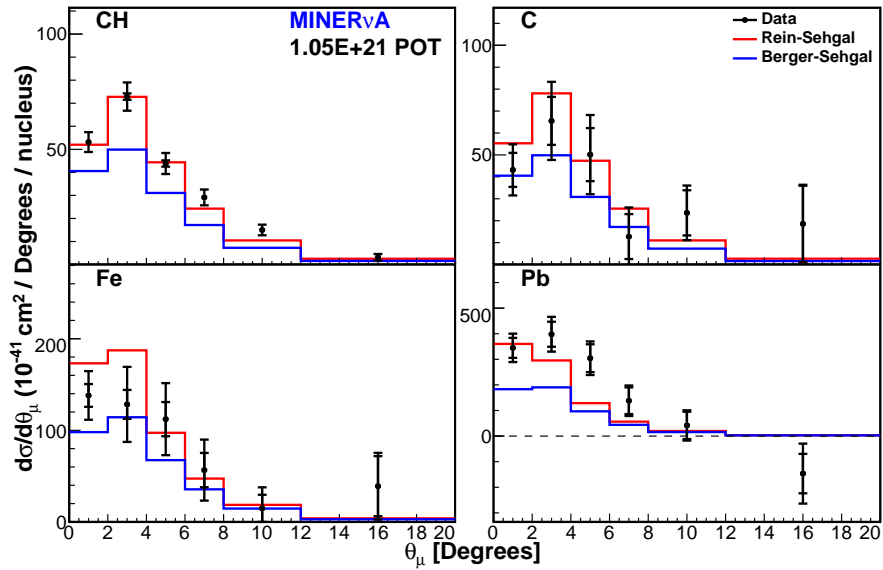


FIG. 9. Differential cross sections as function of  $\theta_\mu$ : CH, C, Fe, and Pb, in reading order. Data is compared to the R-S (red) and B-S (blue) models.

Cross section ratios of C, Fe and Pb relative to CH, as a function of  $E_\pi$ ,  $\theta_\pi$ ,  $Q^2$ ,  $E_\mu$ , and  $\theta_\mu$

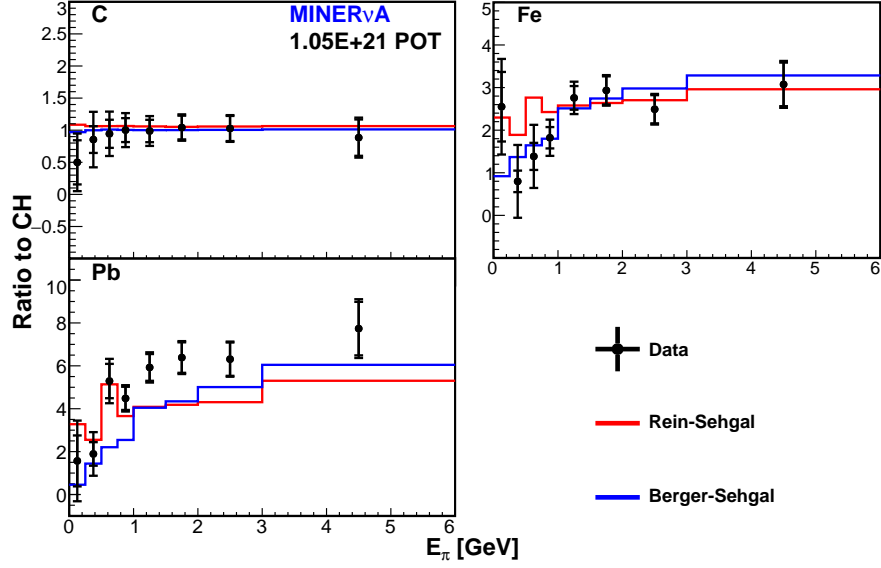


FIG. 10. Ratios of the differential cross section as a function of  $E_\pi$ . C, Fe and Pb with respect to CH, in reading order. Data is compared to the Rein-Sehgal (red) and Berger-Sehgal (blue) models.

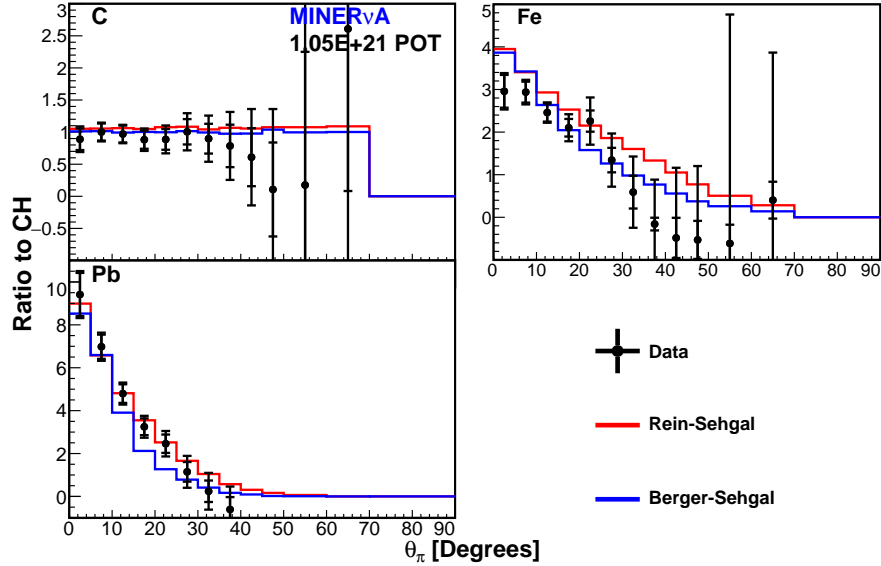


FIG. 11. Ratios of the differential cross section as a function of  $\theta_\pi$ . C, Fe and Pb with respect to CH, in reading order. Data is compared to the Rein-Sehgal (red) and Berger-Sehgal (blue) models.

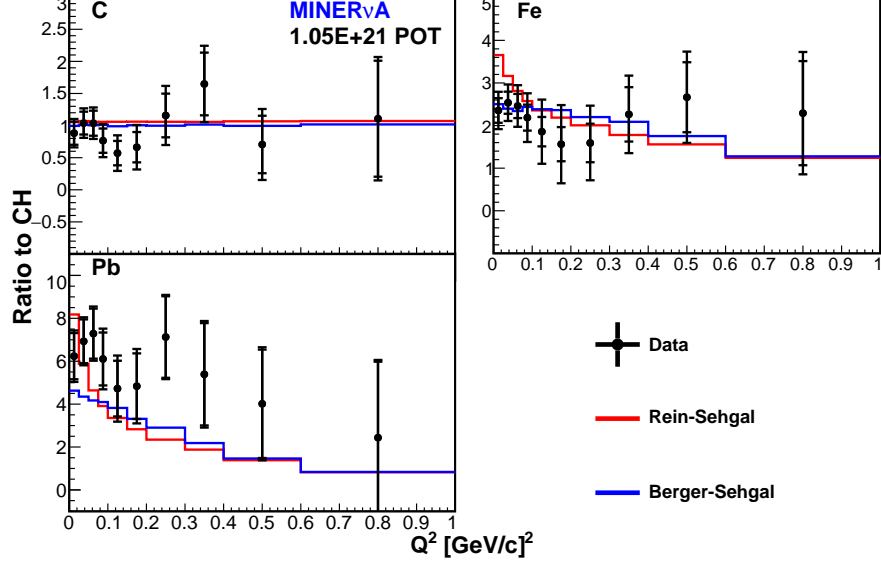


FIG. 12. Ratios of the differential cross section as a function of  $Q^2$ . C, Fe and Pb with respect to CH, in reading order. Data is compared to the Rein-Sehgal (red) and Berger-Sehgal (blue) models.

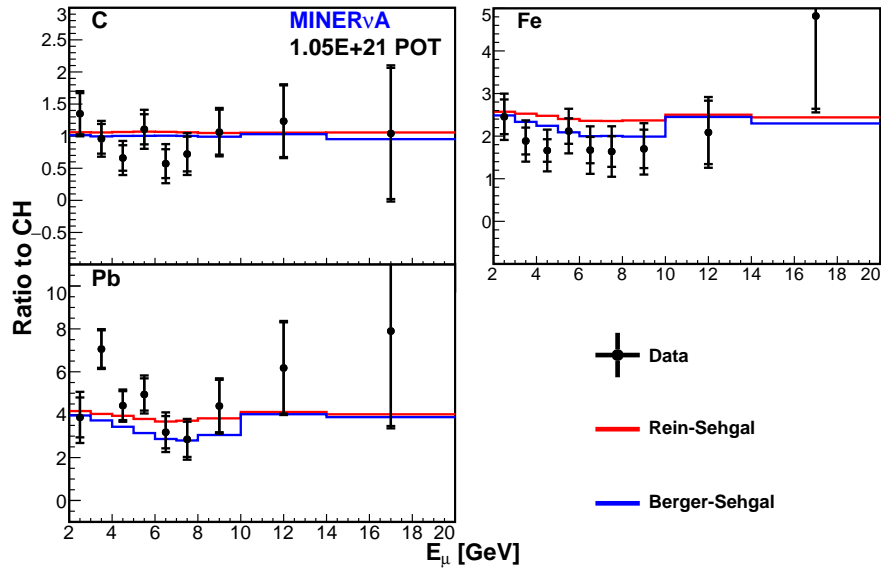


FIG. 13. Ratios of the differential cross section as a function of  $E_\mu$ . C, Fe and Pb with respect to CH, in reading order. Data is compared to the Rein-Sehgal (red) and Berger-Sehgal (blue) models.

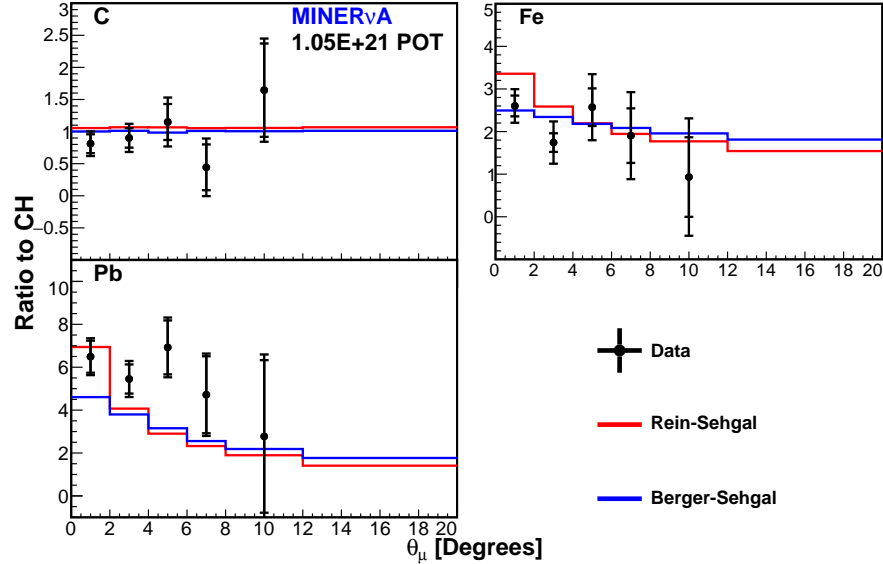


FIG. 14. Ratios of the differential cross section as a function of  $\theta_\mu$ . C, Fe and Pb with respect to CH, in reading order. Data is compared to the Rein-Sehgal (red) and Berger-Sehgal (blue) models.

### Cross section tables

TABLE II. Measured cross section as a function of  $E_\nu$  on CH, in units of  $10^{-39} \text{ cm}^2/\text{GeV}/{}^{12}\text{CH}$ , and the absolute and fractional cross section uncertainties.

Bin edges (GeV)	$\sigma$	Abs. Stat. Unc.	Abs. Tot. Unc.	Frac. Stat. Unc.	Frac. Tot. Unc.
2.0 - 3.0	2.377	0.254	0.586	0.107	0.246
3.0 - 4.0	3.317	0.144	0.486	0.043	0.147
4.0 - 5.0	4.183	0.127	0.504	0.030	0.120
5.0 - 6.0	4.661	0.114	0.478	0.024	0.103
6.0 - 7.0	4.888	0.112	0.452	0.023	0.092
7.0 - 8.0	5.512	0.137	0.534	0.025	0.097
8.0 - 10.0	6.836	0.209	0.785	0.031	0.115
10.0 - 14.0	10.097	0.482	1.177	0.048	0.117
14.0 - 20.0	12.147	1.064	1.836	0.088	0.151

TABLE III. Statistical covariance matrix of the measured  $\sigma(E_\nu)$  on CH, in units of  $10^{-78} (\text{cm}^2/\text{GeV}/\text{CH})^2$ .

Bin edges (GeV)	2.0 - 3.0	3.0 - 4.0	4.0 - 5.0	5.0 - 6.0	6.0 - 7.0	7.0 - 8.0	8.0 - 10.0	10.0 - 14.0	14.0 - 20.0
2.0 - 3.0	0.0644	0.0020	-0.0020	-0.0005	-0.0001	-0.0001	-0.0001	-0.0001	-0.0001
3.0 - 4.0	0.0020	0.0206	0.0020	-0.0014	-0.0006	-0.0002	-0.0001	-0.0001	-0.0001
4.0 - 5.0	-0.0020	0.0020	0.0163	0.0031	-0.0016	-0.0012	-0.0006	-0.0002	-0.0002
5.0 - 6.0	-0.0005	-0.0014	0.0031	0.0130	0.0041	-0.0016	-0.0021	-0.0010	-0.0003
6.0 - 7.0	-0.0001	-0.0006	-0.0016	0.0041	0.0126	0.0071	-0.0019	-0.0037	-0.0012
7.0 - 8.0	-0.0001	-0.0002	-0.0012	-0.0016	0.0071	0.0187	0.0123	-0.0061	-0.0051
8.0 - 10.0	-0.0001	-0.0001	-0.0006	-0.0021	-0.0019	0.0123	0.0436	0.0211	-0.0159
10.0 - 14.0	-0.0001	-0.0001	-0.0002	-0.0010	-0.0037	-0.0061	0.0211	0.2323	0.0425
14.0 - 20.0	-0.0001	-0.0001	-0.0002	-0.0003	-0.0012	-0.0051	-0.0159	0.0425	1.1320

TABLE IV. Systematic covariance matrix of the measured  $\sigma(E_\nu)$  on CH, in units of  $10^{-78} (\text{cm}^2/\text{GeV}/\text{CH})^2$ .

Bin edges (GeV)	2.0 - 3.0	3.0 - 4.0	4.0 - 5.0	5.0 - 6.0	6.0 - 7.0	7.0 - 8.0	8.0 - 10.0	10.0 - 14.0	14.0 - 20.0
2.0 - 3.0	0.2790	0.2301	0.2266	0.1924	0.1171	0.0043	-0.1085	-0.1252	0.1389
3.0 - 4.0	0.2301	0.2160	0.2209	0.1998	0.1455	0.0598	-0.0266	-0.0267	0.2827
4.0 - 5.0	0.2266	0.2209	0.2374	0.2200	0.1673	0.0824	-0.0027	0.0159	0.3826
5.0 - 6.0	0.1924	0.1998	0.2200	0.2158	0.1828	0.1236	0.0625	0.0847	0.4231
6.0 - 7.0	0.1171	0.1455	0.1673	0.1828	0.1913	0.1871	0.1828	0.2154	0.4366
7.0 - 8.0	0.0043	0.0598	0.0824	0.1236	0.1871	0.2667	0.3574	0.4281	0.4455
8.0 - 10.0	-0.1085	-0.0266	-0.0027	0.0625	0.1828	0.3574	0.5728	0.7394	0.5060
10.0 - 14.0	-0.1252	-0.0267	0.0159	0.0847	0.2154	0.4281	0.7394	1.1522	0.9222
14.0 - 20.0	0.1389	0.2827	0.3826	0.4231	0.4366	0.4455	0.5060	0.9222	2.2386

TABLE V. Measured cross section as a function of  $E_\nu$  on C, in units of  $10^{-39} \text{ cm}^2/\text{GeV}/{}^{12}\text{C}$ , and the absolute and fractional cross section uncertainties.

Bin edges (GeV)	$\sigma$	Abs. Stat. Unc.	Abs. Tot. Unc.	Frac. Stat. Unc.	Frac. Tot. Unc.
2.0 - 3.0	2.764	2.219	2.863	0.803	1.036
3.0 - 4.0	3.712	1.252	1.687	0.337	0.454
4.0 - 5.0	5.088	1.120	1.685	0.220	0.331
5.0 - 6.0	3.236	0.896	1.336	0.277	0.413
6.0 - 7.0	2.848	0.835	1.297	0.293	0.455
7.0 - 8.0	5.287	1.189	1.537	0.225	0.291
8.0 - 10.0	6.614	1.644	2.114	0.249	0.320
10.0 - 14.0	13.743	4.093	4.476	0.298	0.326
14.0 - 20.0	6.877	6.947	7.366	1.010	1.071

TABLE VI. Statistical covariance matrix of the measured  $\sigma(E_\nu)$  on C, in units of  $10^{-78}$  ( $\text{cm}^2/\text{GeV}/\text{C}$ ) $^2$ .  
 Bin edges (GeV) || 2.0 - 3.0 3.0 - 4.0 4.0 - 5.0 5.0 - 6.0 6.0 - 7.0 7.0 - 8.0 8.0 - 10.0 10.0 - 14.0 14.0 - 20.0

2.0 - 3.0	4.9248	0.1154	-0.1384	-0.0182	-0.0012	-0.0035	0.0010	-0.0031	-0.0023
3.0 - 4.0	0.1154	1.5675	0.0466	-0.0840	-0.0237	-0.0049	-0.0049	-0.0056	0.0007
4.0 - 5.0	-0.1384	0.0466	1.2547	0.1217	-0.0881	-0.0675	-0.0227	-0.0139	-0.0034
5.0 - 6.0	-0.0182	-0.0840	0.1217	0.8025	0.2216	-0.1081	-0.0935	-0.0354	-0.0106
6.0 - 7.0	-0.0012	-0.0237	-0.0881	0.2216	0.6965	0.3806	-0.1354	-0.1647	-0.0150
7.0 - 8.0	-0.0035	-0.0049	-0.0675	-0.1081	0.3806	1.4138	0.5926	-0.5660	-0.1693
8.0 - 10.0	0.0010	-0.0049	-0.0227	-0.0935	-0.1354	0.5926	2.7026	0.7314	-0.5316
10.0 - 14.0	-0.0031	-0.0056	-0.0139	-0.0354	-0.1647	-0.5660	0.7314	16.7528	1.5120
14.0 - 20.0	-0.0023	0.0007	-0.0034	-0.0106	-0.0150	-0.1693	-0.5316	1.5120	48.2633

TABLE VII. Systematic covariance matrix of the measured  $\sigma(E_\nu)$  on C, in units of  $10^{-78}$  ( $\text{cm}^2/\text{GeV}/\text{C}$ ) $^2$ .  
 Bin edges (GeV) || 2.0 - 3.0 3.0 - 4.0 4.0 - 5.0 5.0 - 6.0 6.0 - 7.0 7.0 - 8.0 8.0 - 10.0 10.0 - 14.0 14.0 - 20.0

2.0 - 3.0	3.2724	1.7230	1.8016	0.9754	0.9961	0.7259	-0.9863	-0.5744	0.7490
3.0 - 4.0	1.7230	1.2776	1.3792	0.9590	0.9541	0.7800	-0.1119	0.1359	1.3682
4.0 - 5.0	1.8016	1.3792	1.5859	1.1263	1.1064	0.9143	-0.0131	0.3331	1.7378
5.0 - 6.0	0.9754	0.9590	1.1263	0.9813	0.9464	0.8497	0.4505	0.6405	1.8201
6.0 - 7.0	0.9961	0.9541	1.1064	0.9464	0.9860	0.9121	0.4968	0.6462	1.6526
7.0 - 8.0	0.7259	0.7800	0.9143	0.8497	0.9121	0.9484	0.7463	0.9362	1.5766
8.0 - 10.0	-0.9863	-0.1119	-0.0131	0.4505	0.4968	0.7463	1.7679	1.9288	1.7080
10.0 - 14.0	-0.5744	0.1359	0.3331	0.6405	0.6462	0.9362	1.9288	3.2803	2.6492
14.0 - 20.0	0.7490	1.3682	1.7378	1.8201	1.6526	1.5766	1.7080	2.6492	5.9903

TABLE VIII. Measured cross section as a function of  $E_\nu$  on Fe, in units of  $10^{-39}$   $\text{cm}^2/\text{GeV}/{}^{56}\text{Fe}$ , and the absolute and fractional cross section uncertainties.

Bin edges (GeV)	$\sigma$	Abs. Stat. Unc.	Abs. Tot. Unc.	Frac. Stat. Unc.	Frac. Tot. Unc.
2.0 - 3.0	3.645	2.600	4.099	0.713	1.125
3.0 - 4.0	7.275	1.651	3.116	0.227	0.428
4.0 - 5.0	6.119	1.305	2.862	0.213	0.468
5.0 - 6.0	7.976	1.178	2.914	0.148	0.365
6.0 - 7.0	9.672	1.211	2.726	0.125	0.282
7.0 - 8.0	11.415	1.424	2.895	0.125	0.254
8.0 - 10.0	15.748	2.205	3.734	0.140	0.237
10.0 - 14.0	24.823	5.127	6.448	0.207	0.260
14.0 - 20.0	29.653	11.370	13.041	0.383	0.440

TABLE IX. Statistical covariance matrix of the measured  $\sigma(E_\nu)$  on Fe, in units of  $10^{-78}$  ( $\text{cm}^2/\text{GeV}/\text{Fe}$ ) $^2$ .  
 Bin edges (GeV) || 2.0 - 3.0 3.0 - 4.0 4.0 - 5.0 5.0 - 6.0 6.0 - 7.0 7.0 - 8.0 8.0 - 10.0 10.0 - 14.0 14.0 - 20.0

2.0 - 3.0	6.7618	0.2772	-0.1783	-0.0454	-0.0060	-0.0041	-0.0047	-0.0097	-0.0004
3.0 - 4.0	0.2772	2.7247	0.1849	-0.1708	-0.0691	-0.0199	-0.0121	-0.0162	-0.0188
4.0 - 5.0	-0.1783	0.1849	1.7034	0.3364	-0.1621	-0.1079	-0.0466	-0.0211	-0.0227
5.0 - 6.0	-0.0454	-0.1708	0.3364	1.3873	0.4109	-0.1928	-0.2062	-0.0926	-0.0349
6.0 - 7.0	-0.0060	-0.0691	-0.1621	0.4109	1.4674	0.7105	-0.2779	-0.3884	-0.1054
7.0 - 8.0	-0.0041	-0.0199	-0.1079	-0.1928	0.7105	2.0276	1.1923	-0.7401	-0.4978
8.0 - 10.0	-0.0047	-0.0121	-0.0466	-0.2062	-0.2779	1.1923	4.8623	2.0433	-1.7170
10.0 - 14.0	-0.0097	-0.0162	-0.0211	-0.0926	-0.3884	-0.7401	2.0433	26.2871	3.7779
14.0 - 20.0	-0.0004	-0.0188	-0.0227	-0.0349	-0.1054	-0.4978	-1.7170	3.7779	129.2868

TABLE X. Systematic covariance matrix of the measured  $\sigma(E_\nu)$  on Fe, in units of  $10^{-78}$  ( $\text{cm}^2/\text{GeV}/\text{Fe}$ ) $^2$ .  
 Bin edges (GeV) || 2.0 - 3.0 3.0 - 4.0 4.0 - 5.0 5.0 - 6.0 6.0 - 7.0 7.0 - 8.0 8.0 - 10.0 10.0 - 14.0 14.0 - 20.0

2.0 - 3.0	10.0401	7.5886	6.5583	6.5540	4.1295	2.1339	0.2314	1.3701	4.8032
3.0 - 4.0	7.5886	6.9875	6.4540	6.6337	5.0889	3.7535	2.4344	3.5779	8.9142
4.0 - 5.0	6.5583	6.4540	6.4872	6.7361	5.6069	4.5848	3.6393	4.8048	10.8173
5.0 - 6.0	6.5540	6.6337	6.7361	7.1030	6.0831	5.1319	4.2520	5.4613	11.9276
6.0 - 7.0	4.1295	5.0889	5.6069	6.0831	5.9642	5.7731	5.6431	6.5948	12.3660
7.0 - 8.0	2.1339	3.7535	4.5848	5.1319	5.7731	6.3506	7.0722	7.9518	12.3611
8.0 - 10.0	0.2314	2.4344	3.6393	4.2520	5.6431	7.0722	9.0818	10.6140	12.8714
10.0 - 14.0	1.3701	3.5779	4.8048	5.4613	6.5948	7.9518	10.6140	15.2864	18.2801
14.0 - 20.0	4.8032	8.9142	10.8173	11.9276	12.3660	12.3611	12.8714	18.2801	40.7697

TABLE XI. Measured cross section as a function of  $E_\nu$  on Pb, in units of  $10^{-39}$   $\text{cm}^2/\text{GeV}/{}^{207}\text{Pb}$ , and the absolute and fractional cross section uncertainties.

Bin edges (GeV)	$\sigma$	Abs. Stat. Unc.	Abs. Tot. Unc.	Frac. Stat. Unc.	Frac. Tot. Unc.
2.0 - 3.0	-2.085	4.016	5.184	-1.926	-2.487
3.0 - 4.0	13.667	3.134	4.579	0.229	0.335
4.0 - 5.0	19.545	2.777	4.373	0.142	0.224
5.0 - 6.0	23.350	2.609	4.031	0.112	0.173
6.0 - 7.0	24.214	2.670	3.819	0.110	0.158
7.0 - 8.0	25.476	3.191	4.425	0.125	0.174
8.0 - 10.0	33.061	4.730	6.124	0.143	0.185
10.0 - 14.0	63.446	11.662	13.263	0.184	0.209
14.0 - 20.0	82.615	28.103	29.643	0.340	0.359

TABLE XII. Statistical covariance matrix of the measured  $\sigma(E_\nu)$  on Pb, in units of  $10^{-78}$  ( $\text{cm}^2/\text{GeV}/\text{Pb}$ ) $^2$ .

Bin edges (GeV)	2.0 - 3.0	3.0 - 4.0	4.0 - 5.0	5.0 - 6.0	6.0 - 7.0	7.0 - 8.0	8.0 - 10.0	10.0 - 14.0	14.0 - 20.0
2.0 - 3.0	16.1250	3.2152	0.4663	0.0804	0.0356	0.0142	0.0150	0.0006	0.0251
3.0 - 4.0	3.2152	9.8220	3.0035	0.5524	0.1496	0.0768	0.0431	0.0582	0.1578
4.0 - 5.0	0.4663	3.0035	7.7132	3.3863	0.8484	0.2482	0.1378	0.1873	0.1200
5.0 - 6.0	0.0804	0.5524	3.3863	6.8069	3.7850	1.3710	0.5196	0.2818	0.1661
6.0 - 7.0	0.0356	0.1496	0.8484	3.7850	7.1306	5.1985	2.3620	1.0254	0.5773
7.0 - 8.0	0.0142	0.0768	0.2482	1.3710	5.1985	10.1811	9.3051	4.2276	0.9908
8.0 - 10.0	0.0150	0.0431	0.1378	0.5196	2.3620	9.3051	22.3683	24.5201	8.7950
10.0 - 14.0	0.0006	0.0582	0.1873	0.2818	1.0254	4.2276	24.5201	136.0103	107.0414
14.0 - 20.0	0.0251	0.1578	0.1200	0.1661	0.5773	0.9908	8.7950	107.0414	789.7512

TABLE XIII. Systematic covariance matrix of the measured  $\sigma(E_\nu)$  on Pb, in units of  $10^{-78}$  ( $\text{cm}^2/\text{GeV}/\text{Pb}$ ) $^2$ .

Bin edges (GeV)	2.0 - 3.0	3.0 - 4.0	4.0 - 5.0	5.0 - 6.0	6.0 - 7.0	7.0 - 8.0	8.0 - 10.0	10.0 - 14.0	14.0 - 20.0
2.0 - 3.0	10.7501	10.2017	9.4881	7.6136	4.6177	1.5630	-0.6901	-1.1925	2.2098
3.0 - 4.0	10.2017	11.1466	10.9766	9.1403	5.5968	1.9597	-0.7532	-0.4484	5.2480
4.0 - 5.0	9.4881	10.9766	11.4078	9.9918	6.7780	3.4311	0.8750	2.1669	9.8261
5.0 - 6.0	7.6136	9.1403	9.9918	9.4440	7.3828	5.1562	3.4300	5.5130	13.2359
6.0 - 7.0	4.6177	5.5968	6.7780	7.3828	7.4514	7.2947	7.1126	10.0302	15.8811
7.0 - 8.0	1.5630	1.9597	3.4311	5.1562	7.2947	9.3996	11.1009	15.2224	18.2495
8.0 - 10.0	-0.6901	-0.7532	0.8750	3.4300	7.1126	11.1009	15.1331	22.2243	22.8958
10.0 - 14.0	-1.1925	-0.4484	2.1669	5.5130	10.0302	15.2224	22.2243	39.9002	45.8082
14.0 - 20.0	2.2098	5.2480	9.8261	13.2359	15.8811	18.2495	22.8958	45.8082	88.9614

TABLE XIV. Measured cross section as a function of  $E_\pi$  on CH, in units of  $10^{-39} \text{ cm}^2/\text{GeV}/{}^{12}\text{CH}$ , and the absolute and fractional cross section uncertainties.

Bin edges (GeV)	$d\sigma/dE_\pi$	Abs.	Stat.	Unc.	Abs.	Tot.	Unc.	Frac.	Stat.	Unc.	Frac.	Tot.	Unc.
0 - 0.25	0.708		0.053		0.278		0.074		0.392				
0.25 - 0.5	3.440		0.107		0.563		0.031		0.164				
0.5 - 0.75	1.725		0.063		0.235		0.037		0.136				
0.75 - 1.0	1.974		0.055		0.197		0.028		0.100				
1.0 - 1.5	1.629		0.043		0.168		0.026		0.103				
1.5 - 2.0	1.246		0.035		0.137		0.028		0.110				
2.0 - 3.0	0.880		0.026		0.086		0.030		0.098				
3.0 - 6.0	0.299		0.012		0.041		0.040		0.137				

TABLE XV. Statistical covariance matrix of the measured  $d\sigma/dE_\pi$  on CH, in units of  $10^{-80} (\text{cm}^2/\text{GeV}/\text{CH})^2$ .

Bin edges (GeV)	0 - 0.25	0.25 - 0.5	0.5 - 0.75	0.75 - 1.0	1.0 - 1.5	1.5 - 2.0	2.0 - 3.0	3.0 - 6.0
0 - 0.25	0.2760	-0.0408	-0.0353	-0.0106	0.0010	0.0018	0.0005	0.0000
0.25 - 0.5	-0.0408	1.1345	0.0136	-0.0975	-0.0497	-0.0050	0.0030	0.0006
0.5 - 0.75	-0.0353	0.0136	0.4026	0.1914	-0.0234	-0.0415	-0.0085	0.0008
0.75 - 1.0	-0.0106	-0.0975	0.1914	0.3024	0.1234	-0.0285	-0.0261	-0.0008
1.0 - 1.5	0.0010	-0.0497	-0.0234	0.1234	0.1823	0.0665	-0.0158	-0.0056
1.5 - 2.0	0.0018	-0.0050	-0.0415	-0.0285	0.0665	0.1259	0.0451	-0.0097
2.0 - 3.0	0.0005	0.0030	-0.0085	-0.0261	-0.0158	0.0451	0.0685	0.0037
3.0 - 6.0	0.0000	0.0006	0.0008	-0.0008	-0.0056	-0.0097	0.0037	0.0140

TABLE XVI. Systematic covariance matrix of the measured  $d\sigma/dE_\pi$  on CH, in units of  $10^{-80} (\text{cm}^2/\text{GeV}/\text{CH})^2$ .

Bin edges (GeV)	0 - 0.25	0.25 - 0.5	0.5 - 0.75	0.75 - 1.0	1.0 - 1.5	1.5 - 2.0	2.0 - 3.0	3.0 - 6.0
0 - 0.25	7.4352	6.6553	-2.1796	0.0648	1.7209	1.7141	0.3655	-0.6048
0.25 - 0.5	6.6553	30.5695	5.9236	3.6695	2.3474	1.7564	1.0188	0.0588
0.5 - 0.75	-2.1796	5.9236	5.1158	3.3984	1.3836	0.6822	0.9287	0.6777
0.75 - 1.0	0.0648	3.6695	3.3984	3.5701	2.6030	1.8554	1.3722	0.5266
1.0 - 1.5	1.7209	2.3474	1.3836	2.6030	2.6241	2.0963	1.2584	0.2569
1.5 - 2.0	1.7141	1.7564	0.6822	1.8554	2.0963	1.7386	0.9981	0.1575
2.0 - 3.0	0.3655	1.0188	0.9287	1.3722	1.2584	0.9981	0.6778	0.2097
3.0 - 6.0	-0.6048	0.0588	0.6777	0.5266	0.2569	0.1575	0.2097	0.1529

TABLE XVII. Measured cross section as a function of  $E_\pi$  on C, in units of  $10^{-39} \text{ cm}^2/\text{GeV}/{}^{12}\text{C}$ , and the absolute and fractional cross section uncertainties.

Bin edges (GeV)	$d\sigma/dE_\pi$	Abs.	Stat.	Unc.	Abs.	Tot.	Unc.	Frac.	Stat.	Unc.	Frac.	Tot.	Unc.
0 - 0.25	0.308		0.210		0.350		0.682		1.135				
0.25 - 0.5	2.893		0.698		1.682		0.241		0.581				
0.5 - 0.75	1.636		0.373		0.649		0.228		0.397				
0.75 - 1.0	1.929		0.353		0.570		0.183		0.295				
1.0 - 1.5	1.587		0.276		0.413		0.174		0.260				
1.5 - 2.0	1.334		0.233		0.287		0.174		0.215				
2.0 - 3.0	0.913		0.171		0.192		0.188		0.210				
3.0 - 6.0	0.251		0.080		0.100		0.317		0.399				

TABLE XVIII. Statistical covariance matrix of the measured  $d\sigma/dE_\pi$  on C, in units of  $10^{-80} (\text{cm}^2/\text{GeV}/\text{C})^2$ .

Bin edges (GeV)	0 - 0.25	0.25 - 0.5	0.5 - 0.75	0.75 - 1.0	1.0 - 1.5	1.5 - 2.0	2.0 - 3.0	3.0 - 6.0
0 - 0.25	4.4170	5.7037	-0.7952	-0.6720	-0.2486	-0.0324	0.0016	-0.0007
0.25 - 0.5	5.7037	48.6925	5.3324	-1.6066	-2.1061	-0.8416	-0.1604	-0.0071
0.5 - 0.75	-0.7952	5.3324	13.9190	8.5817	0.9126	-1.1168	-0.4201	-0.0343
0.75 - 1.0	-0.6720	-1.6066	8.5817	12.4958	6.3305	-0.1191	-0.7724	-0.0890
1.0 - 1.5	-0.2486	-2.1061	0.9126	6.3305	7.6198	3.1542	-0.2496	-0.1697
1.5 - 2.0	-0.0324	-0.8416	-1.1168	-0.1191	3.1542	5.4208	2.1045	-0.2151
2.0 - 3.0	0.0016	-0.1604	-0.4201	-0.7724	-0.2496	2.1045	2.9358	0.3287
3.0 - 6.0	-0.0007	-0.0071	-0.0343	-0.0890	-0.1697	-0.2151	0.3287	0.6341

TABLE XIX. Systematic covariance matrix of the measured  $d\sigma/dE_\pi$  on C, in units of  $10^{-80}$  ( $\text{cm}^2/\text{GeV}/\text{C}$ ) $^2$ .

Bin edges (GeV)	0 - 0.25	0.25 - 0.5	0.5 - 0.75	0.75 - 1.0	1.0 - 1.5	1.5 - 2.0	2.0 - 3.0	3.0 - 6.0
0 - 0.25	7.8336	37.0751	6.0245	2.0742	1.0786	0.6509	-0.8443	-1.0527
0.25 - 0.5	37.0751	234.2113	60.8254	33.8527	16.9079	6.5851	-2.7988	-4.4001
0.5 - 0.75	6.0245	60.8254	28.1731	21.6607	12.0346	4.7428	0.9579	-0.2510
0.75 - 1.0	2.0742	33.8527	21.6607	20.0101	12.8231	5.8221	1.5520	-0.0197
1.0 - 1.5	1.0786	16.9079	12.0346	12.8231	9.4153	4.8126	1.0894	-0.2466
1.5 - 2.0	0.6509	6.5851	4.7428	5.8221	4.8126	2.8133	0.7237	-0.1653
2.0 - 3.0	-0.8443	-2.7988	0.9579	1.5520	1.0894	0.7237	0.7465	0.3833
3.0 - 6.0	-1.0527	-4.4001	-0.2510	-0.0197	-0.2466	-0.1653	0.3833	0.3703

TABLE XX. Measured cross section as a function of  $E_\pi$  on Fe, in units of  $10^{-39}$   $\text{cm}^2/\text{GeV}/^{56}\text{Fe}$ , and the absolute and fractional cross section uncertainties.

Bin edges (GeV)	$d\sigma/dE_\pi$	Abs.	Stat.	Unc.	Abs.	Tot.	Unc.	Frac.	Stat.	Unc.	Frac.	Tot.	Unc.
0 - 0.25	1.984	0.613			1.262			0.309			0.636		
0.25 - 0.5	2.804	0.880			3.226			0.314			1.150		
0.5 - 0.75	2.318	0.521			1.419			0.225			0.612		
0.75 - 1.0	3.641	0.482			0.978			0.132			0.269		
1.0 - 1.5	4.654	0.441			0.856			0.095			0.184		
1.5 - 2.0	3.695	0.391			0.509			0.106			0.138		
2.0 - 3.0	2.176	0.275			0.327			0.126			0.150		
3.0 - 6.0	0.986	0.156			0.216			0.158			0.219		

TABLE XXI. Statistical covariance matrix of the measured  $d\sigma/dE_\pi$  on Fe, in units of  $10^{-80}$  ( $\text{cm}^2/\text{GeV}/\text{Fe}$ ) $^2$ .

Bin edges (GeV)	0 - 0.25	0.25 - 0.5	0.5 - 0.75	0.75 - 1.0	1.0 - 1.5	1.5 - 2.0	2.0 - 3.0	3.0 - 6.0
0 - 0.25	37.5947	2.3571	-7.7105	-4.3877	-0.8628	0.4330	0.1895	0.0066
0.25 - 0.5	2.3571	77.4070	12.8532	-3.0434	-5.4244	-1.5835	0.0508	0.0642
0.5 - 0.75	-7.7105	12.8532	27.0992	15.7089	-0.5231	-3.5119	-0.7574	0.0805
0.75 - 1.0	-4.3877	-3.0434	15.7089	23.2364	11.3064	-3.7754	-2.3192	0.0062
1.0 - 1.5	-0.8628	-5.4244	-0.5231	11.3064	19.4475	6.2474	-2.1927	-0.6301
1.5 - 2.0	0.4330	-1.5835	-3.5119	-3.7754	6.2474	15.2930	5.3661	-1.3946
2.0 - 3.0	0.1895	0.0508	-0.7574	-2.3192	-2.1927	5.3661	7.5669	0.4711
3.0 - 6.0	0.0066	0.0642	0.0805	0.0062	-0.6301	-1.3946	0.4711	2.4289

TABLE XXII. Systematic covariance matrix of the measured  $d\sigma/dE_\pi$  on Fe, in units of  $10^{-80}$  ( $\text{cm}^2/\text{GeV}/\text{Fe}$ ) $^2$ .

Bin edges (GeV)	0 - 0.25	0.25 - 0.5	0.5 - 0.75	0.75 - 1.0	1.0 - 1.5	1.5 - 2.0	2.0 - 3.0	3.0 - 6.0
0 - 0.25	121.5712	123.3174	22.8534	49.7716	55.1985	14.8221	2.8513	-8.7838
0.25 - 0.5	123.3174	963.1823	379.7737	175.6837	40.7910	20.6318	25.5564	14.6491
0.5 - 0.75	22.8534	379.7737	174.1696	84.4061	20.1848	12.5757	13.3942	9.4542
0.75 - 1.0	49.7716	175.6837	84.4061	72.3703	49.3928	19.4188	9.2768	0.8456
1.0 - 1.5	55.1985	40.7910	20.1848	49.3928	53.7995	20.1270	6.1711	-3.1294
1.5 - 2.0	14.8221	20.6318	12.5757	19.4188	20.1270	10.6391	4.8107	0.9558
2.0 - 3.0	2.8513	25.5564	13.3942	9.2768	6.1711	4.8107	3.1322	1.6987
3.0 - 6.0	-8.7838	14.6491	9.4542	0.8456	-3.1294	0.9558	1.6987	2.2431

TABLE XXIII. Measured cross section as a function of  $E_\pi$  on Pb, in units of  $10^{-39}$   $\text{cm}^2/\text{GeV}/^{207}\text{Pb}$ , and the absolute and fractional cross section uncertainties.

Bin edges (GeV)	$d\sigma/dE_\pi$	Abs.	Stat.	Unc.	Abs.	Tot.	Unc.	Frac.	Stat.	Unc.	Frac.	Tot.	Unc.
0 - 0.25	1.111	0.839			1.522			0.755			1.370		
0.25 - 0.5	6.546	1.888			3.964			0.288			0.606		
0.5 - 0.75	9.105	1.334			2.026			0.147			0.223		
0.75 - 1.0	8.854	1.035			1.302			0.117			0.147		
1.0 - 1.5	9.703	0.988			1.346			0.102			0.139		
1.5 - 2.0	7.977	0.856			1.059			0.107			0.133		
2.0 - 3.0	5.517	0.657			0.746			0.119			0.135		
3.0 - 6.0	2.379	0.371			0.492			0.156			0.207		

TABLE XXIV. Statistical covariance matrix of the measured  $d\sigma/dE_\pi$  on Pb, in units of  $10^{-80}$  ( $\text{cm}^2/\text{GeV/Pb}$ ) $^2$ .

Bin edges (GeV)	0 - 0.25	0.25 - 0.5	0.5 - 0.75	0.75 - 1.0	1.0 - 1.5	1.5 - 2.0	2.0 - 3.0	3.0 - 6.0
0 - 0.25	70.3302	57.2517	-4.6570	-7.4049	-3.6718	-0.9772	-0.1680	-0.0341
0.25 - 0.5	57.2517	356.6308	91.8816	-8.8042	-21.3034	-9.6179	-2.4860	-0.2734
0.5 - 0.75	-4.6570	91.8816	177.9462	82.7665	5.7367	-14.9631	-5.4753	-0.5958
0.75 - 1.0	-7.4049	-8.8042	82.7665	107.2260	60.9311	-2.0950	-8.5282	-1.4282
1.0 - 1.5	-3.6718	-21.3034	5.7367	60.9311	97.6004	45.5293	-1.4870	-3.7291
1.5 - 2.0	-0.9772	-9.6179	-14.9631	-2.0950	45.5293	73.2230	29.1632	-3.6135
2.0 - 3.0	-0.1680	-2.4860	-5.4753	-8.5282	-1.4870	29.1632	43.1505	6.5841
3.0 - 6.0	-0.0341	-0.2734	-0.5958	-1.4282	-3.7291	-3.6135	6.5841	13.7705

TABLE XXV. Systematic covariance matrix of the measured  $d\sigma/dE_\pi$  on Pb, in units of  $10^{-80}$  ( $\text{cm}^2/\text{GeV/Pb}$ ) $^2$ .

Bin edges (GeV)	0 - 0.25	0.25 - 0.5	0.5 - 0.75	0.75 - 1.0	1.0 - 1.5	1.5 - 2.0	2.0 - 3.0	3.0 - 6.0
0 - 0.25	161.3889	274.5015	79.0755	57.1965	73.5423	44.9724	13.7603	-24.4509
0.25 - 0.5	274.5015	1214.8783	472.2045	143.9961	60.3931	32.5159	27.5435	-3.9565
0.5 - 0.75	79.0755	472.2045	232.4696	84.5246	34.1260	21.7769	23.5233	12.4378
0.75 - 1.0	57.1965	143.9961	84.5246	62.3161	60.4339	40.0911	22.1608	-1.4281
1.0 - 1.5	73.5423	60.3931	34.1260	60.4339	83.5409	55.5527	23.6323	-11.9043
1.5 - 2.0	44.9724	32.5159	21.7769	40.0911	55.5527	38.8312	18.4448	-5.2071
2.0 - 3.0	13.7603	27.5435	23.5233	22.1608	23.6323	18.4448	12.4749	3.1934
3.0 - 6.0	-24.4509	-3.9565	12.4378	-1.4281	-11.9043	-5.2071	3.1934	10.3920

TABLE XXVI. Measured cross section as a function of  $\theta_\pi$  on CH, in units of  $10^{-41}$   $\text{cm}^2/\text{Degrees}/^{12}\text{CH}$ , and the absolute and fractional cross section uncertainties.

Bin edges (Degrees)	$ d\sigma/d\theta_\pi $	Abs. Stat. Unc.	Abs. Tot. Unc.	Frac. Stat. Unc.	Frac. Tot. Unc.
0 - 5	15.847	0.388	1.695	0.024	0.107
5 - 10	24.663	0.430	2.273	0.017	0.092
10 - 15	19.800	0.342	1.693	0.017	0.086
15 - 20	14.322	0.275	1.244	0.019	0.087
20 - 25	9.965	0.235	0.897	0.024	0.090
25 - 30	6.918	0.179	0.680	0.026	0.098
30 - 35	4.723	0.148	0.552	0.031	0.117
35 - 40	2.997	0.128	0.476	0.043	0.159
40 - 45	1.872	0.112	0.354	0.060	0.189
45 - 50	0.997	0.099	0.326	0.100	0.327
50 - 60	0.341	0.084	0.318	0.247	0.932
60 - 70	-0.152	0.084	0.365	-0.553	-2.405

TABLE XXVII. Measured cross section as a function of  $\theta_\pi$  on C, in units of  $10^{-41}$   $\text{cm}^2/\text{Degrees}/^{12}\text{C}$ , and the absolute and fractional cross section uncertainties.

Bin edges (Degrees)	$ d\sigma/d\theta_\pi $	Abs. Stat. Unc.	Abs. Tot. Unc.	Frac. Stat. Unc.	Frac. Tot. Unc.
0 - 5	14.113	2.644	3.735	0.187	0.265
5 - 10	24.197	3.166	4.343	0.131	0.180
10 - 15	18.827	2.513	3.271	0.133	0.174
15 - 20	12.399	1.961	2.803	0.158	0.226
20 - 25	8.693	1.557	2.405	0.179	0.277
25 - 30	6.948	1.348	2.255	0.194	0.325
30 - 35	4.271	1.092	1.868	0.256	0.437
35 - 40	2.289	0.957	1.644	0.418	0.718
40 - 45	1.120	0.827	1.426	0.738	1.273
45 - 50	0.107	0.736	1.263	6.859	11.779
50 - 60	0.056	0.658	1.116	11.818	20.040
60 - 70	-0.635	0.562	0.851	-0.886	-1.339

TABLE XXVIII. Measured cross section as a function of  $\theta_\pi$  on Fe, in units of  $10^{-41} \text{ cm}^2/\text{Degrees}/{}^{56}\text{Fe}$ , and the absolute and fractional cross section uncertainties.

Bin edges (Degrees)	$d\sigma/d\theta_\pi$	Abs. Stat. Unc.	Abs. Tot. Unc.	Frac. Stat. Unc.	Frac. Tot. Unc.
0 - 5	47.141	5.930	7.924	0.126	0.168
5 - 10	74.730	6.020	9.424	0.081	0.126
10 - 15	50.799	4.233	6.204	0.083	0.122
15 - 20	31.157	2.965	5.762	0.095	0.185
20 - 25	23.392	2.500	6.476	0.107	0.277
25 - 30	9.536	2.017	4.787	0.212	0.502
30 - 35	2.794	1.815	4.108	0.650	1.470
35 - 40	-0.479	0.448	3.138	-0.934	-6.547
40 - 45	-0.905	0.880	2.991	-0.972	-3.304
45 - 50	-0.520	0.433	1.466	-0.832	-2.821
50 - 60	-0.208	0.132	0.474	-0.637	-2.280
60 - 70	-0.052	0.035	0.116	-0.673	-2.242

TABLE XXIX. Measured cross section as a function of  $\theta_\pi$  on Pb, in units of  $10^{-41} \text{ cm}^2/\text{Degrees}/{}^{207}\text{Pb}$ , and the absolute and fractional cross section uncertainties.

Bin edges (Degrees)	$d\sigma/d\theta_\pi$	Abs. Stat. Unc.	Abs. Tot. Unc.	Frac. Stat. Unc.	Frac. Tot. Unc.
0 - 5	149.597	15.574	20.378	0.104	0.136
5 - 10	174.018	13.720	18.445	0.079	0.106
10 - 15	95.970	8.498	11.789	0.089	0.123
15 - 20	46.906	5.578	8.244	0.119	0.176
20 - 25	24.608	4.248	6.437	0.173	0.262
25 - 30	7.935	3.163	5.315	0.399	0.670
30 - 35	1.138	2.361	4.080	2.075	3.586
35 - 40	-1.836	1.742	3.128	-0.949	-1.703
40 - 45	-2.219	1.129	2.043	-0.509	-0.921
45 - 50	-2.875	1.184	1.789	-0.412	-0.622
50 - 60	-1.287	0.685	0.859	-0.532	-0.667
60 - 70	0.000	0.000	0.000	—	—

Bin edges (Degrees)		0 - 5	5 - 10	10 - 15	15 - 20	20 - 25	25 - 30	30 - 35	35 - 40	40 - 45	45 - 50	50 - 60	60 - 70
0 - 5		0.15022	0.06762	0.01108	0.00271	0.00119	0.00061	0.00037	0.00023	0.00017	0.00012	0.00009	0.00006
5 - 10		0.06762	0.18463	0.05092	0.01023	0.00352	0.00167	0.00097	0.00060	0.00038	0.00024	0.00015	0.00008
10 - 15		0.01108	0.05092	0.11678	0.03526	0.00842	0.00302	0.00156	0.00094	0.00059	0.00038	0.00024	0.00012
15 - 20		0.00271	0.01023	0.03526	0.07563	0.02695	0.00641	0.00246	0.00136	0.00085	0.00056	0.00033	0.00017
20 - 25		0.00119	0.00352	0.00842	0.02695	0.05540	0.01816	0.00480	0.00203	0.00113	0.00073	0.00044	0.00022
25 - 30		0.00061	0.00167	0.00302	0.00641	0.01816	0.03206	0.01243	0.00372	0.00161	0.00095	0.00054	0.00028
30 - 35		0.00037	0.00097	0.00156	0.00246	0.00480	0.01243	0.02188	0.00964	0.00296	0.00127	0.00067	0.00033
35 - 40		0.00023	0.00060	0.00094	0.00136	0.00203	0.00372	0.00964	0.01626	0.00755	0.00241	0.00088	0.00039
40 - 45		0.00017	0.00038	0.00059	0.00085	0.00113	0.00161	0.00296	0.00755	0.01247	0.00617	0.00155	0.00050
45 - 50		0.00012	0.00024	0.00038	0.00056	0.00073	0.00095	0.00127	0.00241	0.00617	0.00090	0.00405	0.00087
50 - 60		0.00009	0.00015	0.00024	0.00033	0.00044	0.00054	0.00067	0.00088	0.00155	0.00405	0.00711	0.00253
60 - 70		0.00006	0.00008	0.00012	0.00017	0.00022	0.00028	0.00033	0.00039	0.00050	0.00087	0.00253	0.00703

TABLE XXXI. Systematic covariance matrix of the measured  $d\sigma/d\theta_\pi$  on CH, in units of  $10^{-82} (\text{cm}^2/\text{Degrees}/\text{CH})^2$ .

Bin edges (Degrees)	0 - 5	5 - 10	10 - 15	15 - 20	20 - 25	25 - 30	30 - 35	35 - 40	40 - 45	45 - 50	50 - 60	60 - 70
0 - 5	2.72379	3.64432	2.59066	1.71175	1.04589	0.68129	0.45271	0.35331	0.18791	0.11965	0.10532	0.19777
5 - 10	3.64432	4.98285	3.62489	2.45822	1.53001	0.99810	0.64144	0.46551	0.23676	0.13264	0.10081	0.20472
10 - 15	2.59066	3.62489	2.74969	1.95433	1.27232	0.85674	0.55764	0.39361	0.19909	0.10231	0.05973	0.12776
15 - 20	1.71175	2.45822	1.95433	1.47295	1.01639	0.71259	0.47978	0.33507	0.17657	0.08817	0.03451	0.06223
20 - 25	1.04589	1.53001	1.27232	1.01639	0.74909	0.55221	0.39722	0.28684	0.16337	0.08799	0.03185	0.03333
25 - 30	0.68129	0.99810	0.85674	0.71259	0.55221	0.42986	0.33101	0.25180	0.15462	0.09421	0.04326	0.03802
30 - 35	0.45271	0.64144	0.55764	0.47978	0.39722	0.33101	0.28272	0.23342	0.15472	0.10584	0.06055	0.05348
35 - 40	0.35331	0.46551	0.39361	0.33507	0.28684	0.25180	0.23342	0.21071	0.14610	0.11014	0.07672	0.07945
40 - 45	0.18791	0.23676	0.19909	0.17657	0.16337	0.15462	0.14610	0.11302	0.09637	0.07528	0.06780	
45 - 50	0.11965	0.13264	0.10231	0.08817	0.08799	0.09421	0.10584	0.11014	0.09637	0.09617	0.08786	0.08008
50 - 60	0.10532	0.10081	0.05973	0.03451	0.03185	0.04326	0.06055	0.07672	0.07528	0.08786	0.09406	0.09559
60 - 70	0.19777	0.20472	0.12776	0.06223	0.03333	0.03802	0.05348	0.07945	0.06780	0.08008	0.09559	0.12606

TABLE XXXII. Statistical covariance matrix of the measured  $d\sigma/d\theta_\pi$  on C, in units of  $10^{-82} (\text{cm}^2/\text{Degrees}/\text{C})^2$ .

Bin edges (Degrees)	0 - 5	5 - 10	10 - 15	15 - 20	20 - 25	25 - 30	30 - 35	35 - 40	40 - 45	45 - 50	50 - 60	60 - 70
0 - 5	6.98980	3.84301	0.677443	0.14305	0.08112	0.03548	0.02212	0.01966	0.01251	0.00793	0.00849	0.01550
5 - 10	3.84301	10.02638	3.10618	0.64788	0.25251	0.13271	0.07565	0.04025	0.02159	0.01995	0.02230	0.01501
10 - 15	0.67443	3.10618	6.31476	2.02052	0.53587	0.21131	0.12503	0.06753	0.04492	0.03438	0.02526	0.01268
15 - 20	0.14305	0.64788	2.02052	3.84585	1.37971	0.41266	0.17748	0.09676	0.06915	0.03837	0.02314	0.01246
20 - 25	0.08112	0.25251	0.53587	1.37971	2.42569	1.05707	0.34085	0.15226	0.09125	0.05684	0.03786	0.02042
25 - 30	0.03548	0.13271	0.21131	0.41266	1.05707	1.81715	0.78115	0.29038	0.14797	0.09071	0.06102	0.03514
30 - 35	0.02212	0.07565	0.12503	0.17748	0.34085	0.78115	1.19178	0.58065	0.22222	0.11877	0.07560	0.03664
35 - 40	0.01966	0.04025	0.06753	0.09676	0.15226	0.29038	0.58065	0.91606	0.49124	0.19236	0.09862	0.05227
40 - 45	0.01251	0.02159	0.04492	0.06915	0.09125	0.14797	0.22922	0.49124	0.68318	0.37083	0.13331	0.04651
45 - 50	0.00793	0.01995	0.03438	0.03837	0.05684	0.09071	0.11877	0.19236	0.37083	0.54116	0.29857	0.08034
50 - 60	0.00849	0.02230	0.02526	0.02314	0.03786	0.06102	0.07560	0.09862	0.13331	0.29857	0.43341	0.18068
60 - 70	0.01550	0.01501	0.01268	0.01246	0.02042	0.03514	0.03664	0.05227	0.04651	0.08034	0.18068	0.31627

Bin edges (Degrees)		Systematic covariance matrix of the measured $d\sigma/d\theta_\pi$ on C, in units of $10^{-82} \text{ cm}^2/\text{Degrees/C}^2$ .													
		0 - 5	5 - 10	10 - 15	15 - 20	20 - 25	25 - 30	30 - 35	35 - 40	40 - 45	45 - 50	50 - 60	60 - 70		
0 - 5		6.95677	7.26890	3.07948	2.04259	1.53132	1.41817	1.17586	1.20298	1.23229	0.79065	0.49969	0.38967		
5 - 10		7.26890	8.83938	4.94581	3.66890	2.89344	2.76229	2.16670	1.95206	1.77766	1.23827	0.79736	0.44907		
10 - 15		3.07948	4.94581	4.38309	3.91850	3.34185	3.20779	2.52158	2.07264	1.62714	1.22479	0.83741	0.37920		
15 - 20		2.04259	3.66890	3.91850	4.00877	3.60273	3.45696	2.76270	2.26945	1.74443	1.30781	0.86964	0.38599		
20 - 25		1.53132	2.89344	3.34185	3.60273	3.35998	3.26355	2.65265	2.2307	1.72323	1.30426	0.86581	0.38884		
25 - 30		1.41817	2.76229	3.20779	3.45696	3.26355	3.26608	2.69645	2.27838	1.81686	1.41218	0.97143	0.45127		
30 - 35		1.17586	2.16670	2.52158	2.76270	2.65265	2.69645	2.29635	1.98365	1.61540	1.28512	0.90824	0.45110		
35 - 40		1.20298	1.95206	2.07264	2.26945	2.21307	2.27838	1.98365	1.78638	1.50990	1.23392	0.90095	0.48104		
40 - 45		1.23229	1.77766	1.62714	1.74443	1.72323	1.81686	1.61540	1.50990	1.35026	1.14470	0.87503	0.50487		
45 - 50		0.79065	1.23827	1.22479	1.30781	1.30426	1.41218	1.28512	1.23392	1.14470	1.05499	0.87711	0.53907		
50 - 60		0.49969	0.79736	0.83741	0.86964	0.86581	0.97143	0.90824	0.90095	0.87503	0.87711	0.81284	0.54262		
60 - 70		0.38967	0.44907	0.37920	0.38599	0.38884	0.45127	0.45110	0.48104	0.50487	0.53907	0.54262	0.40731		

TABLE XXXIV. Statistical covariance matrix of the measured  $d\sigma/d\theta_\pi$  on Fe, in units of  $10^{-82} \text{ (cm}^2/\text{Degrees/Fe)}^2$ .

Bin edges (Degrees)	0 - 5	5 - 10	10 - 15	15 - 20	20 - 25	25 - 30	30 - 35	35 - 40	40 - 45	45 - 50	50 - 60	60 - 70
0 - 5	35.16603	6.89135	-2.49103	-0.97904	-0.39292	-0.07174	0.07874	-0.04683	-0.09115	-0.04485	-0.01244	-0.00029
5 - 10	6.89135	36.24242	5.05513	-1.57726	-1.12329	-0.15973	0.25032	-0.11827	-0.23437	-0.11345	-0.03396	-0.01652
10 - 15	-2.49103	5.05513	17.91881	3.80610	-0.73742	-0.30101	0.23834	-0.11640	-0.23119	-0.10911	-0.03177	-0.00721
15 - 20	-0.97904	-1.57726	3.80610	8.78915	2.82792	0.20231	0.37448	-0.13168	-0.26310	-0.12414	-0.03464	-0.01014
20 - 25	-0.39292	-1.12329	-0.73742	2.82792	6.25186	2.54411	1.19428	-0.22547	-0.45027	-0.22320	-0.06514	-0.01776
25 - 30	-0.07174	-0.15973	-0.30101	0.20231	2.54411	4.06903	2.79543	-0.40654	-0.79125	-0.39381	-0.12556	-0.02911
30 - 35	0.07874	0.25032	0.23834	0.37448	1.19428	2.79543	3.29282	-0.61462	-1.19251	-0.58760	-0.18622	-0.04427
35 - 40	-0.04683	-0.11827	-0.11640	-0.13168	-0.22547	-0.40654	-0.61462	0.20046	0.39392	0.19351	0.05906	0.01524
40 - 45	-0.09115	-0.23437	-0.23119	-0.26310	-0.45027	-0.79125	-1.19251	0.39392	0.77485	0.38049	0.11601	0.02999
45 - 50	-0.04485	-0.11345	-0.10911	-0.12414	-0.22320	-0.39381	-0.58760	0.19351	0.38049	0.18710	0.05700	0.01473
50 - 60	-0.01244	-0.03396	-0.03177	-0.03464	-0.06514	-0.12556	-0.18622	0.05906	0.11601	0.05700	0.01749	0.00448
60 - 70	-0.00029	-0.01652	-0.00721	-0.01014	-0.01776	-0.02911	-0.04427	0.01524	0.02999	0.01473	0.00448	0.00121

TABLE XXXV. Systematic covariance matrix of the measured  $d\sigma/d\theta_\pi$  on Fe, in units of  $10^{-82} (\text{cm}^2/\text{Degrees}/\text{Fe})^2$ .

Bin edges (Degrees)	0 - 5	5 - 10	10 - 15	15 - 20	20 - 25	25 - 30	30 - 35	35 - 40	40 - 45	45 - 50	50 - 60	60 - 70
0 - 5	27.61667	32.96602	15.68630	12.11356	11.05214	5.72072	4.18748	0.386531	-1.08606	-0.71713	-0.18880	-0.05342
5 - 10	32.96602	52.57652	27.75217	28.55298	31.39175	18.19445	14.05411	2.32195	-2.87945	-2.16256	-0.56650	-0.17188
10 - 15	15.68630	27.75217	20.57183	19.94198	19.96012	11.64074	7.37233	-1.23172	-3.59124	-2.06450	-0.63074	-0.16455
15 - 20	12.11356	28.55298	19.94198	24.41427	28.29986	18.43032	13.58408	-0.16180	-4.98354	-3.07918	-0.91758	-0.24900
20 - 25	11.05214	31.39175	19.96012	28.29986	35.69179	24.51090	19.23526	0.29319	-6.76264	-4.24555	-1.25867	-0.34549
25 - 30	5.72072	18.19445	11.64074	18.43032	24.51090	18.84836	15.42946	0.39506	-5.44913	-3.38528	-1.03853	-0.28161
30 - 35	4.18748	14.05411	7.37233	13.58408	19.23526	15.42946	13.58248	2.36798	-3.08583	-2.20023	-0.65940	-0.18982
35 - 40	0.38531	2.32195	-1.23172	-0.16180	0.29319	0.39506	2.36798	9.64452	7.75041	3.45279	1.14582	0.26172
40 - 45	-1.08606	-2.87945	-3.59124	-4.98354	-6.76264	-5.44913	-3.08583	7.75041	8.17273	3.96125	1.28993	0.30995
45 - 50	-0.71713	-2.16256	-2.06450	-3.07918	-4.24555	-3.38528	-2.20023	3.45279	3.96125	1.96260	0.63515	0.15457
50 - 60	-0.18880	-0.56650	-0.63074	-0.91758	-1.25867	-1.03853	-0.65940	1.14582	1.28993	0.63515	0.20672	0.05009
60 - 70	-0.05342	-0.17188	-0.16455	-0.24900	-0.34549	-0.28161	-0.18982	0.26172	0.30995	0.15457	0.05009	0.01224

TABLE XXXVI. Statistical covariance matrix of the measured  $d\sigma/d\theta\pi$  on Pb, in units of  $10^{-82} \text{ cm}^2/\text{Degrees/Pb}$ <sup>2</sup>.

TABLE XXXVII. Systematic covariance matrix of the measured  $d\sigma/d\theta\pi$  on Pb, in units of  $10^{-82} \text{ cm}^2/\text{Degrees/Pb}^2$ .

TABLE XXXVIII. Measured cross section as a function of  $Q^2$  on CH, in units of  $10^{-39} \text{ cm}^2/[\text{GeV}/c]^2/^{12}\text{CH}$ , and the absolute and fractional cross section uncertainties.

Bin edges ([GeV/c] $^2$ )	$d\sigma/dQ^2$	Abs.	Stat.	Unc.	Abs.	Tot.	Unc.	Frac.	Stat.	Unc.	Frac.	Tot.	Unc.
0 - 0.025	26.020	0.718			2.346			0.028			0.090		
0.025 - 0.05	23.506	0.581			1.982			0.025			0.084		
0.05 - 0.075	18.405	0.479			1.629			0.026			0.088		
0.075 - 0.1	14.895	0.400			1.367			0.027			0.092		
0.1 - 0.15	11.247	0.314			1.074			0.028			0.095		
0.15 - 0.2	8.307	0.270			0.862			0.033			0.104		
0.2 - 0.3	5.711	0.225			0.674			0.039			0.118		
0.3 - 0.4	3.771	0.179			0.481			0.047			0.127		
0.4 - 0.6	2.345	0.126			0.310			0.054			0.132		
0.6 - 1.0	0.848	0.073			0.162			0.086			0.191		

TABLE XXXIX. Statistical covariance matrix of the measured  $d\sigma/dQ^2$  on CH, in units of  $10^{-78} (\text{cm}^2/(\text{GeV}/c)^2/\text{CH})^2$ .

Bin edges ([GeV/c] $^2$ )	0 - 0.025	0.025 - 0.05	0.05 - 0.075	0.075 - 0.1	0.1 - 0.15	0.15 - 0.2	0.2 - 0.3	0.3 - 0.4	0.4 - 0.6	0.6 - 1.0
0 - 0.025	0.5156	0.0459	-0.0416	-0.0233	-0.0069	-0.0016	-0.0004	-0.0001	-0.0000	-0.0000
0.025 - 0.05	0.0459	0.3380	0.1158	-0.0040	-0.0178	-0.0073	-0.0018	-0.0003	-0.0001	-0.0000
0.05 - 0.075	-0.0416	0.1158	0.2292	0.1122	0.0034	-0.0130	-0.0050	-0.0011	-0.0002	-0.0000
0.075 - 0.1	-0.0233	-0.0040	0.1122	0.1596	0.0662	-0.0040	-0.0089	-0.0026	-0.0004	-0.0000
0.1 - 0.15	-0.0069	-0.0178	0.0034	0.0662	0.0987	0.0392	-0.0037	-0.0049	-0.0012	-0.0001
0.15 - 0.2	-0.0016	-0.0073	-0.0130	-0.0040	0.0392	0.0731	0.0280	-0.0030	-0.0031	-0.0004
0.2 - 0.3	-0.0004	-0.0018	-0.0050	-0.0089	-0.0037	0.0280	0.0507	0.0158	-0.0022	-0.0010
0.3 - 0.4	-0.0001	-0.0003	-0.0011	-0.0026	-0.0049	-0.0030	0.0158	0.0320	0.0092	-0.0014
0.4 - 0.6	-0.0000	-0.0001	-0.0002	-0.0004	-0.0012	-0.0031	-0.0022	0.0092	0.0159	0.0022
0.6 - 1.0	-0.0000	-0.0000	-0.0000	-0.0000	-0.0001	-0.0004	-0.0010	-0.0014	0.0022	0.0053

TABLE XL. Systematic covariance matrix of the measured  $d\sigma/dQ^2$  on CH, in units of  $10^{-78} (\text{cm}^2/(\text{GeV}/c)^2/\text{CH})^2$ .

Bin edges ([GeV/c] $^2$ )	0 - 0.025	0.025 - 0.05	0.05 - 0.075	0.075 - 0.1	0.1 - 0.15	0.15 - 0.2	0.2 - 0.3	0.3 - 0.4	0.4 - 0.6	0.6 - 1.0
0 - 0.025	4.9885	4.1479	3.2820	2.6012	1.8610	1.2879	0.7812	0.4455	0.2212	0.0983
0.025 - 0.05	4.1479	3.5895	2.9131	2.3747	1.7624	1.2641	0.8109	0.4847	0.2615	0.1164
0.05 - 0.075	3.2820	2.9131	2.4234	2.0130	1.5237	1.1189	0.7470	0.4564	0.2556	0.1154
0.075 - 0.1	2.6012	2.3747	2.0130	1.7087	1.3224	0.9877	0.6733	0.4156	0.2423	0.1119
0.1 - 0.15	1.8610	1.7624	1.5237	1.3224	1.0546	0.8101	0.5702	0.3568	0.2136	0.1002
0.15 - 0.2	1.2879	1.2641	1.1189	0.9877	0.8101	0.6694	0.5009	0.3237	0.1955	0.0908
0.2 - 0.3	0.7812	0.8109	0.7470	0.6733	0.5702	0.5009	0.4039	0.2731	0.1634	0.0755
0.3 - 0.4	0.4455	0.4847	0.4564	0.4156	0.3568	0.3237	0.2731	0.1989	0.1195	0.0538
0.4 - 0.6	0.2212	0.2615	0.2556	0.2423	0.2136	0.1955	0.1634	0.1195	0.0804	0.0384
0.6 - 1.0	0.0983	0.1164	0.1154	0.1119	0.1002	0.0908	0.0755	0.0538	0.0384	0.0209

TABLE XLI. Measured cross section as a function of  $Q^2$  on C, in units of  $10^{-39} \text{ cm}^2/[\text{GeV}/c]^2/^{12}\text{C}$ , and the absolute and fractional cross section uncertainties.

Bin edges ([GeV/c] $^2$ )	$d\sigma/dQ^2$	Abs.	Stat.	Unc.	Abs.	Tot.	Unc.	Frac.	Stat.	Unc.	Frac.	Tot.	Unc.
0 - 0.025	22.794	4.605			6.511			0.202			0.286		
0.025 - 0.05	24.134	4.070			6.173			0.169			0.256		
0.05 - 0.075	18.964	3.519			5.132			0.186			0.271		
0.075 - 0.1	11.425	2.800			4.210			0.245			0.368		
0.1 - 0.15	6.534	2.161			3.362			0.331			0.515		
0.15 - 0.2	5.486	1.942			3.031			0.354			0.552		
0.2 - 0.3	6.298	1.828			2.709			0.290			0.430		
0.3 - 0.4	6.217	1.812			2.354			0.291			0.379		
0.4 - 0.6	1.727	1.091			1.389			0.632			0.804		
0.6 - 1.0	0.877	0.709			0.771			0.809			0.880		

TABLE XLII. Statistical covariance matrix of the measured  $d\sigma/dQ^2$  on C, in units of  $10^{-78}$  ( $\text{cm}^2/(\text{GeV}/c)^2/\text{C})^2$ .

Bin edges ([GeV/c] $^2$ )	0 - 0.025	0.025 - 0.05	0.05 - 0.075	0.075 - 0.1	0.1 - 0.15	0.15 - 0.2	0.2 - 0.3	0.3 - 0.4	0.4 - 0.6	0.6 - 1.0
0 - 0.025	21.2085	3.2886	-2.3019	-1.4152	-0.3826	-0.0771	-0.0201	-0.0020	-0.0013	-0.0006
0.025 - 0.05	3.2886	16.5632	6.8748	0.1440	-1.0024	-0.5313	-0.1513	-0.0121	-0.0039	-0.0005
0.05 - 0.075	-2.3019	6.8748	12.3855	6.6510	0.7848	-0.7211	-0.4276	-0.0784	-0.0072	-0.0010
0.075 - 0.1	-1.4152	0.1440	6.6510	7.8383	3.7387	0.3250	-0.4746	-0.2207	-0.0297	-0.0026
0.1 - 0.15	-0.3826	-1.0024	0.7848	3.7387	4.6694	2.3752	0.0629	-0.3995	-0.0611	-0.0048
0.15 - 0.2	-0.0771	-0.5313	-0.7211	0.3250	2.3752	3.7715	1.9818	-0.3312	-0.1747	-0.0240
0.2 - 0.3	-0.0201	-0.1513	-0.4276	-0.4746	0.0629	1.9818	3.3407	1.0917	-0.1886	-0.0831
0.3 - 0.4	-0.0020	-0.0121	-0.0784	-0.2207	-0.3995	-0.3312	1.0917	3.2830	0.8365	-0.0829
0.4 - 0.6	-0.0013	-0.0039	-0.0072	-0.0297	-0.0611	-0.1747	-0.1886	0.8365	1.1897	0.2141
0.6 - 1.0	-0.0006	-0.0005	-0.0010	-0.0026	-0.0048	-0.0240	-0.0831	-0.0829	0.2141	0.5030

TABLE XLIII. Systematic covariance matrix of the measured  $d\sigma/dQ^2$  on C, in units of  $10^{-78}$  ( $\text{cm}^2/(\text{GeV}/c)^2/\text{C})^2$ .

Bin edges ([GeV/c] $^2$ )	0 - 0.025	0.025 - 0.05	0.05 - 0.075	0.075 - 0.1	0.1 - 0.15	0.15 - 0.2	0.2 - 0.3	0.3 - 0.4	0.4 - 0.6	0.6 - 1.0
0 - 0.025	21.1782	20.8529	16.5509	13.0947	9.8807	7.2547	4.6254	1.1915	0.1300	-0.0556
0.025 - 0.05	20.8529	21.5445	16.8088	12.9548	9.8018	7.3992	5.0006	1.4909	0.2115	0.0110
0.05 - 0.075	16.5509	16.8088	13.9511	11.3377	8.5919	6.4868	4.3881	1.7351	0.6126	0.1352
0.075 - 0.1	13.0947	12.9548	11.3377	9.8829	7.7727	6.0761	4.2276	2.0885	0.9718	0.2513
0.1 - 0.15	9.8807	9.8018	8.5919	7.7727	6.6324	5.6620	4.2262	2.2825	1.0771	0.2989
0.15 - 0.2	7.2547	7.3992	6.4868	6.0761	5.6620	5.4143	4.4157	2.5392	1.1839	0.3469
0.2 - 0.3	4.6254	5.0006	4.3881	4.2276	4.2262	4.4157	3.9978	2.5293	1.1517	0.3539
0.3 - 0.4	1.1915	1.4909	1.7351	2.0885	2.2825	2.5392	2.5293	2.2606	1.1786	0.3929
0.4 - 0.6	0.1300	0.2115	0.6126	0.9718	1.0771	1.1839	1.1517	1.1786	0.7394	0.2431
0.6 - 1.0	-0.0556	0.0110	0.1352	0.2513	0.2989	0.3469	0.3539	0.3929	0.2431	0.0918

TABLE XLIV. Measured cross section as a function of  $Q^2$  on Fe, in units of  $10^{-39}$   $\text{cm}^2/[\text{GeV}/c]^2/^{56}\text{Fe}$ , and the absolute and fractional cross section uncertainties.

Bin edges ([GeV/c] $^2$ )	$d\sigma/dQ^2$	Abs. Stat. Unc.	Abs. Tot. Unc.	Frac. Stat. Unc.	Frac. Tot. Unc.
0 - 0.025	62.420	7.342	14.558	0.118	0.233
0.025 - 0.05	60.968	5.938	12.758	0.097	0.209
0.05 - 0.075	46.116	5.092	10.833	0.110	0.235
0.075 - 0.1	32.553	4.390	9.614	0.135	0.295
0.1 - 0.15	20.223	3.681	8.842	0.182	0.437
0.15 - 0.2	12.698	3.209	7.940	0.253	0.625
0.2 - 0.3	9.747	2.727	5.854	0.280	0.601
0.3 - 0.4	8.747	2.402	3.957	0.275	0.452
0.4 - 0.6	5.949	1.779	2.728	0.299	0.459
0.6 - 1.0	1.995	1.040	1.374	0.521	0.689

TABLE XLV. Statistical covariance matrix of the measured  $d\sigma/dQ^2$  on Fe, in units of  $10^{-78}$  ( $\text{cm}^2/(\text{GeV}/c)^2/\text{Fe})^2$ .

Bin edges ([GeV/c] $^2$ )	0 - 0.025	0.025 - 0.05	0.05 - 0.075	0.075 - 0.1	0.1 - 0.15	0.15 - 0.2	0.2 - 0.3	0.3 - 0.4	0.4 - 0.6	0.6 - 1.0
0 - 0.025	53.9093	9.8563	-4.6831	-4.1620	-1.7732	-0.5040	-0.1217	-0.0154	0.0006	-0.0008
0.025 - 0.05	9.8563	35.2577	16.2897	1.8021	-2.5618	-1.7315	-0.6075	-0.1155	-0.0133	0.0042
0.05 - 0.075	-4.6831	16.2897	25.9331	15.2838	2.7306	-1.6184	-1.1431	-0.3493	-0.0639	-0.0031
0.075 - 0.1	-4.1620	1.8021	15.2838	19.2685	10.8811	1.4779	-1.2938	-0.7641	-0.1602	-0.0161
0.1 - 0.15	-1.7732	-2.5618	2.7306	10.8811	13.5488	7.3639	0.8530	-0.8988	-0.3741	-0.0418
0.15 - 0.2	-0.5040	-1.7315	-1.6184	1.4779	7.3639	10.2951	5.4149	0.0842	-0.6205	-0.1348
0.2 - 0.3	-0.1217	-0.6075	-1.1431	-1.2938	0.8530	5.4149	7.4355	3.2239	-0.1595	-0.2564
0.3 - 0.4	-0.0154	-0.1155	-0.3493	-0.7641	-0.8988	0.0842	3.2239	5.7674	2.1027	-0.2192
0.4 - 0.6	0.0006	-0.0133	-0.0639	-0.1602	-0.3741	-0.6205	-0.1595	2.1027	3.1631	0.7486
0.6 - 1.0	-0.0008	0.0042	-0.0031	-0.0161	-0.0418	-0.1348	-0.2564	-0.2192	0.7486	1.0815

TABLE XLVI. Systematic covariance matrix of the measured  $d\sigma/dQ^2$  on Fe, in units of  $10^{-78}$   $\text{cm}^2/(\text{GeV}/c)^2/\text{Fe})^2$ .

Bin edges ( $[\text{GeV}/c]^2$ )	0 - 0.025	0.025 - 0.05	0.05 - 0.075	0.075 - 0.1	0.1 - 0.15	0.15 - 0.2	0.2 - 0.3	0.3 - 0.4	0.4 - 0.6	0.6 - 1.0	
0 - 0.025	158.0199	139.2672	112.5007	92.9769	73.9032	54.8548	35.4647	20.1997	12.7493	6.1379	
0.025 - 0.05	139.2672	127.5045	105.4226	89.0236	73.7072	57.3144	38.0409	22.0698	13.5930	6.3087	
0.05 - 0.075	112.5007	105.4226	91.4213	80.2486	69.5391	56.0659	37.8044	21.9036	13.1953	5.9120	
0.075 - 0.1	92.9769	89.0236	80.2486	73.1524	66.2580	55.0588	37.4289	21.6069	12.8510	5.5542	
0.1 - 0.15	73.9032	73.7072	69.5391	66.2580	64.6355	56.7803	38.7721	21.4257	12.1988	5.2286	
0.15 - 0.2	54.8548	57.3144	56.0659	55.0588	56.7803	52.7465	36.8141	19.6967	10.6476	4.6008	
0.2 - 0.3	35.4647	38.0409	37.8044	37.4289	38.7721	36.8141	26.8377	15.0496	8.2108	3.4812	
0.3 - 0.4	20.1997	22.0698	21.9036	21.6069	21.4257	19.6967	15.0496	9.8908	6.0788	2.4110	
0.4 - 0.6	12.7493	13.5930	13.1953	12.8510	12.1988	10.6476	8.2108	6.0788	4.2797	1.7170	
0.6 - 1.0	6.1379	6.3087	5.9120	5.5542	5.2286	4.6008	3.4812	2.4110	1.7170	0.8060	

TABLE XLVII. Measured cross section as a function of  $Q^2$  on Pb, in units of  $10^{-39}$   $\text{cm}^2/[\text{GeV}/c]^2/^{207}\text{Pb}$ , and the absolute and fractional cross section uncertainties.

Bin edges ( $[\text{GeV}/c]^2$ )	$d\sigma/dQ^2$	Abs.	Stat.	Unc.	Abs.	Tot.	Unc.	Frac.	Stat.	Unc.	Frac.	Tot.	Unc.
0 - 0.025	162.537	27.690			36.478			0.170			0.224		
0.025 - 0.05	163.617	23.783			30.257			0.145			0.185		
0.05 - 0.075	134.554	21.250			24.932			0.158			0.185		
0.075 - 0.1	90.890	18.198			21.752			0.200			0.239		
0.1 - 0.15	52.927	14.471			17.724			0.273			0.335		
0.15 - 0.2	40.035	12.595			14.975			0.315			0.374		
0.2 - 0.3	41.531	10.954			11.824			0.264			0.285		
0.3 - 0.4	20.404	8.973			9.533			0.440			0.467		
0.4 - 0.6	9.253	5.801			6.288			0.627			0.680		
0.6 - 1.0	2.090	3.034			3.168			1.452			1.516		

Bin edges [ $(\text{GeV}/c)^2$ ]		$d\sigma/dQ^2$ on Pb, in units of $10^{-78} (\text{cm}^2/(\text{GeV}/c)^2/\text{Pb})^2$ .										
		0 - 0.025	0 - 0.025	0.025 - 0.05	0.05 - 0.075	0.075 - 0.1	0.1 - 0.15	0.15 - 0.2	0.2 - 0.3	0.3 - 0.4	0.4 - 0.6	0.6 - 1.0
0.025 - 0.05	15.6754	766.7597	15.6754	-144.3387	-64.3224	-9.9106	4.4781	3.8054	0.8008	0.0961	0.0222	
0.05 - 0.075	-144.3387	565.6100	210.9321	-51.3156	-67.5893	-22.5181	0.9094	2.5645	0.6372	0.0575		
0.075 - 0.1	-64.3224	210.9321	451.5643	211.3721	-4.6529	-45.9334	-17.4375	0.8687	0.9438	0.1104		
0.1 - 0.15	-9.9106	-51.3156	211.3721	331.1799	170.0820	-3.6173	-36.6134	-6.7536	1.2920	0.0489		
0.15 - 0.2	4.4781	-67.5893	-4.6529	170.0820	209.4085	94.5342	-15.4491	-16.5666	-1.1175	0.3888		
0.2 - 0.3	3.8054	4.4781	-22.5181	-45.9334	-3.6173	94.5342	158.6382	61.6261	-21.6106	-10.6635	0.4829	
0.3 - 0.4	0.8008	3.8054	0.9094	-17.4375	-36.6134	-15.4491	61.6261	119.9990	27.4612	-11.2340	-2.1432	
0.4 - 0.6	0.0961	2.5645	0.8687	-6.7536	-16.5666	-21.6106	27.4612	80.5172	21.7022	-6.5241		
0.6 - 1.0	0.0222	0.6372	0.9438	1.2920	-1.1175	-10.6635	-11.2340	21.7022	33.6513	4.6152		
		0.1104	0.0489	0.1104	0.0489	0.3888	0.4829	-2.1432	-6.5241	4.6152	9.2049	

Bin edges ([GeV/c <sup>2</sup> ])		0 - 0.025	0.025 - 0.05	0.05 - 0.075	0.075 - 0.1	0.1 - 0.15	0.15 - 0.2	0.2 - 0.3	0.3 - 0.4	0.4 - 0.6	0.6 - 1.0
0 - 0.025	563.8980	428.2168	260.1724	190.3170	141.1061	120.1973	49.7337	15.9567	26.7687	8.3174	
0.025 - 0.05	428.2168	349.8708	222.8117	166.6936	126.3446	101.6364	47.9531	17.5967	22.1924	6.5905	
0.05 - 0.075	260.1724	222.8117	170.0262	143.9018	108.1825	77.0201	38.4767	16.7428	13.7118	4.2189	
0.075 - 0.1	190.3170	166.6936	143.9018	141.9843	115.8184	78.3015	37.5177	16.2120	10.4763	4.0533	
0.1 - 0.15	141.1061	126.3446	108.1825	115.8184	104.7343	74.2326	34.5556	13.3751	8.7370	3.9600	
0.15 - 0.2	120.1973	101.6364	77.0201	78.3015	74.2326	65.6092	30.3815	10.6700	10.1841	3.9561	
0.2 - 0.3	49.7337	47.9531	38.4767	37.5177	34.5556	30.3815	19.8144	10.6333	7.2494	2.7198	
0.3 - 0.4	15.9567	17.5967	16.7428	16.2120	13.3751	10.6700	10.6333	10.3550	6.3430	2.0666	
0.4 - 0.6	26.7687	22.1924	13.7118	10.4763	8.7370	10.1841	7.2494	6.3430	5.8819	1.8055	
0.6 - 1.0	8.3174	6.5905	4.2189	4.0533	3.9600	3.9561	2.7198	2.0666	1.8055	0.8304	

TABLE L. Measured cross section as a function of  $E_\mu$  on CH, in units of  $10^{-39} \text{ cm}^2/\text{GeV}/^{12}\text{CH}$ , and the absolute and fractional cross section uncertainties.

Bin edges (GeV)	$d\sigma/dE_\mu$	Abs. Stat. Unc.	Abs. Tot. Unc.	Frac. Stat. Unc.	Frac. Tot. Unc.
0.0 - 2.0	0.229	0.024	0.052	0.107	0.225
2.0 - 3.0	0.748	0.026	0.086	0.035	0.115
3.0 - 4.0	0.875	0.026	0.089	0.029	0.102
4.0 - 5.0	0.919	0.024	0.085	0.026	0.093
5.0 - 6.0	0.722	0.020	0.069	0.028	0.095
6.0 - 7.0	0.471	0.015	0.051	0.031	0.108
7.0 - 8.0	0.270	0.010	0.030	0.036	0.113
8.0 - 10.0	0.112	0.005	0.013	0.045	0.113
10.0 - 14.0	0.034	0.002	0.004	0.068	0.110
14.0 - 20.0	0.009	0.001	0.002	0.140	0.192

TABLE LI. Measured cross section as a function of  $E_\mu$  on C, in units of  $10^{-39} \text{ cm}^2/\text{GeV}/^{12}\text{C}$ , and the absolute and fractional cross section uncertainties.

Bin edges (GeV)	$d\sigma/dE_\mu$	Abs. Stat. Unc.	Abs. Tot. Unc.	Frac. Stat. Unc.	Frac. Tot. Unc.
0.0 - 2.0	0.580	0.485	0.595	0.837	1.025
2.0 - 3.0	0.982	0.230	0.293	0.235	0.298
3.0 - 4.0	0.834	0.199	0.271	0.239	0.324
4.0 - 5.0	0.588	0.176	0.257	0.299	0.437
5.0 - 6.0	0.814	0.170	0.247	0.209	0.304
6.0 - 7.0	0.268	0.105	0.152	0.392	0.568
7.0 - 8.0	0.197	0.073	0.092	0.372	0.469
8.0 - 10.0	0.117	0.038	0.044	0.325	0.374
10.0 - 14.0	0.043	0.019	0.020	0.446	0.471
14.0 - 20.0	0.010	0.010	0.010	0.969	1.022

TABLE LII. Measured cross section as a function of  $E_\mu$  on Fe, in units of  $10^{-39} \text{ cm}^2/\text{GeV}/^{56}\text{Fe}$ , and the absolute and fractional cross section uncertainties.

Bin edges (GeV)	$d\sigma/dE_\mu$	Abs. Stat. Unc.	Abs. Tot. Unc.	Frac. Stat. Unc.	Frac. Tot. Unc.
0.0 - 2.0	0.027	0.192	0.218	7.197	8.185
2.0 - 3.0	1.875	0.299	0.521	0.159	0.278
3.0 - 4.0	1.666	0.271	0.508	0.163	0.305
4.0 - 5.0	1.563	0.243	0.531	0.155	0.339
5.0 - 6.0	1.546	0.211	0.455	0.137	0.294
6.0 - 7.0	0.809	0.146	0.310	0.181	0.383
7.0 - 8.0	0.446	0.096	0.182	0.215	0.409
8.0 - 10.0	0.191	0.049	0.074	0.259	0.388
10.0 - 14.0	0.066	0.023	0.027	0.344	0.417
14.0 - 20.0	0.034	0.014	0.015	0.401	0.437

TABLE LIII. Measured cross section as a function of  $E_\mu$  on Pb, in units of  $10^{-39} \text{ cm}^2/\text{GeV}/^{207}\text{Pb}$ , and the absolute and fractional cross section uncertainties.

Bin edges (GeV)	$d\sigma/dE_\mu$	Abs. Stat. Unc.	Abs. Tot. Unc.	Frac. Stat. Unc.	Frac. Tot. Unc.
0.0 - 2.0	0.064	0.088	0.539	1.366	8.375
2.0 - 3.0	2.919	0.693	1.035	0.237	0.355
3.0 - 4.0	6.196	0.745	0.969	0.120	0.156
4.0 - 5.0	4.080	0.614	0.795	0.150	0.195
5.0 - 6.0	3.580	0.535	0.712	0.149	0.199
6.0 - 7.0	1.498	0.351	0.479	0.234	0.320
7.0 - 8.0	0.770	0.220	0.280	0.286	0.363
8.0 - 10.0	0.496	0.136	0.153	0.274	0.308
10.0 - 14.0	0.210	0.071	0.076	0.338	0.361
14.0 - 20.0	0.071	0.038	0.040	0.543	0.561

Bin edges (GeV)		$d\sigma/dE_\mu$ on CH, in units of $10^{-82} \text{ cm}^2/\text{GeV/CH}^2$ .									
		0.0 - 2.0	2.0 - 3.0	3.0 - 4.0	4.0 - 5.0	5.0 - 6.0	6.0 - 7.0	7.0 - 8.0	8.0 - 10.0	10.0 - 14.0	14.0 - 20.0
0.0 - 2.0	5.9983	-0.1652	-0.1679	-0.0290	-0.0072	-0.0032	-0.0017	-0.0004	-0.0001	-0.0001	-0.0000
2.0 - 3.0	-0.1652	6.8097	-0.0810	-0.3248	-0.0707	-0.0145	-0.0049	-0.0017	-0.0004	-0.0004	-0.0001
3.0 - 4.0	-0.1679	-0.0810	6.5748	0.3286	-0.4154	-0.1143	-0.0232	-0.0042	-0.0010	-0.0010	-0.0002
4.0 - 5.0	-0.0290	-0.3248	0.3286	5.8782	0.7528	-0.3712	-0.1438	-0.0222	-0.0022	-0.0004	-0.0004
5.0 - 6.0	-0.0072	-0.0707	-0.4154	0.7528	3.9922	0.8930	-0.1768	-0.0832	-0.0077	-0.0006	-0.0006
6.0 - 7.0	-0.0032	-0.0145	-0.1143	-0.3712	0.8930	2.1049	0.6932	-0.0411	-0.0217	-0.0017	-0.0017
7.0 - 8.0	-0.0017	-0.0049	-0.0232	-0.1438	-0.1768	0.6932	0.9185	0.2253	-0.0181	-0.0045	-0.0045
8.0 - 10.0	-0.0004	-0.0017	-0.0042	-0.0222	-0.0832	-0.0411	0.2253	0.2552	0.0244	-0.0049	-0.0049
10.0 - 14.0	-0.0001	-0.0004	-0.0010	-0.0022	-0.0077	-0.0217	-0.0181	0.0244	0.0542	0.0034	-0.0034
14.0 - 20.0	-0.0000	-0.0001	-0.0002	-0.0004	-0.0006	-0.0017	-0.0045	-0.0049	0.0034	0.0161	-0.0034

TABLE IV. Systematic covariance matrix of the measured  $d\sigma/dE_\mu$  on CH, in units of  $10^{-82} \text{ cm}^2/\text{GeV/CH}^2$ .

Bin edges (GeV)	0.0 - 2.0	2.0 - 3.0	3.0 - 4.0	4.0 - 5.0	5.0 - 6.0	6.0 - 7.0	7.0 - 8.0	8.0 - 10.0	10.0 - 14.0	14.0 - 20.0
0.0 - 2.0	20.6460	32.2814	30.7820	26.0871	14.6225	0.4146	-2.5442	-1.3780	-0.0203	0.1464
2.0 - 3.0	32.2814	67.2170	68.6912	62.9193	42.6163	17.2048	5.6259	1.9454	1.0703	0.6432
3.0 - 4.0	30.7820	68.6912	72.6789	68.4847	49.1464	23.4771	9.3034	3.3725	1.3732	0.7296
4.0 - 5.0	26.0871	62.9193	68.4847	66.8710	50.7996	27.5544	12.1855	4.4966	1.5290	0.7389
5.0 - 6.0	14.6225	42.6163	49.1464	50.7996	43.4029	28.0873	13.9716	5.1412	1.4490	0.5791
6.0 - 7.0	0.4146	17.2048	23.4771	27.5544	28.0873	23.8790	13.6583	5.2521	1.2713	0.4035
7.0 - 8.0	-2.5442	5.6259	9.3034	12.1855	13.9716	13.6583	8.3560	3.2937	0.7700	0.2109
8.0 - 10.0	-1.3780	1.9454	3.3725	4.4966	5.1412	5.2521	3.2937	1.3516	0.3215	0.0902
10.0 - 14.0	-0.0203	1.0703	1.3732	1.5290	1.4490	1.2713	0.7700	0.3215	0.0884	0.0286
14.0 - 20.0	0.1464	0.6432	0.7296	0.7389	0.5791	0.4035	0.2109	0.0902	0.0286	0.0143

TABLE LVI. Statistical covariance matrix of the measured  $d\sigma/dE_\mu$  on C, in units of  $10^{-82} \text{ cm}^2/\text{GeV}/\text{C}^2$ .

Bin edges (GeV)	0.0 - 2.0	2.0 - 3.0	3.0 - 4.0	4.0 - 5.0	5.0 - 6.0	6.0 - 7.0	7.0 - 8.0	8.0 - 10.0	10.0 - 14.0	14.0 - 20.0
0.0 - 2.0	2356.5129	-14.0042	-18.7831	-2.6560	-0.3640	-0.0678	-0.0596	-0.0274	-0.007	-0.0061
2.0 - 3.0	-14.0042	529.9013	-17.2562	-15.8343	-3.4403	-0.4735	-0.2382	-0.0885	-0.0388	0.0000
3.0 - 4.0	-18.7831	-17.2562	396.3338	13.5114	-24.5105	-3.7515	-0.6188	-0.2286	-0.0515	-0.0070
4.0 - 5.0	-2.6560	-15.8343	13.5114	308.7779	27.2149	-14.8828	-4.1985	-0.7458	-0.0714	-0.0119
5.0 - 6.0	-0.3640	-3.4403	-24.5105	27.2149	290.6316	38.5761	-11.2031	-4.4329	-0.3151	-0.0288
6.0 - 7.0	-0.0678	-0.4735	-3.7515	-14.8828	38.5761	109.9253	35.1045	-2.5113	-1.0297	-0.0234
7.0 - 8.0	-0.0596	-0.2382	-0.6188	-4.1985	-11.2031	35.1045	53.6783	10.6857	-1.4337	-0.1391
8.0 - 10.0	-0.0274	-0.0885	-0.2286	-0.7458	-4.4329	-2.5113	10.6857	14.5823	0.7809	-0.2367
10.0 - 14.0	-0.0007	-0.0388	-0.0515	-0.0714	-0.3151	-1.0297	-1.4337	0.7809	3.6189	0.0349
14.0 - 20.0	-0.0061	0.0000	-0.0070	-0.0119	-0.0288	-0.0234	-0.1391	-0.2367	0.0349	0.9821

TABLE LVII. Systematic covariance matrix of the measured  $d\sigma/dE_\mu$  on C, in units of  $10^{-82} \text{ (cm}^2/\text{GeV/C)}^2$ .

Bin edges (GeV)	0.0 - 2.0	2.0 - 3.0	3.0 - 4.0	4.0 - 5.0	5.0 - 6.0	6.0 - 7.0	7.0 - 8.0	8.0 - 10.0	10.0 - 14.0	14.0 - 20.0
0.0 - 2.0	1179.8379	473.8654	286.2156	293.4031	113.4690	-59.3452	-8.6769	-26.9745	-4.3152	0.3377
2.0 - 3.0	473.8654	328.3690	298.3790	295.8041	236.2814	86.1262	47.7439	8.2687	3.5817	3.0791
3.0 - 4.0	286.2156	298.3790	336.0060	329.0601	293.2896	138.5268	71.4242	20.0272	6.6170	4.5006
4.0 - 5.0	293.4031	295.8041	329.0601	350.5658	308.2426	153.4144	81.0098	22.3089	6.6001	4.6614
5.0 - 6.0	113.4690	236.2814	293.2896	308.2426	321.0841	179.8772	89.2087	30.1654	8.2929	4.7473
6.0 - 7.0	-59.3452	86.1262	138.5268	153.4144	179.8772	121.6017	59.5178	22.2734	5.5556	2.7806
7.0 - 8.0	-8.6769	47.7439	71.4242	81.0098	89.2087	59.5178	31.6735	11.0328	2.8379	1.3127
8.0 - 10.0	-26.9745	8.2687	20.0272	22.3089	30.1654	22.2734	11.0328	4.6549	1.1614	0.5075
10.0 - 14.0	-4.3152	3.5817	6.6170	6.6001	8.2929	5.5556	2.8379	1.1614	0.4171	0.1432
14.0 - 20.0	0.3377	3.0791	4.5006	4.6614	4.7473	2.7806	1.3127	0.5075	0.1432	0.1101

TABLE LVIII. Statistical covariance matrix of the measured  $d\sigma/dE_\mu$  on Fe, in units of  $10^{-82} \text{ cm}^2/\text{GeV}/\text{Fe}^2$ .

Bin edges (GeV)		0.0 - 2.0	2.0 - 3.0	3.0 - 4.0	4.0 - 5.0	5.0 - 6.0	6.0 - 7.0	7.0 - 8.0	8.0 - 10.0	10.0 - 14.0	14.0 - 20.0
0.0 - 2.0		367.2053	55.3952	-4.1850	-1.3363	-0.2193	0.1963	0.0664	-0.0389	-0.0121	-0.0025
2.0 - 3.0		55.3952	891.2884	-24.9819	-34.2073	-7.6393	-1.3319	-0.5176	-0.1663	-0.0612	-0.0397
3.0 - 4.0		-4.1850	-24.9819	733.6458	31.2789	-44.5082	-9.6031	-1.7568	-0.4213	-0.0706	-0.0438
4.0 - 5.0		-1.3363	-34.2073	31.2789	590.3850	64.2338	-35.2384	-11.2500	-1.5777	-0.2211	-0.0631
5.0 - 6.0		-0.2193	-7.6393	-44.5082	64.2338	446.3657	73.9177	-20.2857	-7.0830	-0.6560	-0.0960
6.0 - 7.0		0.1963	-1.3319	-9.6031	-35.2384	73.9177	212.9967	64.2227	-4.7805	-1.9368	-0.1512
7.0 - 8.0		0.0664	-0.5176	-1.7568	-11.2500	-20.2857	64.2227	91.7466	19.2517	-1.8061	-0.5212
8.0 - 10.0		-0.0389	-0.1663	-0.4213	-1.5777	-7.0830	-4.7805	19.2517	24.3987	2.6730	-0.5955
10.0 - 14.0		-0.0121	-0.0612	-0.0706	-0.2211	-0.6560	-1.9368	-1.8061	2.6730	5.0828	0.3213
14.0 - 20.0		-0.0025	-0.0397	-0.0438	-0.0631	-0.0960	-0.1512	-0.5212	-0.5955	0.3213	1.8951

TABLE LIX. Systematic covariance matrix of the measured  $d\sigma/dE_\mu$  on Fe, in units of  $10^{-82} \text{ cm}^2/\text{GeV}/\text{Fe}^2$ .

Bin edges (GeV)	0.0 - 2.0	2.0 - 3.0	3.0 - 4.0	4.0 - 5.0	5.0 - 6.0	6.0 - 7.0	7.0 - 8.0	8.0 - 10.0	10.0 - 14.0	14.0 - 20.0
0.0 - 2.0	107.6961	387.4369	277.4287	291.2239	156.6640	40.6955	0.0955	-0.6898	1.3373	0.6191
2.0 - 3.0	387.4369	1824.9817	1626.6269	1735.6605	1184.8009	550.5953	222.0599	72.5604	26.4450	11.8133
3.0 - 4.0	277.4287	1626.6269	1842.2601	1995.5565	1595.2967	923.4858	457.0605	156.2215	47.6087	19.3696
4.0 - 5.0	291.2239	1735.6605	1995.5565	2224.2938	1802.6740	1074.9500	539.3353	183.4038	53.9563	22.0006
5.0 - 6.0	156.6640	1184.8009	1595.2967	1802.6740	1620.9488	1052.0093	557.0614	190.3114	53.7496	20.6563
6.0 - 7.0	40.6955	550.5953	923.4858	1074.9500	1052.0093	746.6329	416.0345	142.9569	38.1409	13.9530
7.0 - 8.0	0.0955	222.0599	457.0605	539.3353	557.0614	416.0345	241.2994	84.2851	21.8422	7.6162
8.0 - 10.0	-0.6898	72.5604	156.2215	183.4038	190.3114	142.9569	84.2851	30.3550	7.9684	2.6153
10.0 - 14.0	1.3373	26.4450	47.6087	53.9563	53.7496	38.1409	21.8422	7.9684	2.3850	0.7850
14.0 - 20.0	0.6191	11.8133	19.3696	22.0006	20.6563	13.9530	7.6162	2.6153	0.7850	0.3531

TABLE LX. Statistical covariance matrix of the measured  $d\sigma/dE_\mu$  on Pb, in units of  $10^{-82} \text{ cm}^2/\text{GeV/Pb}^2$ .

Bin edges (GeV)	0.0 - 2.0	2.0 - 3.0	3.0 - 4.0	4.0 - 5.0	5.0 - 6.0	6.0 - 7.0	7.0 - 8.0	8.0 - 10.0	10.0 - 14.0	14.0 - 20.0
0.0 - 2.0	77.1977	-191.1797	-6.2704	1.5369	0.7824	0.1944	0.0401	0.0066	0.0080	-0.0035
2.0 - 3.0	-191.1797	4797.3987	-135.2686	-170.7986	-34.7420	-6.9866	-1.8858	-0.3702	-0.6050	-0.0939
3.0 - 4.0	-6.2704	-135.2686	551.4135	162.0535	-345.2708	-69.5061	-14.3699	-4.6617	-0.6870	-0.2685
4.0 - 5.0	1.5369	-170.7986	162.0535	3769.8006	426.2942	-184.8799	-58.3174	-13.5982	-2.1290	-0.2303
5.0 - 6.0	0.7824	-34.7420	-345.2708	426.2942	2861.2386	492.4456	-83.5987	-54.7202	-7.4660	-0.7174
6.0 - 7.0	0.1944	-6.9866	-69.5061	-184.8799	492.4456	1229.3465	392.8174	-13.0668	-15.4123	-1.5038
7.0 - 8.0	0.0401	-1.8858	-14.3699	-58.3174	-83.5987	392.8174	485.3247	134.4762	-12.0857	-3.4391
8.0 - 10.0	0.0066	-0.3702	-4.6617	-13.5982	-54.7202	-13.0668	134.4762	184.2351	16.8204	-5.0433
10.0 - 14.0	0.0080	-0.6050	-0.6870	-2.1290	-7.4660	-15.4123	-12.0857	16.8204	50.3066	3.6303
14.0 - 20.0	-0.0035	-0.0939	-0.2685	-0.2303	-0.7174	-1.5038	-3.4391	-5.0433	3.6303	14.7562

TABLE LXI. Systematic covariance matrix of the measured  $d\sigma/dE_\mu$  on Pb, in units of  $10^{-82} \text{ cm}^2/\text{GeV/Pb}$  $^2$ .

Bin edges (GeV)	0.0 - 2.0	2.0 - 3.0	3.0 - 4.0	4.0 - 5.0	5.0 - 6.0	6.0 - 7.0	7.0 - 8.0	8.0 - 10.0	10.0 - 14.0	14.0 - 20.0
0.0 - 2.0	2822.8124	-3737.0979	-2101.6989	-1160.9305	-786.1595	-85.7685	88.8671	106.0995	17.7201	9.8633
2.0 - 3.0	-3737.0979	5918.2321	4109.9688	2471.4035	1'737.5037	329.3346	24.1097	-54.8404	15.0465	-1.4167
3.0 - 4.0	-2101.6989	4109.9688	3835.0760	2734.2490	2108.3561	740.5671	293.4790	88.6675	60.1865	18.8045
4.0 - 5.0	-1160.9305	2471.4035	2734.2490	2547.4180	2207.5103	1180.4204	558.6266	178.5853	77.0052	25.6929
5.0 - 6.0	-786.1595	1737.5037	2108.3561	2207.5103	2201.4897	1346.0873	656.0709	214.8864	83.3849	26.7815
6.0 - 7.0	-85.7685	329.3346	740.5671	1180.4204	1346.0873	1061.2996	540.8800	173.1065	59.2936	18.1981
7.0 - 8.0	88.8671	24.1097	293.4790	558.6266	656.0709	540.8800	298.1334	105.3169	33.8665	9.4386
8.0 - 10.0	106.0995	-54.8404	88.6675	178.5853	214.8864	173.1065	105.3169	49.3980	16.2835	4.3772
10.0 - 14.0	17.7201	15.0465	60.1865	77.0052	83.3849	59.2936	33.8665	16.2835	7.1500	2.1358
14.0 - 20.0	9.8633	-1.4167	18.8045	25.6929	26.7815	18.1981	9.4386	4.3772	2.1358	1.0236

TABLE LXII. Measured cross section as a function of  $\theta_\mu$  on CH, in units of  $10^{-41} \text{ cm}^2/\text{Degrees}/{}^{12}\text{CH}$ , and the absolute and fractional cross section uncertainties.

Bin edges (Degrees)	$d\sigma/d\theta_\mu$	Abs. Stat. Unc.	Abs. Tot. Unc.	Frac. Stat. Unc.	Frac. Tot. Unc.
0 - 2	53.146	1.112	4.305	0.021	0.081
2 - 4	72.881	1.400	6.132	0.019	0.084
4 - 6	43.843	1.359	4.563	0.031	0.104
6 - 8	29.134	1.266	3.426	0.043	0.118
8 - 12	15.003	0.822	2.307	0.055	0.154
12 - 20	3.157	0.736	1.430	0.233	0.453

TABLE LXIII. Statistical covariance matrix of the measured  $d\sigma/d\theta_\mu$  on CH, in units of  $10^{-82} (\text{cm}^2/\text{Degrees}/\text{CH})^2$ .

Bin edges (Degrees)	0 - 2	2 - 4	4 - 6	6 - 8	8 - 12	12 - 20
0 - 2	1.23759	-0.08711	-0.04958	-0.00088	0.00009	-0.00042
2 - 4	-0.08711	1.95870	-0.04121	-0.05016	-0.00090	-0.00057
4 - 6	-0.04958	-0.04121	1.84762	-0.02906	-0.02943	-0.00105
6 - 8	-0.00088	-0.05016	-0.02906	1.60362	-0.03510	-0.01733
8 - 12	0.00009	-0.00090	-0.02943	-0.03510	0.67648	-0.01653
12 - 20	-0.00042	-0.00057	-0.00105	-0.01733	-0.01653	0.54230

TABLE LXIV. Systematic covariance matrix of the measured  $d\sigma/d\theta_\mu$  on CH, in units of  $10^{-82} (\text{cm}^2/\text{Degrees}/\text{CH})^2$ .

Bin edges (Degrees)	0 - 2	2 - 4	4 - 6	6 - 8	8 - 12	12 - 20
0 - 2	17.29504	23.21110	13.62761	7.81278	4.27958	1.66791
2 - 4	23.21110	35.64265	23.80553	15.20949	8.81648	3.50405
4 - 6	13.62761	23.80553	18.97604	13.31870	8.25253	3.70790
6 - 8	7.81278	15.20949	13.31870	10.13509	6.57531	3.08291
8 - 12	4.27958	8.81648	8.25253	6.57531	4.64706	2.41325
12 - 20	1.66791	3.50405	3.70790	3.08291	2.41325	1.50122

TABLE LXV. Measured cross section as a function of  $\theta_\mu$  on C, in units of  $10^{-41} \text{ cm}^2/\text{Degrees}/{}^{12}\text{C}$ , and the absolute and fractional cross section uncertainties.

Bin edges (Degrees)	$d\sigma/d\theta_\mu$	Abs. Stat. Unc.	Abs. Tot. Unc.	Frac. Stat. Unc.	Frac. Tot. Unc.
0 - 2	43.173	7.755	11.654	0.180	0.270
2 - 4	65.513	10.939	17.814	0.167	0.272
4 - 6	50.137	12.100	18.065	0.241	0.360
6 - 8	12.757	10.236	13.280	0.802	1.041
8 - 12	23.589	10.300	12.452	0.437	0.528
12 - 20	18.554	17.404	17.829	0.938	0.961

TABLE LXVI. Statistical covariance matrix of the measured  $d\sigma/d\theta_\mu$  on C, in units of  $10^{-82} (\text{cm}^2/\text{Degrees}/\text{C})^2$ .

Bin edges (Degrees)	0 - 2	2 - 4	4 - 6	6 - 8	8 - 12	12 - 20
0 - 2	60.13758	-3.44584	-4.61150	-0.16505	0.03088	0.00651
2 - 4	-3.44584	119.65768	-3.55463	-4.14315	-0.42015	0.05787
4 - 6	-4.61150	-3.55463	146.41443	7.23272	-5.48475	-0.59039
6 - 8	-0.16505	-4.14315	7.23272	104.78224	6.19822	-4.97330
8 - 12	0.03088	-0.42015	-5.48475	6.19822	106.08489	-8.29479
12 - 20	0.00651	0.05787	-0.59039	-4.97330	-8.29479	302.89844

TABLE LXVII. Systematic covariance matrix of the measured  $d\sigma/d\theta_\mu$  on C, in units of  $10^{-82} (\text{cm}^2/\text{Degrees}/\text{C})^2$ .

Bin edges (Degrees)	0 - 2	2 - 4	4 - 6	6 - 8	8 - 12	12 - 20
0 - 2	75.68600	112.34260	73.96793	26.55311	19.52057	5.23643
2 - 4	112.34260	197.68648	163.73613	77.24754	59.38123	20.44799
4 - 6	73.96793	163.73613	179.93202	101.85083	82.49403	34.06233
6 - 8	26.55311	77.24754	101.85083	71.56708	54.62803	23.86098
8 - 12	19.52057	59.38123	82.49403	54.62803	48.97492	21.83461
12 - 20	5.23643	20.44799	34.06233	23.86098	21.83461	14.97286

TABLE LXVIII. Measured cross section as a function of  $\theta_\mu$  on Fe, in units of  $10^{-41} \text{ cm}^2/\text{Degrees}/{}^{56}\text{Fe}$ , and the absolute and fractional cross section uncertainties.

Bin edges (Degrees)	$d\sigma/d\theta_\mu$	Abs. Stat. Unc.	Abs. Tot. Unc.	Frac. Stat. Unc.	Frac. Tot. Unc.
0 - 2	138.083	12.423	26.542	0.090	0.192
2 - 4	128.303	15.788	40.983	0.123	0.319
4 - 6	112.200	18.660	39.322	0.166	0.350
6 - 8	56.564	18.746	33.303	0.331	0.589
8 - 12	14.822	14.806	22.952	0.999	1.549
12 - 20	39.007	32.816	36.404	0.841	0.933

TABLE LXIX. Statistical covariance matrix of the measured  $d\sigma/d\theta_\mu$  on Fe, in units of  $10^{-82} (\text{cm}^2/\text{Degrees}/\text{Fe})^2$ .

Bin edges (Degrees)	0 - 2	2 - 4	4 - 6	6 - 8	8 - 12	12 - 20
0 - 2	154.31919	-1.84906	-17.82977	-1.23957	-0.00733	0.01066
2 - 4	-1.84906	249.25761	9.35276	-17.39404	-1.31784	0.16002
4 - 6	-17.82977	9.35276	348.19990	15.63820	-16.42002	-4.08125
6 - 8	-1.23957	-17.39404	15.63820	351.41508	31.02038	-28.20155
8 - 12	-0.00733	-1.31784	-16.42002	31.02038	219.23200	24.48856
12 - 20	0.01066	0.16002	-4.08125	-28.20155	24.48856	1076.91290

TABLE LXX. Systematic covariance matrix of the measured  $d\sigma/d\theta_\mu$  on Fe, in units of  $10^{-82} (\text{cm}^2/\text{Degrees}/\text{Fe})^2$ .

Bin edges (Degrees)	0 - 2	2 - 4	4 - 6	6 - 8	8 - 12	12 - 20
0 - 2	550.17774	812.08077	604.82336	422.88272	250.68015	209.91760
2 - 4	812.08077	1430.34981	1216.76117	894.75072	518.66757	425.24654
4 - 6	604.82336	1216.76117	1198.05527	920.15579	544.76161	447.58681
6 - 8	422.88272	894.75072	920.15579	757.65175	463.92102	369.41237
8 - 12	250.68015	518.66757	544.76161	463.92102	307.54418	245.48632
12 - 20	209.91760	425.24654	447.58681	369.41237	245.48632	248.36387

TABLE LXXI. Measured cross section as a function of  $\theta_\mu$  on Pb, in units of  $10^{-41} \text{ cm}^2/\text{Degrees}/{}^{207}\text{Pb}$ , and the absolute and fractional cross section uncertainties.

Bin edges (Degrees)	$d\sigma/d\theta_\mu$	Abs. Stat. Unc.	Abs. Tot. Unc.	Frac. Stat. Unc.	Frac. Tot. Unc.
0 - 2	344.795	39.005	55.498	0.113	0.161
2 - 4	397.971	48.903	68.000	0.123	0.171
4 - 6	304.390	54.436	65.667	0.179	0.216
6 - 8	138.111	52.196	59.532	0.378	0.431
8 - 12	41.697	53.430	59.160	1.281	1.419
12 - 20	-146.540	77.052	117.135	-0.526	-0.799

TABLE LXXII. Statistical covariance matrix of the measured  $d\sigma/d\theta_\mu$  on Pb, in units of  $10^{-82} (\text{cm}^2/\text{Degrees}/\text{Pb})^2$ .

Bin edges (Degrees)	0 - 2	2 - 4	4 - 6	6 - 8	8 - 12	12 - 20
0 - 2	1521.40006	-24.82221	-162.20611	-9.76556	0.90789	-8.68319
2 - 4	-24.82221	2391.53908	71.27696	-151.90168	-8.67385	-47.52392
4 - 6	-162.20611	71.27696	2963.33097	175.27484	-203.44463	287.06722
6 - 8	-9.76556	-151.90168	175.27484	2724.37400	65.56213	1458.73765
8 - 12	0.90789	-8.67385	-203.44463	65.56213	2854.80333	-664.60304
12 - 20	-8.68319	-47.52392	287.06722	1458.73765	-664.60304	5936.97296

TABLE LXXXIII. Systematic covariance matrix of the measured  $d\sigma/d\theta_\mu$  on Pb, in units of  $10^{-82} (\text{cm}^2/\text{Degrees}/\text{Pb})^2$ .

Bin edges (Degrees)	0 - 2	2 - 4	4 - 6	6 - 8	8 - 12	12 - 20
0 - 2	1558.62580	1668.07935	999.67795	601.95184	496.71163	754.64704
2 - 4	1668.07935	2232.49070	1498.83133	911.67399	716.16319	1455.12501
4 - 6	999.67795	1498.83133	1348.88822	927.52338	716.88860	771.05559
6 - 8	601.95184	911.67399	927.52338	819.66937	620.03734	447.32671
8 - 12	496.71163	716.16319	716.88860	620.03734	645.10342	691.96377
12 - 20	754.64704	1455.12501	771.05559	447.32671	691.96377	7783.73906

**Tables of cross section ratios**

TABLE LXXIV. Measured cross section ratio of C with respect to CH as a function of  $E_\nu$ , and the absolute and fractional uncertainties.

Bin edges (GeV)	$\sigma(E_\nu)_C/\sigma(E_\nu)_{CH}$	Abs.	Stat.	Unc.	Abs.	Tot.	Unc.	Frac.	Stat.	Unc.	Frac.	Tot.	Unc.
2.0 - 3.0	1.197	0.974			1.122			0.814			0.937		
3.0 - 4.0	1.118	0.381			0.445			0.341			0.398		
4.0 - 5.0	1.217	0.272			0.341			0.223			0.280		
5.0 - 6.0	0.698	0.194			0.261			0.278			0.374		
6.0 - 7.0	0.594	0.175			0.251			0.294			0.422		
7.0 - 8.0	0.988	0.224			0.272			0.227			0.275		
8.0 - 10.0	0.988	0.248			0.277			0.251			0.281		
10.0 - 14.0	1.335	0.404			0.415			0.303			0.311		
14.0 - 20.0	0.534	0.542			0.564			1.015			1.057		

TABLE LXXV. Statistical covariance matrix of the measured  $\sigma(E_\nu)_C/\sigma(E_\nu)_{CH}$

Bin edges (GeV)	2.0 - 3.0	3.0 - 4.0	4.0 - 5.0	5.0 - 6.0	6.0 - 7.0	7.0 - 8.0	8.0 - 10.0	10.0 - 14.0	14.0 - 20.0
2.0 - 3.0	0.9490	0.0151	-0.0143	-0.0017	-0.0001	-0.0003	0.0001	-0.0001	-0.0001
3.0 - 4.0	0.0151	0.1454	0.0034	-0.0055	-0.0015	-0.0003	-0.0002	-0.0002	0.0000
4.0 - 5.0	-0.0143	0.0034	0.0737	0.0063	-0.0044	-0.0030	-0.0008	-0.0003	-0.0001
5.0 - 6.0	-0.0017	-0.0055	0.0063	0.0378	0.0100	-0.0044	-0.0030	-0.0007	-0.0002
6.0 - 7.0	-0.0001	-0.0015	-0.0044	0.0100	0.0306	0.0148	-0.0042	-0.0033	-0.0002
7.0 - 8.0	-0.0003	-0.0003	-0.0030	-0.0044	0.0148	0.0502	0.0165	-0.0103	-0.0025
8.0 - 10.0	0.0001	-0.0002	-0.0008	-0.0030	-0.0042	0.0165	0.0616	0.0106	-0.0062
10.0 - 14.0	-0.0001	-0.0002	-0.0003	-0.0007	-0.0033	-0.0103	0.0106	0.1636	0.0114
14.0 - 20.0	-0.0001	0.0000	-0.0001	-0.0002	-0.0002	-0.0025	-0.0062	0.0114	0.2938

TABLE LXXVI. Systematic covariance matrix of the measured  $\sigma(E_\nu)_C/\sigma(E_\nu)_{CH}$

Bin edges (GeV)	2.0 - 3.0	3.0 - 4.0	4.0 - 5.0	5.0 - 6.0	6.0 - 7.0	7.0 - 8.0	8.0 - 10.0	10.0 - 14.0	14.0 - 20.0
2.0 - 3.0	0.3090	0.0956	0.0763	0.0421	0.0550	0.0550	-0.0145	0.0160	0.0168
3.0 - 4.0	0.0956	0.0528	0.0448	0.0342	0.0367	0.0318	0.0089	0.0132	0.0211
4.0 - 5.0	0.0763	0.0448	0.0424	0.0326	0.0345	0.0294	0.0109	0.0133	0.0204
5.0 - 6.0	0.0421	0.0342	0.0326	0.0305	0.0298	0.0239	0.0142	0.0114	0.0219
6.0 - 7.0	0.0550	0.0367	0.0345	0.0298	0.0324	0.0268	0.0131	0.0117	0.0197
7.0 - 8.0	0.0550	0.0318	0.0294	0.0239	0.0268	0.0237	0.0098	0.0104	0.0154
8.0 - 10.0	-0.0145	0.0089	0.0109	0.0142	0.0131	0.0098	0.0154	0.0076	0.0142
10.0 - 14.0	0.0160	0.0132	0.0133	0.0114	0.0117	0.0104	0.0076	0.0089	0.0102
14.0 - 20.0	0.0168	0.0211	0.0204	0.0219	0.0197	0.0154	0.0142	0.0102	0.0246

TABLE LXXVII. Measured cross section ratio of Fe with respect to CH as a function of  $E_\nu$ , and the absolute and fractional uncertainties.

Bin edges (GeV)	$\sigma(E_\nu)_{Fe}/\sigma(E_\nu)_{CH}$	Abs.	Stat.	Unc.	Abs.	Tot.	Unc.	Frac.	Stat.	Unc.	Frac.	Tot.	Unc.
2.0 - 3.0	1.412	1.020			1.411			0.722			0.999		
3.0 - 4.0	2.205	0.516			0.784			0.234			0.356		
4.0 - 5.0	1.492	0.324			0.606			0.217			0.406		
5.0 - 6.0	1.680	0.253			0.522			0.151			0.311		
6.0 - 7.0	1.900	0.244			0.453			0.129			0.238		
7.0 - 8.0	1.977	0.255			0.410			0.129			0.207		
8.0 - 10.0	2.248	0.328			0.415			0.146			0.185		
10.0 - 14.0	2.520	0.544			0.585			0.216			0.232		
14.0 - 20.0	2.849	1.151			1.216			0.404			0.427		

TABLE LXXVIII. Statistical covariance matrix of the measured  $\sigma(E_\nu)_{Fe}/\sigma(E_\nu)_{CH}$ 

Bin edges (GeV)	2.0 - 3.0	3.0 - 4.0	4.0 - 5.0	5.0 - 6.0	6.0 - 7.0	7.0 - 8.0	8.0 - 10.0	10.0 - 14.0	14.0 - 20.0
2.0 - 3.0	1.0395	0.0326	-0.0168	-0.0037	-0.0005	-0.0003	-0.0003	-0.0004	-0.0000
3.0 - 4.0	0.0326	0.2658	0.0137	-0.0109	-0.0041	-0.0010	-0.0005	-0.0005	-0.0005
4.0 - 5.0	-0.0168	0.0137	0.1048	0.0173	-0.0078	-0.0046	-0.0016	-0.0005	-0.0005
5.0 - 6.0	-0.0037	-0.0109	0.0173	0.0643	0.0170	-0.0070	-0.0062	-0.0020	-0.0007
6.0 - 7.0	-0.0005	-0.0041	-0.0078	0.0170	0.0597	0.0242	-0.0078	-0.0077	-0.0020
7.0 - 8.0	-0.0003	-0.0010	-0.0046	-0.0070	0.0242	0.0650	0.0295	-0.0130	-0.0083
8.0 - 10.0	-0.0003	-0.0005	-0.0016	-0.0062	-0.0078	0.0295	0.1073	0.0296	-0.0236
10.0 - 14.0	-0.0004	-0.0005	-0.0005	-0.0020	-0.0077	-0.0130	0.0296	0.2961	0.0368
14.0 - 20.0	-0.0000	-0.0005	-0.0005	-0.0007	-0.0020	-0.0083	-0.0236	0.0368	1.3247

TABLE LXXIX. Systematic covariance matrix of the measured  $\sigma(E_\nu)_{Fe}/\sigma(E_\nu)_{CH}$ 

Bin edges (GeV)	2.0 - 3.0	3.0 - 4.0	4.0 - 5.0	5.0 - 6.0	6.0 - 7.0	7.0 - 8.0	8.0 - 10.0	10.0 - 14.0	14.0 - 20.0
2.0 - 3.0	0.9502	0.4983	0.3858	0.3378	0.2183	0.1543	0.1080	0.1180	0.1497
3.0 - 4.0	0.4983	0.3489	0.2885	0.2562	0.1970	0.1548	0.1138	0.1020	0.1646
4.0 - 5.0	0.3858	0.2885	0.2629	0.2324	0.1854	0.1474	0.1094	0.0939	0.1582
5.0 - 6.0	0.3378	0.2562	0.2324	0.2079	0.1671	0.1335	0.0997	0.0855	0.1432
6.0 - 7.0	0.2183	0.1970	0.1854	0.1671	0.1451	0.1202	0.0915	0.0738	0.1311
7.0 - 8.0	0.1543	0.1548	0.1474	0.1335	0.1202	0.1031	0.0799	0.0618	0.1100
8.0 - 10.0	0.1080	0.1138	0.1094	0.0997	0.0915	0.0799	0.0649	0.0500	0.0839
10.0 - 14.0	0.1180	0.1020	0.0939	0.0855	0.0738	0.0618	0.0500	0.0460	0.0704
14.0 - 20.0	0.1497	0.1646	0.1582	0.1432	0.1311	0.1100	0.0839	0.0704	0.1533

TABLE LXXX. Measured cross section ratio of Pb with respect to CH as a function of  $E_\nu$ , and the absolute and fractional uncertainties.

Bin edges (GeV)	$\sigma(E_\nu)_{Pb}/\sigma(E_\nu)_{CH}$	Abs. Stat. Unc.	Abs. Tot. Unc.	Frac. Stat. Unc.	Frac. Tot. Unc.
2.0 - 3.0	-0.869	1.676	2.291	-1.929	-2.637
3.0 - 4.0	4.113	0.961	1.130	0.234	0.275
4.0 - 5.0	4.684	0.681	0.812	0.145	0.173
5.0 - 6.0	4.989	0.571	0.682	0.114	0.137
6.0 - 7.0	4.910	0.554	0.671	0.113	0.137
7.0 - 8.0	4.570	0.584	0.686	0.128	0.150
8.0 - 10.0	4.823	0.706	0.768	0.146	0.159
10.0 - 14.0	6.354	1.208	1.256	0.190	0.198
14.0 - 20.0	7.023	2.472	2.527	0.352	0.360

TABLE LXXXI. Statistical covariance matrix of the measured  $\sigma(E_\nu)_{Pb}/\sigma(E_\nu)_{CH}$ 

Bin edges (GeV)	2.0 - 3.0	3.0 - 4.0	4.0 - 5.0	5.0 - 6.0	6.0 - 7.0	7.0 - 8.0	8.0 - 10.0	10.0 - 14.0	14.0 - 20.0
2.0 - 3.0	2.8079	0.4032	0.0466	0.0072	0.0030	0.0011	0.0009	0.0000	0.0009
3.0 - 4.0	0.4032	0.9228	0.2166	0.0355	0.0091	0.0041	0.0019	0.0018	0.0040
4.0 - 5.0	0.0466	0.2166	0.4639	0.1734	0.0412	0.0107	0.0048	0.0045	0.0024
5.0 - 6.0	0.0072	0.0355	0.1734	0.3260	0.1640	0.0525	0.0162	0.0060	0.0030
6.0 - 7.0	0.0030	0.0091	0.0412	0.1640	0.3064	0.1891	0.0699	0.0208	0.0100
7.0 - 8.0	0.0011	0.0041	0.0107	0.0525	0.1891	0.3411	0.2435	0.0760	0.0151
8.0 - 10.0	0.0009	0.0019	0.0048	0.0162	0.0699	0.2435	0.4987	0.3582	0.1091
10.0 - 14.0	0.0000	0.0018	0.0045	0.0060	0.0208	0.0760	0.3582	1.4600	0.9113
14.0 - 20.0	0.0009	0.0040	0.0024	0.0030	0.0100	0.0151	0.1091	0.9113	6.1121

TABLE LXXXII. Systematic covariance matrix of the measured  $\sigma(E_\nu)_{Pb}/\sigma(E_\nu)_{CH}$ 

Bin edges (GeV)	2.0 - 3.0	3.0 - 4.0	4.0 - 5.0	5.0 - 6.0	6.0 - 7.0	7.0 - 8.0	8.0 - 10.0	10.0 - 14.0	14.0 - 20.0
2.0 - 3.0	2.4408	0.8114	0.5081	0.3181	0.2136	0.1779	0.1866	0.2020	0.0586
3.0 - 4.0	0.8114	0.3548	0.2447	0.1810	0.1521	0.1285	0.1117	0.1044	0.0490
4.0 - 5.0	0.5081	0.2447	0.1950	0.1561	0.1400	0.1247	0.1024	0.0943	0.0549
5.0 - 6.0	0.3181	0.1810	0.1561	0.1398	0.1336	0.1230	0.0984	0.0878	0.0679
6.0 - 7.0	0.2136	0.1521	0.1400	0.1336	0.1432	0.1339	0.1030	0.0863	0.0938
7.0 - 8.0	0.1779	0.1285	0.1247	0.1230	0.1339	0.1296	0.1017	0.0844	0.0938
8.0 - 10.0	0.1866	0.1117	0.1024	0.0984	0.1030	0.1017	0.0916	0.0857	0.0825
10.0 - 14.0	0.2020	0.1044	0.0943	0.0878	0.0863	0.0844	0.0857	0.1187	0.0876
14.0 - 20.0	0.0586	0.0490	0.0549	0.0679	0.0938	0.0938	0.0825	0.0876	0.2728

TABLE LXXXIII. Measured cross section ratio of C with respect to CH as a function of  $E_\pi$ , and the absolute and fractional uncertainties.

Bin edges (GeV)	$\frac{d\sigma_C}{dE_\pi} / \frac{d\sigma_{CH}}{dE_\pi}$	Abs. Stat. Unc.	Abs. Tot. Unc.	Frac. Stat. Unc.	Frac. Tot. Unc.
0 - 0.25	0.499	0.344	0.449	0.689	0.899
0.25 - 0.5	0.854	0.208	0.432	0.244	0.506
0.5 - 0.75	0.944	0.219	0.346	0.232	0.366
0.75 - 1.0	1.002	0.186	0.265	0.186	0.264
1.0 - 1.5	0.988	0.174	0.232	0.177	0.235
1.5 - 2.0	1.041	0.185	0.206	0.177	0.197
2.0 - 3.0	1.027	0.196	0.208	0.191	0.203
3.0 - 6.0	0.884	0.283	0.312	0.320	0.352

TABLE LXXXIV. Statistical covariance matrix of the measured  $\frac{d\sigma_C}{dE_\pi} / \frac{d\sigma_{CH}}{dE_\pi}$ 

Bin edges (GeV)	0 - 0.25	0.25 - 0.5	0.5 - 0.75	0.75 - 1.0	1.0 - 1.5	1.5 - 2.0	2.0 - 3.0	3.0 - 6.0
0 - 0.25	0.1182	0.0273	-0.0074	-0.0056	-0.0025	-0.0004	0.0000	-0.0000
0.25 - 0.5	0.0273	0.0434	0.0091	-0.0025	-0.0039	-0.0019	-0.0005	-0.0001
0.5 - 0.75	-0.0074	0.0091	0.0479	0.0257	0.0033	-0.0050	-0.0027	-0.0007
0.75 - 1.0	-0.0056	-0.0025	0.0257	0.0347	0.0204	-0.0005	-0.0045	-0.0016
1.0 - 1.5	-0.0025	-0.0039	0.0033	0.0204	0.0304	0.0153	-0.0017	-0.0037
1.5 - 2.0	-0.0004	-0.0019	-0.0050	-0.0005	0.0153	0.0341	0.0185	-0.0059
2.0 - 3.0	0.0000	-0.0005	-0.0027	-0.0045	-0.0017	0.0185	0.0383	0.0130
3.0 - 6.0	-0.0000	-0.0001	-0.0007	-0.0016	-0.0037	-0.0059	0.0130	0.0801

TABLE LXXXV. Systematic covariance matrix of the measured  $\frac{d\sigma_C}{dE_\pi} / \frac{d\sigma_{CH}}{dE_\pi}$ 

Bin edges (GeV)	0 - 0.25	0.25 - 0.5	0.5 - 0.75	0.75 - 1.0	1.0 - 1.5	1.5 - 2.0	2.0 - 3.0	3.0 - 6.0
0 - 0.25	0.0830	0.0859	0.0369	0.0047	-0.0077	-0.0105	-0.0120	-0.0182
0.25 - 0.5	0.0859	0.1433	0.0858	0.0356	0.0125	-0.0022	-0.0147	-0.0291
0.5 - 0.75	0.0369	0.0858	0.0716	0.0432	0.0264	0.0089	-0.0062	-0.0168
0.75 - 1.0	0.0047	0.0356	0.0432	0.0354	0.0271	0.0130	0.0008	-0.0046
1.0 - 1.5	-0.0077	0.0125	0.0264	0.0271	0.0236	0.0129	0.0030	-0.0002
1.5 - 2.0	-0.0105	-0.0022	0.0089	0.0130	0.0129	0.0081	0.0034	0.0026
2.0 - 3.0	-0.0120	-0.0147	-0.0062	0.0008	0.0030	0.0034	0.0051	0.0084
3.0 - 6.0	-0.0182	-0.0291	-0.0168	-0.0046	-0.0002	0.0026	0.0084	0.0170

TABLE LXXXVI. Measured cross section ratio of Fe with respect to CH as a function of  $E_\pi$ , and the absolute and fractional uncertainties.

Bin edges (GeV)	$\frac{d\sigma_{Fe}}{dE_\pi} / \frac{d\sigma_{CH}}{dE_\pi}$	Abs. Stat. Unc.	Abs. Tot. Unc.	Frac. Stat. Unc.	Frac. Tot. Unc.
0 - 0.25	2.550	0.816	1.122	0.320	0.440
0.25 - 0.5	0.798	0.252	0.855	0.316	1.071
0.5 - 0.75	1.384	0.318	0.741	0.230	0.535
0.75 - 1.0	1.822	0.250	0.425	0.137	0.233
1.0 - 1.5	2.758	0.278	0.380	0.101	0.138
1.5 - 2.0	2.934	0.330	0.359	0.112	0.122
2.0 - 3.0	2.491	0.331	0.360	0.133	0.144
3.0 - 6.0	3.075	0.512	0.550	0.166	0.179

TABLE LXXXVII. Statistical covariance matrix of the measured  $\frac{d\sigma_{Fe}}{dE_\pi} / \frac{d\sigma_{CH}}{dE_\pi}$ 

Bin edges (GeV)	0 - 0.25	0.25 - 0.5	0.5 - 0.75	0.75 - 1.0	1.0 - 1.5	1.5 - 2.0	2.0 - 3.0	3.0 - 6.0
0 - 0.25	0.6664	0.0086	-0.0592	-0.0282	-0.0066	0.0044	0.0028	0.0003
0.25 - 0.5	0.0086	0.0637	0.0219	-0.0043	-0.0092	-0.0036	0.0002	0.0006
0.5 - 0.75	-0.0592	0.0219	0.1011	0.0470	-0.0019	-0.0167	-0.0052	0.0015
0.75 - 1.0	-0.0282	-0.0043	0.0470	0.0627	0.0335	-0.0150	-0.0133	0.0001
1.0 - 1.5	-0.0066	-0.0092	-0.0019	0.0335	0.0771	0.0294	-0.0149	-0.0116
1.5 - 2.0	0.0044	-0.0036	-0.0167	-0.0150	0.0294	0.1087	0.0488	-0.0345
2.0 - 3.0	0.0028	0.0002	-0.0052	-0.0133	-0.0149	0.0488	0.1094	0.0168
3.0 - 6.0	0.0003	0.0006	0.0015	0.0001	-0.0116	-0.0345	0.0168	0.2619

TABLE LXXXVIII. Systematic covariance matrix of the measured  $\frac{d\sigma_{Fe}}{dE_\pi} / \frac{d\sigma_{CH}}{dE_\pi}$ 

Bin edges (GeV)	0 - 0.25	0.25 - 0.5	0.5 - 0.75	0.75 - 1.0	1.0 - 1.5	1.5 - 2.0	2.0 - 3.0	3.0 - 6.0
0 - 0.25	0.5924	0.3989	0.2567	0.1334	0.0832	0.0161	0.0096	-0.0399
0.25 - 0.5	0.3989	0.6667	0.5148	0.1815	0.0426	0.0361	0.0386	0.0130
0.5 - 0.75	0.2567	0.5148	0.4479	0.1785	0.0546	0.0365	0.0333	0.0085
0.75 - 1.0	0.1334	0.1815	0.1785	0.1180	0.0737	0.0085	0.0003	-0.0292
1.0 - 1.5	0.0832	0.0426	0.0546	0.0737	0.0674	0.0026	-0.0059	-0.0323
1.5 - 2.0	0.0161	0.0361	0.0365	0.0085	0.0026	0.0198	0.0183	0.0163
2.0 - 3.0	0.0096	0.0386	0.0333	0.0003	-0.0059	0.0183	0.0200	0.0222
3.0 - 6.0	-0.0399	0.0130	0.0085	-0.0292	-0.0323	0.0163	0.0222	0.0410

TABLE LXXXIX. Measured cross section ratio of Pb with respect to CH as a function of  $E_\pi$ , and the absolute and fractional uncertainties.

Bin edges (GeV)	$\frac{d\sigma_{Pb}}{dE_\pi} / \frac{d\sigma_{CH}}{dE_\pi}$	Abs. Stat. Unc.	Abs. Tot. Unc.	Frac. Stat. Unc.	Frac. Tot. Unc.
0 - 0.25	1.566	1.188	1.881	0.758	1.201
0.25 - 0.5	1.892	0.549	1.017	0.290	0.538
0.5 - 0.75	5.291	0.800	1.034	0.151	0.195
0.75 - 1.0	4.483	0.540	0.614	0.120	0.137
1.0 - 1.5	5.926	0.624	0.706	0.105	0.119
1.5 - 2.0	6.385	0.710	0.767	0.111	0.120
2.0 - 3.0	6.311	0.777	0.820	0.123	0.130
3.0 - 6.0	7.736	1.248	1.370	0.161	0.177

TABLE XC. Statistical covariance matrix of the measured  $\frac{d\sigma_{Pb}}{dE_\pi} / \frac{d\sigma_{CH}}{dE_\pi}$ 

Bin edges (GeV)	0 - 0.25	0.25 - 0.5	0.5 - 0.75	0.75 - 1.0	1.0 - 1.5	1.5 - 2.0	2.0 - 3.0	3.0 - 6.0
0 - 0.25	1.4116	0.2333	-0.0382	-0.0529	-0.0316	-0.0110	-0.0027	-0.0016
0.25 - 0.5	0.2333	0.3014	0.1543	-0.0129	-0.0376	-0.0222	-0.0082	-0.0026
0.5 - 0.75	-0.0382	0.1543	0.6403	0.2435	0.0204	-0.0696	-0.0364	-0.0113
0.75 - 1.0	-0.0529	-0.0129	0.2435	0.2919	0.1884	-0.0085	-0.0494	-0.0235
1.0 - 1.5	-0.0316	-0.0376	0.0204	0.1884	0.3898	0.2225	-0.0104	-0.0741
1.5 - 2.0	-0.0110	-0.0222	-0.0696	-0.0085	0.2225	0.5045	0.2670	-0.0940
2.0 - 3.0	-0.0027	-0.0082	-0.0364	-0.0494	-0.0104	0.2670	0.6033	0.2449
3.0 - 6.0	-0.0016	-0.0026	-0.0113	-0.0235	-0.0741	-0.0940	0.2449	1.5572

TABLE XCI. Systematic covariance matrix of the measured  $\frac{d\sigma_{Pb}}{dE_\pi} / \frac{d\sigma_{CH}}{dE_\pi}$ 

Bin edges (GeV)	0 - 0.25	0.25 - 0.5	0.5 - 0.75	0.75 - 1.0	1.0 - 1.5	1.5 - 2.0	2.0 - 3.0	3.0 - 6.0
0 - 0.25	2.1252	0.7029	0.5880	0.2067	0.1665	-0.0014	-0.0388	-0.5146
0.25 - 0.5	0.7029	0.7325	0.4706	0.0766	0.0125	0.0066	0.0022	-0.0981
0.5 - 0.75	0.5880	0.4706	0.4295	0.1418	0.1015	0.0405	0.0313	-0.0882
0.75 - 1.0	0.2067	0.0766	0.1418	0.0852	0.0866	0.0440	0.0369	-0.0105
1.0 - 1.5	0.1665	0.0125	0.1015	0.0866	0.1081	0.0725	0.0604	0.0184
1.5 - 2.0	-0.0014	0.0066	0.0405	0.0440	0.0725	0.0844	0.0732	0.0825
2.0 - 3.0	-0.0388	0.0022	0.0313	0.0369	0.0604	0.0732	0.0685	0.0968
3.0 - 6.0	-0.5146	-0.0981	-0.0882	-0.0105	0.0184	0.0825	0.0968	0.3191

TABLE XCII. Measured cross section ratio of C with respect to CH as a function of  $\theta_\pi$ , and the absolute and fractional uncertainties.

Bin edges (Degrees)	$\frac{d\sigma_C}{d\theta_\pi} / \frac{d\sigma_{CH}}{d\theta_\pi}$	Abs. Stat. Unc.	Abs. Tot. Unc.	Frac. Stat. Unc.	Frac. Tot. Unc.
0 - 5	0.889	0.168	0.200	0.189	0.224
5 - 10	1.002	0.133	0.146	0.132	0.146
10 - 15	0.970	0.131	0.143	0.135	0.148
15 - 20	0.882	0.141	0.175	0.160	0.198
20 - 25	0.886	0.161	0.217	0.181	0.245
25 - 30	1.005	0.197	0.289	0.196	0.288
30 - 35	0.898	0.232	0.360	0.258	0.400
35 - 40	0.785	0.331	0.529	0.421	0.674
40 - 45	0.609	0.452	0.751	0.741	1.232
45 - 50	0.107	0.732	1.253	6.860	11.747
50 - 60	0.175	2.075	3.861	11.822	21.999
60 - 70	2.608	2.526	19.967	0.968	7.656

TABLE XCIII. Measured cross section ratio of Fe with respect to CH as a function of  $\theta_\pi$ , and the absolute and fractional uncertainties.

Bin edges (Degrees)	$\frac{d\sigma_{Fe}}{d\theta_\pi} / \frac{d\sigma_{CH}}{d\theta_\pi}$	Abs. Stat. Unc.	Abs. Tot. Unc.	Frac. Stat. Unc.	Frac. Tot. Unc.
0 - 5	2.958	0.385	0.427	0.130	0.145
5 - 10	2.938	0.246	0.289	0.084	0.098
10 - 15	2.458	0.212	0.239	0.086	0.097
15 - 20	2.102	0.206	0.317	0.098	0.151
20 - 25	2.259	0.249	0.554	0.110	0.245
25 - 30	1.343	0.287	0.624	0.214	0.465
30 - 35	0.590	0.384	0.837	0.651	1.417
35 - 40	-0.159	0.149	1.043	-0.936	-6.552
40 - 45	-0.484	0.472	1.646	-0.975	-3.401
45 - 50	-0.531	0.447	1.734	-0.842	-3.267
50 - 60	-0.614	0.440	5.374	-0.716	-8.756
60 - 70	0.402	0.432	3.464	1.074	8.608

TABLE XCIV. Measured cross section ratio of Pb with respect to CH as a function of  $\theta_\pi$ , and the absolute and fractional uncertainties.

Bin edges (Degrees)	$\frac{d\sigma_{Pb}}{d\theta_\pi} / \frac{d\sigma_{CH}}{d\theta_\pi}$	Abs. Stat. Unc.	Abs. Tot. Unc.	Frac. Stat. Unc.	Frac. Tot. Unc.
0 - 5	9.413	1.009	1.095	0.107	0.116
5 - 10	6.980	0.565	0.656	0.081	0.094
10 - 15	4.795	0.433	0.513	0.090	0.107
15 - 20	3.247	0.391	0.510	0.121	0.157
20 - 25	2.458	0.428	0.594	0.174	0.241
25 - 30	1.147	0.458	0.744	0.399	0.648
30 - 35	0.241	0.501	0.857	2.075	3.551
35 - 40	-0.608	0.578	1.070	-0.950	-1.760
40 - 45	-1.178	0.604	1.171	-0.512	-0.994
45 - 50	-2.871	1.217	2.245	-0.424	-0.782
50 - 60	-3.656	2.140	5.902	-0.585	-1.614
60 - 70	-0.000	0.000	0.000	—	—

TABLE XCV. Statistical covariance matrix of the measured  $\frac{d\sigma_C}{d\theta_\pi} / \frac{d\sigma_{CH}}{d\theta_\pi}$ 

Bin edges (Degrees)	0 - 5	5 - 10	10 - 15	15 - 20	20 - 25	25 - 30	30 - 35	35 - 40	40 - 45	45 - 50	50 - 60	60 - 70
0 - 5	0.02837	0.01002	0.00219	0.00064	0.00052	0.00032	0.00029	0.00042	0.00043	0.00050	0.00169	-0.00401
5 - 10	0.01002	0.01758	0.00663	0.00191	0.00107	0.00079	0.00066	0.00057	0.00049	0.00082	0.00291	-0.00255
10 - 15	0.00219	0.00663	0.01716	0.00741	0.00282	0.00158	0.00135	0.00119	0.00126	0.00176	0.00410	-0.00268
15 - 20	0.00064	0.00191	0.00741	0.01985	0.01000	0.00425	0.00265	0.00236	0.00267	0.00271	0.00519	-0.00364
20 - 25	0.00052	0.00107	0.00282	0.01000	0.02586	0.01559	0.00731	0.00532	0.00506	0.00576	0.01216	-0.00855
25 - 30	0.00032	0.00079	0.00158	0.00425	0.01559	0.03898	0.02376	0.01441	0.01164	0.01305	0.02782	-0.02088
30 - 35	0.00029	0.00066	0.00135	0.00265	0.00731	0.02376	0.05372	0.04185	0.02620	0.02483	0.05006	-0.03163
35 - 40	0.00042	0.00057	0.00119	0.00236	0.00532	0.01441	0.04185	0.10936	0.09160	0.06560	0.10654	-0.07360
40 - 45	0.00043	0.00049	0.00126	0.00267	0.00506	0.01164	0.02620	0.09160	0.20400	0.20054	0.22289	-0.10386
45 - 50	0.00050	0.00082	0.00176	0.00271	0.00576	0.01305	0.02483	0.06560	0.20054	0.53537	0.93545	-0.32809
50 - 60	0.00169	0.00291	0.00410	0.00519	0.01216	0.02782	0.05006	0.10654	0.22839	0.93545	4.30455	-2.33752
60 - 70	-0.00401	-0.00255	-0.00268	-0.00855	-0.02088	-0.03163	-0.07360	-0.10386	-0.32809	-2.33752	6.37846	

TABLE XCVI. Systematic covariance matrix of the measured  $\frac{d\sigma_C}{d\theta_\pi} / \frac{d\sigma_{CH}}{d\theta_\pi}$ 

Bin edges (Degrees)	0 - 5	5 - 10	10 - 15	15 - 20	20 - 25	25 - 30	30 - 35	35 - 40	40 - 45	45 - 50	50 - 60	60 - 70
0 - 5	0.01147	0.00583	0.00033	0.00096	0.00170	0.00214	0.00263	0.00597	0.01893	0.02666	0.04494	-1.94388
5 - 10	0.00583	0.00377	0.00134	0.00225	0.00334	0.00488	0.00588	0.00947	0.01820	0.02699	0.04984	-0.95507
10 - 15	0.00333	0.00134	0.00337	0.00575	0.00795	0.01119	0.01383	0.01933	0.02404	0.03720	0.08887	0.00197
15 - 20	0.0096	0.00225	0.00575	0.01062	0.01473	0.02035	0.02500	0.03491	0.04387	0.06716	0.15877	-0.15757
20 - 25	0.00170	0.00334	0.00795	0.01473	0.02124	0.03006	0.03757	0.05377	0.07020	0.10847	0.26060	-0.39260
25 - 30	0.00214	0.00488	0.01119	0.02035	0.03006	0.04472	0.05725	0.08333	0.11204	0.17627	0.44553	-0.68275
30 - 35	0.00263	0.00588	0.01383	0.02500	0.03757	0.05725	0.07554	0.11168	0.15243	0.24362	0.63137	-0.92551
35 - 40	0.00597	0.00947	0.01933	0.03491	0.05377	0.08333	0.11168	0.17075	0.23944	0.38872	1.02016	-1.74876
40 - 45	0.01893	0.01820	0.02404	0.04387	0.07020	0.11204	0.15243	0.23944	0.35926	0.59184	1.59627	-4.64498
45 - 50	0.02666	0.02699	0.03720	0.06716	0.10847	0.17627	0.24362	0.38872	0.59184	1.03475	3.00522	-6.70008
50 - 60	0.04494	0.04984	0.08887	0.15877	0.26060	0.44553	0.63137	1.02016	1.59627	3.00522	10.60050	-16.63773
60 - 70	-1.94388	-0.95507	0.00197	-0.15757	-0.39260	-0.68275	-0.92551	-1.74876	-4.64498	-6.70008	-16.63773	392.29784

TABLE XCVII. Statistical covariance matrix of the measured  $\frac{d\sigma_{E_\pi}}{d\theta_\pi} / \frac{d\sigma_{CH}}{d\theta_\pi}$ 

Bin edges (Degrees)	0 - 5	5 - 10	10 - 15	15 - 20	20 - 25	25 - 30	30 - 35	35 - 40	40 - 45	45 - 50	50 - 60	60 - 70
0 - 5	0.14803	0.01700	-0.00756	-0.00414	-0.00238	-0.00063	0.00104	-0.00098	-0.00306	-0.00287	-0.00231	0.00014
5 - 10	0.01700	0.06054	0.00962	-0.00418	-0.00426	-0.00088	0.00208	-0.00154	-0.00493	-0.00455	-0.00395	0.00505
10 - 15	-0.00756	0.00962	0.04492	0.01243	-0.00345	-0.00205	0.00244	-0.00187	-0.00598	-0.00539	-0.00454	0.00271
15 - 20	-0.00414	-0.00418	0.01243	0.04256	0.01842	0.00192	0.00534	-0.00295	-0.00949	-0.00855	-0.00691	0.00532
20 - 25	-0.00238	-0.00426	-0.00345	0.01842	0.06214	0.03459	0.02437	-0.00723	-0.02325	-0.02200	-0.01859	0.01334
25 - 30	-0.00063	-0.00088	-0.00205	0.00192	0.03459	0.08254	0.08317	-0.01902	-0.05957	-0.05661	-0.05225	0.03188
30 - 35	0.00104	0.00208	0.00244	0.00534	0.02437	0.08317	0.14758	-0.04315	-0.13475	-0.12676	-0.11630	0.07277
35 - 40	-0.00098	-0.00154	-0.00187	-0.00295	-0.00723	-0.01902	-0.04315	0.02220	0.06998	0.06563	0.05799	-0.03937
40 - 45	-0.00306	-0.00493	-0.00598	-0.00949	-0.02325	-0.05957	-0.13475	0.06998	0.22284	0.20770	0.18334	-0.12474
45 - 50	-0.00287	-0.00455	-0.00539	-0.00855	-0.02200	-0.05661	-0.12676	0.06563	0.20770	0.19968	0.17198	-0.11696
50 - 60	-0.00231	-0.00395	-0.00454	-0.00691	-0.01859	-0.05225	-0.11630	0.05799	0.18334	0.17198	0.19334	-0.10294
60 - 70	0.00014	0.00505	0.00271	0.00532	0.03134	0.03188	0.07277	-0.03937	-0.12474	-0.11696	-0.10294	0.18692

TABLE XCIVIII. Systematic covariance matrix of the measured  $\frac{d\sigma_{Fe}}{d\theta_\pi} / \frac{d\sigma_{CH}}{d\theta_\pi}$ 

Bin edges (Degrees)	0 - 5	5 - 10	10 - 15	15 - 20	20 - 25	25 - 30	30 - 35	35 - 40	40 - 45	45 - 50	50 - 60	60 - 70
0 - 5	0.03465	0.01248	0.00337	-0.01022	-0.02961	-0.02844	-0.03712	-0.02400	0.00214	0.02415	0.06790	0.27828
5 - 10	0.01248	0.02280	0.01114	0.02402	0.04357	0.04068	0.05150	0.00962	-0.03071	-0.03334	0.00036	0.11483
10 - 15	0.00337	0.01114	0.01215	0.01879	0.02832	0.02944	0.02886	-0.02943	-0.07124	-0.07841	-0.21996	0.02609
15 - 20	-0.01022	0.02402	0.01879	0.05801	0.11498	0.12012	0.14801	-0.01007	-0.15586	-0.19113	-0.44151	-0.02491
20 - 25	-0.02961	0.04357	0.02832	0.11498	0.24507	0.25992	0.33178	0.00080	-0.31769	-0.40006	-0.93116	-0.11641
25 - 30	-0.02844	0.04068	0.02944	0.12012	0.25992	0.30706	0.40076	0.00567	-0.38639	-0.49743	-1.38931	0.01121
30 - 35	-0.03712	0.05150	0.02886	0.14801	0.33178	0.40076	0.55224	0.15140	-0.32734	-0.47469	-1.34810	0.16704
35 - 40	-0.02400	0.00962	-0.02943	-0.01007	0.00080	0.00567	0.15140	1.06634	1.43933	1.41517	4.21407	0.31746
40 - 45	0.00214	-0.03071	-0.07124	-0.15586	-0.31769	-0.38939	-0.32734	1.43933	2.48698	2.61304	7.86513	0.31630
45 - 50	0.02415	-0.03334	-0.07841	-0.19113	-0.40006	-0.49743	-0.47469	1.41517	2.61304	2.80573	8.60435	0.51313
50 - 60	0.06790	0.00036	-0.21996	-0.44151	-0.93116	-1.38931	-1.34810	4.21407	7.86513	8.60435	28.68283	1.13773
60 - 70	0.27828	0.11483	0.02609	-0.02491	-0.11641	0.01121	0.16704	0.31746	0.31630	0.51313	1.13773	11.81072

TABLE XCIX. Statistical covariance matrix of the measured  $\frac{d\sigma_{Pb}}{d\theta_\pi} / \frac{d\sigma_{CH}}{d\theta_\pi}$

TABLE C. Systematic covariance matrix of the measured  $\frac{d\sigma_{Pb}}{d\theta_\pi} / \frac{d\sigma_{CH}}{d\theta_\pi}$

TABLE CI. Measured cross section ratio of C with respect to CH as a function of  $Q^2$ , and the absolute and fractional uncertainties.

Bin edges ([GeV/c] $^2$ )	$\frac{d\sigma_C}{dQ^2} / \frac{d\sigma_{CH}}{dQ^2}$	Abs. Stat. Unc.	Abs. Tot. Unc.	Frac. Stat. Unc.	Frac. Tot. Unc.
0 - 0.025	0.882	0.180	0.221	0.205	0.251
0.025 - 0.05	1.039	0.178	0.230	0.171	0.221
0.05 - 0.075	1.037	0.195	0.245	0.188	0.236
0.075 - 0.1	0.765	0.189	0.257	0.247	0.336
0.1 - 0.15	0.571	0.190	0.277	0.332	0.485
0.15 - 0.2	0.663	0.236	0.347	0.356	0.523
0.2 - 0.3	1.158	0.340	0.460	0.294	0.398
0.3 - 0.4	1.648	0.488	0.595	0.296	0.361
0.4 - 0.6	0.706	0.448	0.553	0.634	0.783
0.6 - 1.0	1.107	0.903	0.961	0.816	0.868

TABLE CII. Statistical covariance matrix of the measured  $\frac{d\sigma_C}{dQ^2} / \frac{d\sigma_{CH}}{dQ^2}$

Bin edges ([GeV/c] $^2$ )	0 - 0.025	0.025 - 0.05	0.05 - 0.075	0.075 - 0.1	0.1 - 0.15	0.15 - 0.2	0.2 - 0.3	0.3 - 0.4	0.4 - 0.6	0.6 - 1.0
0 - 0.025	0.0325	0.0055	-0.0049	-0.0037	-0.0013	-0.0004	-0.0001	-0.0000	-0.0000	-0.0000
0.025 - 0.05	0.0055	0.0316	0.0162	0.0004	-0.0038	-0.0028	-0.0012	-0.0001	-0.0001	-0.0000
0.05 - 0.075	-0.0049	0.0162	0.0381	0.0244	0.0038	-0.0048	-0.0043	-0.0011	-0.0002	-0.0001
0.075 - 0.1	-0.0037	0.0004	0.0244	0.0357	0.0219	0.0026	-0.0058	-0.0039	-0.0008	-0.0002
0.1 - 0.15	-0.0013	-0.0038	0.0038	0.0219	0.0360	0.0251	0.0010	-0.0093	-0.0022	-0.0005
0.15 - 0.2	-0.0004	-0.0028	-0.0048	0.0026	0.0251	0.0557	0.0440	-0.0106	-0.0086	-0.0037
0.2 - 0.3	-0.0001	-0.0012	-0.0043	-0.0058	0.0010	0.0440	0.1157	0.0532	-0.0142	-0.0193
0.3 - 0.4	-0.0000	-0.0001	-0.0011	-0.0039	-0.0093	-0.0106	0.0532	0.2385	0.0906	-0.0278
0.4 - 0.6	-0.0000	-0.0001	-0.0002	-0.0008	-0.0022	-0.0086	-0.0142	0.0906	0.2004	0.1105
0.6 - 1.0	-0.0000	-0.0000	-0.0001	-0.0002	-0.0005	-0.0037	-0.0193	-0.0278	0.1105	0.8158

TABLE CIII. Systematic covariance matrix of the measured  $\frac{d\sigma_C}{dQ^2} / \frac{d\sigma_{CH}}{dQ^2}$

Bin edges ([GeV/c] $^2$ )	0 - 0.025	0.025 - 0.05	0.05 - 0.075	0.075 - 0.1	0.1 - 0.15	0.15 - 0.2	0.2 - 0.3	0.3 - 0.4	0.4 - 0.6	0.6 - 1.0
0 - 0.025	0.0164	0.0178	0.0182	0.0200	0.0217	0.0222	0.0197	0.0033	0.0022	-0.0039
0.025 - 0.05	0.0178	0.0212	0.0205	0.0213	0.0236	0.0249	0.0231	0.0031	0.0015	-0.0050
0.05 - 0.075	0.0182	0.0205	0.0221	0.0247	0.0266	0.0275	0.0248	0.0080	0.0093	-0.0011
0.075 - 0.1	0.0200	0.0213	0.0247	0.0303	0.0337	0.0362	0.0343	0.0192	0.0210	0.0075
0.1 - 0.15	0.0217	0.0236	0.0266	0.0337	0.0409	0.0484	0.0505	0.0332	0.0313	0.0187
0.15 - 0.2	0.0222	0.0249	0.0275	0.0362	0.0484	0.0644	0.0740	0.0530	0.0465	0.0331
0.2 - 0.3	0.0197	0.0231	0.0248	0.0343	0.0505	0.0740	0.0961	0.0786	0.0649	0.0546
0.3 - 0.4	0.0033	0.0031	0.0080	0.0192	0.0332	0.0530	0.0786	0.1154	0.1027	0.1002
0.4 - 0.6	0.0022	0.0015	0.0093	0.0210	0.0313	0.0465	0.0649	0.1027	0.1050	0.0925
0.6 - 1.0	-0.0039	-0.0050	-0.0011	0.0075	0.0187	0.0331	0.0546	0.1002	0.0925	0.1077

TABLE CIV. Measured cross section ratio of Fe with respect to CH as a function of  $Q^2$ , and the absolute and fractional uncertainties.

Bin edges ([GeV/c] $^2$ )	$\frac{d\sigma_{Fe}}{dQ^2} / \frac{d\sigma_{CH}}{dQ^2}$	Abs. Stat. Unc.	Abs. Tot. Unc.	Frac. Stat. Unc.	Frac. Tot. Unc.
0 - 0.025	2.354	0.289	0.438	0.123	0.186
0.025 - 0.05	2.536	0.260	0.429	0.102	0.169
0.05 - 0.075	2.459	0.283	0.489	0.115	0.199
0.075 - 0.1	2.186	0.305	0.572	0.139	0.261
0.1 - 0.15	1.856	0.345	0.753	0.186	0.406
0.15 - 0.2	1.563	0.401	0.918	0.257	0.587
0.2 - 0.3	1.591	0.452	0.875	0.284	0.550
0.3 - 0.4	2.263	0.638	0.910	0.282	0.402
0.4 - 0.6	2.665	0.822	1.071	0.308	0.402
0.6 - 1.0	2.291	1.222	1.436	0.534	0.627

TABLE CV. Statistical covariance matrix of the measured  $\frac{d\sigma_{Fe}}{dQ^2} / \frac{d\sigma_{CH}}{dQ^2}$ 

Bin edges ([GeV/c] <sup>2</sup> )	0 - 0.025	0.025 - 0.05	0.05 - 0.075	0.075 - 0.1	0.1 - 0.15	0.15 - 0.2	0.2 - 0.3	0.3 - 0.4	0.4 - 0.6	0.6 - 1.0
0 - 0.025	0.0835	0.0155	-0.0094	-0.0105	-0.0061	-0.0023	-0.0007	-0.0002	0.0000	-0.0000
0.025 - 0.05	0.0155	0.0674	0.0361	0.0050	-0.0098	-0.0089	-0.0041	-0.0012	-0.0002	0.0002
0.05 - 0.075	-0.0094	0.0361	0.0803	0.0547	0.0134	-0.0106	-0.0100	-0.0048	-0.0015	-0.0002
0.075 - 0.1	-0.0105	0.0050	0.0547	0.0928	0.0671	0.0122	-0.0142	-0.0133	-0.0048	-0.0012
0.1 - 0.15	-0.0061	-0.0098	0.0134	0.0671	0.1189	0.0832	0.0128	-0.0213	-0.0154	-0.0044
0.15 - 0.2	-0.0023	-0.0089	-0.0106	0.0122	0.0832	0.1607	0.1088	0.0027	-0.0342	-0.0191
0.2 - 0.3	-0.0007	-0.0041	-0.0100	-0.0142	0.0128	0.1088	0.2042	0.1361	-0.0117	-0.0481
0.3 - 0.4	-0.0002	-0.0012	-0.0048	-0.0133	-0.0213	0.0027	0.1361	0.4071	0.2436	-0.0651
0.4 - 0.6	0.0000	-0.0002	-0.0015	-0.0048	-0.0154	-0.0342	-0.0117	0.2436	0.6756	0.3850
0.6 - 1.0	-0.0000	0.0002	-0.0002	-0.0012	-0.0044	-0.0191	-0.0481	-0.0651	0.3850	1.4941

TABLE CVI. Systematic covariance matrix of the measured  $\frac{d\sigma_{Fe}}{dQ^2} / \frac{d\sigma_{CH}}{dQ^2}$ 

Bin edges ([GeV/c] <sup>2</sup> )	0 - 0.025	0.025 - 0.05	0.05 - 0.075	0.075 - 0.1	0.1 - 0.15	0.15 - 0.2	0.2 - 0.3	0.3 - 0.4	0.4 - 0.6	0.6 - 1.0
0 - 0.025	0.1082	0.1094	0.1213	0.1381	0.1689	0.1794	0.1530	0.1225	0.1350	0.1701
0.025 - 0.05	0.1094	0.1162	0.1316	0.1518	0.1927	0.2143	0.1845	0.1448	0.1510	0.1861
0.05 - 0.075	0.1213	0.1316	0.1583	0.1892	0.2475	0.2808	0.2441	0.1918	0.1889	0.2215
0.075 - 0.1	0.1381	0.1518	0.1892	0.2338	0.3155	0.3643	0.3181	0.2495	0.2399	0.2642
0.1 - 0.15	0.1689	0.1927	0.2475	0.3155	0.4485	0.5391	0.4696	0.3524	0.3270	0.3543
0.15 - 0.2	0.1794	0.2143	0.2808	0.3643	0.5391	0.6820	0.6047	0.4328	0.3819	0.4268
0.2 - 0.3	0.1530	0.1845	0.2441	0.3181	0.4696	0.6047	0.5623	0.4269	0.3750	0.4071
0.3 - 0.4	0.1225	0.1448	0.1918	0.2495	0.3524	0.4328	0.4269	0.4204	0.4146	0.3790
0.4 - 0.6	0.1350	0.1510	0.1889	0.2399	0.3270	0.3819	0.3750	0.4146	0.4722	0.4468
0.6 - 1.0	0.1701	0.1861	0.2215	0.2642	0.3543	0.4268	0.4071	0.3790	0.4468	0.5674

TABLE CVII. Measured cross section ratio of Pb with respect to CH as a function of  $Q^2$ , and the absolute and fractional uncertainties.

Bin edges ([GeV/c] <sup>2</sup> )	$\frac{d\sigma_{Pb}}{dQ^2} / \frac{d\sigma_{CH}}{dQ^2}$	Abs. Stat. Unc.	Abs. Tot. Unc.	Frac. Stat. Unc.	Frac. Tot. Unc.
0 - 0.025	6.236	1.077	1.199	0.173	0.192
0.025 - 0.05	6.929	1.022	1.119	0.148	0.162
0.05 - 0.075	7.287	1.167	1.263	0.160	0.173
0.075 - 0.1	6.104	1.234	1.415	0.202	0.232
0.1 - 0.15	4.723	1.298	1.541	0.275	0.326
0.15 - 0.2	4.836	1.530	1.735	0.316	0.359
0.2 - 0.3	7.128	1.901	1.964	0.267	0.276
0.3 - 0.4	5.391	2.386	2.484	0.443	0.461
0.4 - 0.6	4.015	2.527	2.636	0.629	0.657
0.6 - 1.0	2.436	3.543	3.623	1.454	1.488

Bin edges ([GeV/c <sup>2</sup> ])		0 - 0.025	0.025 - 0.05	0.05 - 0.075	0.075 - 0.1	0.1 - 0.15	0.15 - 0.2	0.2 - 0.3	0.3 - 0.4	0.4 - 0.6	0.6 - 1.0
0 - 0.025		1.1594	0.0255	-0.2999	-0.1657	-0.0339	0.0268	0.0251	0.0081	0.0016	0.0010
0.025 - 0.05		0.0255	1.0447	0.4837	-0.1459	-0.2554	-0.1152	0.0066	0.0287	0.0117	0.0028
0.05 - 0.075		-0.2999	0.4837	1.3613	0.7688	-0.0225	-0.3005	-0.1621	0.0124	0.0222	0.0070
0.075 - 0.1		-0.1657	-0.1459	0.7688	1.5220	1.0194	-0.0293	-0.4220	-0.1198	0.0376	0.0038
0.1 - 0.15		-0.0339	-0.2554	-0.0225	1.0194	1.6860	1.0191	-0.2366	-0.3906	-0.0433	0.0404
0.15 - 0.2		0.0208	-0.1152	-0.3005	-0.0293	1.0191	2.3411	1.2775	-0.6896	-0.5588	0.0680
0.2 - 0.3		0.0251	0.0066	-0.1621	-0.4220	-0.2366	1.2775	3.6147	1.2452	-0.8365	-0.4287
0.3 - 0.4		0.0081	0.0287	0.0124	-0.1198	-0.3906	-0.6896	1.2452	5.6914	2.4877	-2.0089
0.4 - 0.6		0.0016	0.0117	0.0222	0.0376	-0.0433	-0.5588	-0.8365	2.4877	6.3865	2.3337
0.6 - 1.0		0.0010	0.0028	0.0070	0.0038	0.0404	0.0680	-0.4287	-2.0089	2.3337	12.5505

Bin edges ([GeV/c <sup>2</sup> ])		0 - 0.025	0.025 - 0.05	0.05 - 0.075	0.075 - 0.1	0.1 - 0.15	0.15 - 0.2	0.2 - 0.3	0.3 - 0.4	0.4 - 0.6	0.6 - 1.0
0 - 0.025		0.2781	0.2158	0.1328	0.1573	0.2058	0.2457	0.0262	-0.0170	0.2124	0.1718
0.025 - 0.05		0.2158	0.2075	0.1642	0.1900	0.2298	0.2326	0.0535	-0.0025	0.1492	0.0961
0.05 - 0.075		0.1328	0.1642	0.2347	0.3100	0.3231	0.2660	0.1396	0.0747	0.0663	0.0170
0.075 - 0.1		0.1573	0.1900	0.3100	0.4804	0.5437	0.4405	0.2182	0.1004	0.0529	0.0614
0.1 - 0.15		0.2058	0.2298	0.3231	0.5437	0.6897	0.5994	0.2470	0.0757	0.0869	0.1509
0.15 - 0.2		0.2457	0.2326	0.2660	0.4405	0.5994	0.6679	0.2549	0.0290	0.2009	0.2283
0.2 - 0.3		0.0262	0.0535	0.1396	0.2182	0.2470	0.2549	0.2415	0.1828	0.1047	0.0572
0.3 - 0.4		-0.0170	-0.0025	0.0747	0.1004	0.0757	0.0290	0.1828	0.4791	0.2982	0.1444
0.4 - 0.6		0.2124	0.1492	0.0663	0.0529	0.0869	0.2009	0.1047	0.2982	0.5627	0.3749
0.6 - 1.0		0.1718	0.0961	0.0170	0.0614	0.1509	0.2283	0.0572	0.1444	0.3749	0.5777

TABLE CX. Measured cross section ratio of C with respect to CH as a function of  $E_\mu$ , and the absolute and fractional uncertainties.

Bin edges (GeV)	$\frac{d\sigma_C}{dE_\mu} / \frac{d\sigma_{CH}}{dE_\mu}$	Abs. Stat. Unc.	Abs. Tot. Unc.	Frac. Stat. Unc.	Frac. Tot. Unc.
0.0 - 2.0	2.427	2.048	2.313	0.844	0.953
2.0 - 3.0	1.349	0.321	0.352	0.238	0.261
3.0 - 4.0	0.959	0.231	0.279	0.241	0.291
4.0 - 5.0	0.660	0.198	0.266	0.301	0.402
5.0 - 6.0	1.107	0.235	0.304	0.212	0.275
6.0 - 7.0	0.572	0.225	0.305	0.393	0.533
7.0 - 8.0	0.722	0.270	0.326	0.375	0.452
8.0 - 10.0	1.063	0.350	0.377	0.330	0.355
10.0 - 14.0	1.233	0.558	0.575	0.453	0.466
14.0 - 20.0	1.042	1.022	1.061	0.981	1.018

TABLE CXI. Measured cross section ratio of Fe with respect to CH as a function of  $E_\mu$ , and the absolute and fractional uncertainties.

Bin edges (GeV)	$\frac{d\sigma_{Fe}}{dE_\mu} / \frac{d\sigma_{CH}}{dE_\mu}$	Abs. Stat. Unc.	Abs. Tot. Unc.	Frac. Stat. Unc.	Frac. Tot. Unc.
0.0 - 2.0	0.119	0.858	0.936	7.198	7.850
2.0 - 3.0	2.454	0.407	0.543	0.166	0.221
3.0 - 4.0	1.885	0.315	0.484	0.167	0.257
4.0 - 5.0	1.663	0.265	0.490	0.159	0.295
5.0 - 6.0	2.119	0.299	0.523	0.141	0.247
6.0 - 7.0	1.672	0.309	0.558	0.185	0.333
7.0 - 8.0	1.639	0.360	0.592	0.220	0.362
8.0 - 10.0	1.701	0.451	0.603	0.265	0.354
10.0 - 14.0	2.088	0.744	0.831	0.356	0.398
14.0 - 20.0	4.820	2.178	2.263	0.452	0.469

TABLE CXII. Measured cross section ratio of Pb with respect to CH as a function of  $E_\mu$ , and the absolute and fractional uncertainties.

Bin edges (GeV)	$\frac{d\sigma_{Pb}}{dE_\mu} / \frac{d\sigma_{CH}}{dE_\mu}$	Abs. Stat. Unc.	Abs. Tot. Unc.	Frac. Stat. Unc.	Frac. Tot. Unc.
0.0 - 2.0	0.286	0.392	2.782	1.370	9.726
2.0 - 3.0	3.873	0.930	1.193	0.240	0.308
3.0 - 4.0	7.060	0.875	0.929	0.124	0.132
4.0 - 5.0	4.422	0.676	0.751	0.153	0.170
5.0 - 6.0	4.943	0.751	0.886	0.152	0.179
6.0 - 7.0	3.183	0.752	0.925	0.236	0.291
7.0 - 8.0	2.851	0.822	0.950	0.288	0.333
8.0 - 10.0	4.404	1.223	1.290	0.278	0.293
10.0 - 14.0	6.177	2.129	2.192	0.345	0.355
14.0 - 20.0	7.899	4.428	4.536	0.561	0.574

Bin edges (GeV)	0.0 - 2.0	2.0 - 3.0	3.0 - 4.0	4.0 - 5.0	5.0 - 6.0	6.0 - 7.0	7.0 - 8.0	8.0 - 10.0	10.0 - 14.0	14.0 - 20.0
0.0 - 2.0	4.1957	-0.0081	-0.0090	-0.0012	-0.0002	-0.0001	-0.0001	-0.0001	-0.0000	-0.0003
2.0 - 3.0	-0.0081	0.1031	-0.0027	-0.0024	-0.0006	-0.0001	-0.0001	-0.0001	-0.0002	0.0000
3.0 - 4.0	-0.0090	-0.0027	0.0534	0.0017	-0.0038	-0.0009	-0.0003	-0.0002	-0.0002	-0.0001
4.0 - 5.0	-0.0012	-0.0024	0.0017	0.0394	0.0042	-0.0036	-0.0017	-0.0008	-0.0002	-0.0001
5.0 - 6.0	-0.0002	-0.0006	-0.0038	0.0042	0.0550	0.0112	-0.0056	-0.0055	-0.0012	-0.0004
6.0 - 7.0	-0.0001	-0.0001	-0.0009	-0.0036	0.0112	0.0566	0.0275	-0.0049	-0.0064	-0.0005
7.0 - 8.0	-0.0001	-0.0001	-0.0003	-0.0017	-0.0056	0.0275	0.0731	0.0355	-0.0152	-0.0052
8.0 - 10.0	-0.0001	-0.0001	-0.0002	-0.0008	-0.0055	-0.0049	0.0355	0.1228	0.0204	-0.0219
10.0 - 14.0	-0.0000	-0.0002	-0.0002	-0.0012	-0.0064	-0.0152	0.0204	0.3116	0.0103	
14.0 - 20.0	-0.0003	0.0000	-0.0001	-0.0001	-0.0004	-0.0005	-0.0052	-0.0219	0.0103	1.0450

Bin edges (GeV)	0.0 - 2.0	2.0 - 3.0	3.0 - 4.0	4.0 - 5.0	5.0 - 6.0	6.0 - 7.0	7.0 - 8.0	8.0 - 10.0	10.0 - 14.0	14.0 - 20.0
0.0 - 2.0	1.1524	0.1038	0.0450	0.0686	0.0115	-0.0244	0.0340	-0.0072	-0.0051	0.0200
2.0 - 3.0	0.1038	0.0206	0.0188	0.0220	0.0194	0.0163	0.0188	0.0113	0.0082	0.0222
3.0 - 4.0	0.0450	0.0188	0.0244	0.0261	0.0270	0.0254	0.0241	0.0164	0.0129	0.0319
4.0 - 5.0	0.0686	0.0220	0.0261	0.0311	0.0304	0.0293	0.0285	0.0187	0.0139	0.0368
5.0 - 6.0	0.0115	0.0194	0.0270	0.0304	0.0374	0.0378	0.0322	0.0241	0.0174	0.0394
6.0 - 7.0	-0.0244	0.0163	0.0254	0.0293	0.0378	0.0422	0.0344	0.0261	0.0186	0.0401
7.0 - 8.0	0.0340	0.0188	0.0241	0.0285	0.0322	0.0344	0.0333	0.0231	0.0174	0.0350
8.0 - 10.0	-0.0072	0.0113	0.0164	0.0187	0.0241	0.0261	0.0231	0.0192	0.0139	0.0285
10.0 - 14.0	-0.0051	0.0082	0.0129	0.0139	0.0174	0.0186	0.0174	0.0139	0.0190	0.0233
14.0 - 20.0	0.0200	0.0222	0.0319	0.0368	0.0394	0.0401	0.0350	0.0285	0.0233	0.0804

TABLE CXV. Statistical covariance matrix of the measured  $\frac{d\sigma_{Fe}}{dE_\mu} / \frac{d\sigma_{CH}}{dE_\mu}$ 

Bin edges (GeV)	0.0 - 2.0	2.0 - 3.0	3.0 - 4.0	4.0 - 5.0	5.0 - 6.0	6.0 - 7.0	7.0 - 8.0	8.0 - 10.0	10.0 - 14.0	14.0 - 20.0
0.0 - 2.0	0.7370	0.0325	-0.0021	-0.0006	-0.0001	0.0002	0.0001	-0.0002	-0.0002	-0.0002
2.0 - 3.0	0.0325	0.1656	-0.0037	-0.0048	-0.0014	-0.0004	-0.0002	-0.0002	-0.0003	-0.0007
3.0 - 4.0	-0.0021	-0.0037	0.0992	0.0038	-0.0069	-0.0022	-0.0007	-0.0004	-0.0003	-0.0007
4.0 - 5.0	-0.0006	-0.0048	0.0038	0.0700	0.0094	-0.0078	-0.0044	-0.0015	-0.0007	-0.0009
5.0 - 6.0	-0.0001	-0.0014	-0.0069	0.0094	0.0894	0.0209	-0.0102	-0.0087	-0.0029	-0.0018
6.0 - 7.0	0.0002	-0.0004	-0.0022	-0.0078	0.0209	0.0954	0.0488	-0.0088	-0.0128	-0.0044
7.0 - 8.0	0.0001	-0.0002	-0.0007	-0.0044	-0.0102	0.0488	0.1294	0.0631	-0.0211	-0.0269
8.0 - 10.0	-0.0002	-0.0002	-0.0004	-0.0015	-0.0087	-0.0088	0.0631	0.2037	0.0760	-0.0746
10.0 - 14.0	-0.0002	-0.0003	-0.0003	-0.0007	-0.0029	-0.0128	-0.0211	0.0760	0.5536	0.1437
14.0 - 20.0	-0.0002	-0.0007	-0.0007	-0.0009	-0.0018	-0.0044	-0.0269	-0.0746	0.1437	4.7439

Bin edges (GeV)	0.0 - 2.0	2.0 - 3.0	3.0 - 4.0	4.0 - 5.0	5.0 - 6.0	6.0 - 7.0	7.0 - 8.0	8.0 - 10.0	10.0 - 14.0	14.0 - 20.0
0.0 - 2.0	0.1396	0.1204	0.0818	0.0960	0.0684	0.0531	0.0361	0.0402	0.0511	0.0021
2.0 - 3.0	0.1204	0.1296	0.1074	0.1249	0.1089	0.1016	0.0883	0.0793	0.0758	0.0751
3.0 - 4.0	0.0818	0.1074	0.1353	0.1491	0.1511	0.1543	0.1483	0.1259	0.1151	0.1193
4.0 - 5.0	0.0960	0.1249	0.1491	0.1700	0.1686	0.1729	0.1649	0.1394	0.1268	0.1323
5.0 - 6.0	0.0684	0.1089	0.1511	0.1686	0.1846	0.1953	0.1919	0.1598	0.1438	0.1747
6.0 - 7.0	0.0531	0.1016	0.1543	0.1729	0.1953	0.2155	0.2157	0.1777	0.1554	0.1998
7.0 - 8.0	0.0361	0.0883	0.1483	0.1649	0.1919	0.2157	0.2215	0.1836	0.1550	0.2045
8.0 - 10.0	0.0402	0.0793	0.1259	0.1394	0.1598	0.1777	0.1836	0.1594	0.1349	0.1650
10.0 - 14.0	0.0511	0.0758	0.1151	0.1268	0.1438	0.1554	0.1550	0.1349	0.1361	0.1469
14.0 - 20.0	0.0021	0.0751	0.1193	0.1323	0.1747	0.1998	0.2045	0.1650	0.1469	0.3767

Bin edges (GeV)	0.0 - 2.0	2.0 - 3.0	3.0 - 4.0	4.0 - 5.0	5.0 - 6.0	6.0 - 7.0	7.0 - 8.0	8.0 - 10.0	10.0 - 14.0	14.0 - 20.0
0.0 - 2.0	0.1535	-0.1129	-0.0032	0.0007	0.0005	0.0002	0.0001	0.0000	0.0001	-0.0002
2.0 - 3.0	-0.1129	0.8643	-0.0205	-0.0246	-0.0064	-0.0020	-0.0009	-0.0004	-0.0024	-0.0014
3.0 - 4.0	-0.0032	-0.0205	0.7652	0.0200	-0.0543	-0.0168	-0.0061	-0.0047	-0.0023	-0.0034
4.0 - 5.0	0.0007	-0.0246	0.0200	0.4567	0.0638	-0.0426	-0.0234	-0.0131	-0.0068	-0.0028
5.0 - 6.0	0.0005	-0.0064	-0.0543	0.0638	0.5643	0.1445	-0.0427	-0.0671	-0.0303	-0.0111
6.0 - 7.0	0.0002	-0.0020	-0.0168	-0.0426	0.1445	0.5653	0.3091	-0.0247	-0.0964	-0.0357
7.0 - 8.0	0.0001	-0.0009	-0.0061	-0.0234	-0.0427	0.3091	0.6756	0.4424	-0.1316	-0.1421
8.0 - 10.0	0.0000	-0.0004	-0.0047	-0.0131	-0.0671	-0.0247	0.4424	1.4954	0.4397	-0.5004
10.0 - 14.0	0.0001	-0.0024	-0.0023	-0.0068	-0.0303	-0.0964	-0.1316	0.4397	4.5347	1.1921
14.0 - 20.0	-0.0002	-0.0014	-0.0034	-0.0028	-0.0111	-0.0357	-0.1421	-0.5004	1.1921	19.6094

Bin edges (GeV)	0.0 - 2.0	2.0 - 3.0	3.0 - 4.0	4.0 - 5.0	5.0 - 6.0	6.0 - 7.0	7.0 - 8.0	8.0 - 10.0	10.0 - 14.0	14.0 - 20.0
0.0 - 2.0	7.5866	-1.9707	-0.3895	-0.2481	-0.2914	-0.2635	-0.1367	-0.1432	-0.2818	0.4094
2.0 - 3.0	-1.9707	0.5579	0.1452	0.0982	0.1368	0.1156	0.0825	0.0896	0.1180	-0.1002
3.0 - 4.0	-0.3895	0.1452	0.0972	0.0703	0.1167	0.0963	0.0717	0.0618	0.0597	0.0328
4.0 - 5.0	-0.2481	0.0982	0.0703	0.1077	0.1405	0.1528	0.1301	0.0778	0.0763	0.0567
5.0 - 6.0	-0.2914	0.1368	0.1167	0.1405	0.2207	0.2244	0.1885	0.1336	0.1361	0.1251
6.0 - 7.0	-0.2635	0.1156	0.0963	0.1528	0.2244	0.2900	0.2444	0.1404	0.1506	0.1815
7.0 - 8.0	-0.1367	0.0825	0.0717	0.1301	0.1885	0.2444	0.2265	0.1457	0.1336	0.1122
8.0 - 10.0	-0.1432	0.0896	0.0618	0.0778	0.1336	0.1404	0.1457	0.1700	0.1578	0.0972
10.0 - 14.0	-0.2818	0.1180	0.0597	0.0763	0.1361	0.1506	0.1336	0.1578	0.2691	0.2526
14.0 - 20.0	0.4094	-0.1002	0.0328	0.0567	0.1251	0.1815	0.1122	0.0972	0.2526	0.9652

TABLE CXIX. Measured cross section ratio of C with respect to CH as a function of  $\theta_\mu$ , and the absolute and fractional uncertainties.

Bin edges (Degrees)	$\frac{d\sigma_C}{d\theta_\mu} / \frac{d\sigma_{CH}}{d\theta_\mu}$	Abs. Stat. Unc.	Abs. Tot. Unc.	Frac. Stat. Unc.	Frac. Tot. Unc.
0 - 2	0.811	0.147	0.192	0.181	0.236
2 - 4	0.901	0.152	0.219	0.168	0.243
4 - 6	1.149	0.280	0.381	0.244	0.331
6 - 8	0.443	0.357	0.449	0.804	1.012
8 - 12	1.645	0.727	0.804	0.442	0.489
12 - 20	5.833	5.725	6.548	0.981	1.123

TABLE CXX. Statistical covariance matrix of the measured  $\frac{d\sigma_C}{d\theta_\mu} / \frac{d\sigma_{CH}}{d\theta_\mu}$

Bin edges (Degrees)	0 - 2	2 - 4	4 - 6	6 - 8	8 - 12	12 - 20
0 - 2	0.02161	-0.00089	-0.00199	-0.00011	0.00004	0.00004
2 - 4	-0.00089	0.02306	-0.00112	-0.00198	-0.00040	0.00025
4 - 6	-0.00199	-0.00112	0.07857	0.00576	-0.00877	-0.00426
6 - 8	-0.00011	-0.00198	0.00576	0.12709	0.01503	-0.05436
8 - 12	0.00004	-0.00040	-0.00877	0.01503	0.52870	-0.18190
12 - 20	0.00004	0.00025	-0.00426	-0.05436	-0.18190	32.77880

TABLE CXXI. Systematic covariance matrix of the measured  $\frac{d\sigma_C}{d\theta_\mu} / \frac{d\sigma_{CH}}{d\theta_\mu}$

Bin edges (Degrees)	0 - 2	2 - 4	4 - 6	6 - 8	8 - 12	12 - 20
0 - 2	0.01510	0.01744	0.01919	0.01247	0.00805	-0.08231
2 - 4	0.01744	0.02499	0.03528	0.02931	0.02529	-0.01271
4 - 6	0.01919	0.03528	0.06650	0.06315	0.06553	0.16736
6 - 8	0.01247	0.02931	0.06315	0.07415	0.07214	0.21385
8 - 12	0.00805	0.02529	0.06553	0.07214	0.11751	0.05673
12 - 20	-0.08231	-0.01271	0.16736	0.21385	0.05673	10.10247

TABLE CXXII. Measured cross section ratio of Fe with respect to CH as a function of  $\theta_\mu$ , and the absolute and fractional uncertainties.

Bin edges (Degrees)	$\frac{d\sigma_{Fe}}{d\theta_\mu} / \frac{d\sigma_{CH}}{d\theta_\mu}$	Abs. Stat. Unc.	Abs. Tot. Unc.	Frac. Stat. Unc.	Frac. Tot. Unc.
0 - 2	2.601	0.244	0.394	0.094	0.152
2 - 4	1.741	0.219	0.496	0.126	0.285
4 - 6	2.572	0.441	0.776	0.172	0.302
6 - 8	1.904	0.641	1.021	0.337	0.536
8 - 12	0.932	0.934	1.378	1.002	1.479
12 - 20	10.786	9.491	11.279	0.880	1.046

TABLE CXXIII. Statistical covariance matrix of the measured  $\frac{d\sigma_{Fe}}{d\theta_\mu} / \frac{d\sigma_{CH}}{d\theta_\mu}$

Bin edges (Degrees)	0 - 2	2 - 4	4 - 6	6 - 8	8 - 12	12 - 20
0 - 2	0.05957	-0.00047	-0.00770	-0.00079	-0.00001	0.00006
2 - 4	-0.00047	0.04780	0.00291	-0.00795	-0.00112	0.00060
4 - 6	-0.00770	0.00291	0.19472	0.01207	-0.02367	-0.02587
6 - 8	-0.00079	-0.00795	0.01207	0.41072	0.06565	-0.26253
8 - 12	-0.00001	-0.00112	-0.02367	0.06565	0.87180	0.42570
12 - 20	0.00006	0.00060	-0.02587	-0.26253	0.42570	90.07038

TABLE CXXIV. Systematic covariance matrix of the measured  $\frac{d\sigma_{Fe}}{d\theta_\mu} / \frac{d\sigma_{CH}}{d\theta_\mu}$

Bin edges (Degrees)	0 - 2	2 - 4	4 - 6	6 - 8	8 - 12	12 - 20
0 - 2	0.09584	0.12919	0.15831	0.18404	0.22107	0.26372
2 - 4	0.12919	0.19826	0.26490	0.31183	0.35678	0.64246
4 - 6	0.15831	0.26490	0.40692	0.48999	0.57119	0.86735
6 - 8	0.18404	0.31183	0.48999	0.63216	0.76042	0.93255
8 - 12	0.22107	0.35678	0.57119	0.76042	1.02666	0.47488
12 - 20	0.26372	0.64246	0.86735	0.93255	0.47488	37.15665

TABLE CXXV. Measured cross section ratio of Pb with respect to CH as a function of  $\theta_\mu$ , and the absolute and fractional uncertainties.

Bin edges (Degrees)	$\frac{d\sigma_{Pb}}{d\theta_\mu} / \frac{d\sigma_{CH}}{d\theta_\mu}$	Abs. Stat. Unc.	Abs. Tot. Unc.	Frac. Stat. Unc.	Frac. Tot. Unc.
0 - 2	6.491	0.747	0.860	0.115	0.132
2 - 4	5.451	0.678	0.841	0.124	0.154
4 - 6	6.924	1.258	1.393	0.182	0.201
6 - 8	4.716	1.795	1.920	0.381	0.407
8 - 12	2.773	3.557	3.823	1.283	1.379
12 - 20	-41.696	23.712	43.334	-0.569	-1.039

TABLE CXXVI. Statistical covariance matrix of the measured  $\frac{d\sigma_{Pb}}{d\theta_\mu} / \frac{d\sigma_{CH}}{d\theta_\mu}$

Bin edges (Degrees)	0 - 2	2 - 4	4 - 6	6 - 8	8 - 12	12 - 20
0 - 2	0.55840	-0.00640	-0.06947	-0.00628	0.00114	-0.04651
2 - 4	-0.00640	0.46017	0.02221	-0.07105	-0.00790	-0.18521
4 - 6	-0.06947	0.02221	1.58309	0.13616	-0.30772	1.85807
6 - 8	-0.00628	-0.07105	0.13616	3.22339	0.14887	14.17440
8 - 12	0.00114	-0.00790	-0.30772	0.14887	12.65131	-12.57400
12 - 20	-0.04651	-0.18521	1.85807	14.17440	-12.57400	562.27049

TABLE CXXVII. Systematic covariance matrix of the measured  $\frac{d\sigma_{Pb}}{d\theta_\mu} / \frac{d\sigma_{CH}}{d\theta_\mu}$

Bin edges (Degrees)	0 - 2	2 - 4	4 - 6	6 - 8	8 - 12	12 - 20
0 - 2	0.18089	0.16965	0.14739	0.14741	0.34144	7.72783
2 - 4	0.16965	0.24646	0.24877	0.19977	0.33733	8.09960
4 - 6	0.14739	0.24877	0.35807	0.30008	0.40367	6.20723
6 - 8	0.14741	0.19977	0.30008	0.46411	0.65662	7.98873
8 - 12	0.34144	0.33733	0.40367	0.65662	1.96150	32.80597
12 - 20	7.72783	8.09960	6.20723	7.98873	32.80597	1315.58804